Application of Heat Pipe Technology in Permanent Mold Casting of Nonferrous Alloys

by

Kaled Elalem

Department of Mining, Metals and Materials Engineering
McGill University, Montreal, Canada

A thesis submitted to the Faculty of Graduate Studies and Research
in partial fulfillment of the requirements of the degree of
Doctor of Philosophy

June 2004

Your file Votre référence
ISBN: 0-494-06293-2
Our file Notre référence
ISBN: 0-494-06293-2

ABSTRACT

The issue of mold cooling is one, which presents a foundry with a dilemma. On the one hand, the use of air for cooling is safe and practical, however, it is not very effective and high cost. On the other hand, water-cooling can be very effective but it raises serious concerns about safety, especially with a metal such as magnesium. An alternative option that is being developed at McGill University uses heat pipe technology to carry out the cooling.

The experimental program consisted of designing a permanent mold to produce AZ91E magnesium alloy and A356 aluminum alloy castings with shrinkage defects. Heat pipes were then used to reduce these defects. The heat pipes used in this work are novel and are patent pending. They are referred to as McGill Heat Pipes.

Computer modeling was used extensively in designing the mold and the heat pipes. Final designs for the mold and the heat pipes were chosen based on the modeling results.

Laboratory tests of the heat pipe were performed before conducting the actual experimental plan. The laboratory testing results verified the excellent performance of the heat pipes as anticipated by the model.

An industrial mold made of H13 tool steel was constructed to cast nonferrous alloys. The heat pipes were installed and initial testing and actual industrial trials were conducted. This is the first time where a McGill heat pipe was used in an industrial permanent mold casting process for nonferrous alloys.

The effects of cooling using heat pipes on AZ91E and A356 were evaluated using computer modeling and experimental trials. Microstructural analyses were conducted to measure the secondary dendrite arm spacing, SDAS, and the grain size to evaluate the cooling effects on the castings. The modeling and the experimental results agreed quite well. The metallurgical differences between AZ91E and A356 were investigated using modeling and experimental results. Selected results from modeling, laboratory and industrial trials are presented. The results show a promising future for heat pipe technology in cooling permanent molds for the casting of nonferrous alloys.

Résumé

Pour une fonderie, le refroidissement d'un moule permanent peut poser un dilemme. D'une part, l'utilisation de l'air pour le refroidissement est sécuritaire et pratique, cependant ce n'est pas très efficace et le coût est élevé. D'autre part, le refroidissement par eau peut être très efficace mais il y a des réserves concernant la sécurité, spécialement pour un métal tel que le magnésium. Une option alternative qui a été développée à l'Université McGill utilise la technologie des caloducs pour obtenir le refroidissement.

Le programme expérimental comprenait la conception d'un moule permanent pour produire des pièces coulées en alliage de magnésium AZ91E et en alliage d'aluminium A356 avec des défauts de retassure. Les caloducs ont été utilisés par la suite pour éliminer ces défauts. Les caloducs utilisés dans ce travail et identifiés comme des caloducs de McGill sont innovateurs et font l'objet d'une demande de brevet.

La modélisation par ordinateur a été considérablement utilisée pour la conception du moule et des caloducs. D'ailleurs, c'est en se basant sur les résultats de simulation que le choix final pour la fabrication de ces derniers a été fait.

Des essais préliminaires en laboratoire ont permis d'évaluer le caloduc avant son utilisation dans le programme expérimental de cette étude. Les résultats obtenus ont permis de vérifier l'excellente performance des caloducs telle qu'anticipée par la modélisation.

Un moule industriel en acier H13 a été fabriqué pour couler des alliages non ferreux. Les caloducs ont été installés et des essais initiaux suivis d'essais industriels ont été effectués. C'est la première fois qu'un caloduc de McGill a été utilisé dans un procédé de coulée en moule permanent pour des alliages non ferreux.

Les effets de refroidissement par caloducs pour les alliages AZ91E et A356 ont été évalués en utilisant aussi bien la modélisation que les résultats expérimentaux.

Des analyses microstructurales ont été faites pour mesurer l'espace interdendritique et la taille des grains afin d'évaluer l'influence du refroidissement sur les pièces moulées.

La correspondance entre les résultats expérimentaux et ceux obtenus par modélisation est très bonne. Les différences métallurgiques entre les alliages AZ91E et A356 ont été étudiées en utilisant les résultats expérimentaux ainsi que ceux obtenus par la modélisation. Une sélection des résultats de modélisation, de laboratoire ainsi que ceux obtenus lors des essais industriels est présentée. Les résultats soulignent un avenir prometteur pour l'utilisation de la technologie des caloducs dans le refroidissement des moules permanents utilisés pour la coulée des alliages non ferreux.

Acknowledgements

I hereby thank my supervisors, Prof. John E. Gruzleski and Prof. Frank Mucciardi, for their constant guidance and help throughout this work. It was my pleasure to be under the supervision of such knowledgeable supervisors, in addition to their constant encouragement. Their useful suggestions and innovative ideas have been of great assistance to me in completing this project and without my supervisors help I would not be where I am today.

I would also like to thank the Department of Mining, Metals and Materials Engineering staff at McGill University for their administrative help and assistance. It's been a real great experience to get to know the entire staff.

Special thanks are due to my friend, Mr Walter Greenland, for his help in the fabrication of the heat pipes.

I would like to thank InterMag Technologies and their staff for their help in constructing the mold and allowing me to conduct my experimental trials at their facilities. Special thanks are to Dr Rene Crescent, Dr Zhan Zhang, Mr Yevs Carbonneau, Frederic Rheaume, Luc Gauthier, and Pierre-Luc Gautlier for their help and support during my experimental work.

To my colleagues Juan Hernandez, Claudia Alejandra Neivi Andrade, Lihong Shang, Javier Tavitas, Hujun Zhao, Farzad Jalilan, Ozgyr Ozdemir, and Ramona Vintilla, you'll never be forgotten. Your friendship and invaluable help has made my experience at McGill University much more pleasant.

I would like to thank my friend, Dr. Chunhui Zhang, for his unlimited support and great friendship through all those years. Special thanks for Dr. Florence Paray for her support and kind help.

My sincere thanks are due to my friends, Dr Ahmed Zaid, Saed Musmar, Mohamed Tawalba, Khaled Rahal, Fabian Edelmann, Dr Sofian Benhadad, Demetri Giannitsios and Kajsa Duke for their friendship and moral support.

I am really grateful to my parents, my wife and all my family members for their prayers and patience, which enabled me to complete this work successfully.

Finally, I am grateful for financial support from the Natural Science and Engineering Research Council of Canada (NSERC).

To my father, mother, and all Elalem family

CONTENTS

ABSTRACT I
RÉSUMÉ III
ACKNOWLEDGEMENTS.....V
CONTENTS.....VIII
LIST OF FIGURES.....XI
LIST OF TABLES XVI
NOMENCLATURE.....XVII

CHAPTER 1 INTRODUCTION 1
1.1. SCOPE OF THE PRESENT WORK.....3

CHAPTER 2 LITERATURE SURVEY 5
2.1 Introduction 5
2.2. Air Gap Formation 6
2.2.1. Time for Air Gap Initiation 7
2.3. Freezing Time of Castings Solidifying in Metallic Molds 8
2.3.1. Factors Affecting Freezing Time, t_f 9
2.4 The Interfacial Heat Transfer Coefficient 11
2.5 Latent Heat Liberation 16
2.6. Mold Design 17
2.7. Heat Transfer in Molds 18
2.7.1. Conduction 18
2.7.2. Convection 19
2.7.3. Radiation 20
2.8. Mold Cooling General Approach 21

2.8.1. Control of Mold Temperature 22
2.9. Heat Pipe Technology 24
2.9.1. Heat Pipe Concept 24
2.9.2. Development of Heat Pipe Technology 25
2.9.3. Applications of the Heat Pipe 28
2.9.4. Problems with Heat Pipe Technology 31
2.10. Thermal Modeling of Permanent Mold Casting of Nonferrous 37
2.11. The Relationship between Microstructure and Mechanical Properties vs. Cooling Rate 37

CHAPTER 3 DESIGN AND TESTING OF A WATER-BASED HEAT PIPE AND A PERMANENT MOLD 41

3.1. Heat Pipe Design 41
3.1.1. Introduction 41
3.1.2. Design Guidelines 41
3.1.3. Heat Pipe Configuration 42
3.1.3.1. The condenser section 45
3.1.3.2. The evaporator section 46
3.1.3.3. Vent necessity in McGill heat pipe 51
3.2. Design and Construction of a Permanent Mold for Nonferrous Casting 52
3.2.1. Mold Design 52
3.3. Computer modeling of the casting process 56
3.3.1. Computer modeling of cooling curves 61
3.4. Laboratory Testing of the Novel Heat Pipe 63
3.5. Heat pipe Experimental Studies 67

CHAPTER 4 RESULTS AND DISCUSSION 70
4.1. Industrial Trial for Nonferrous Permanent Mold Casting 70
4.1.1. Industrial Setup 70
4.2. Casting Analysis 74
4.2.1. Visual Analysis of Magnesium AZ91E 75
4.2.2. Visual Analysis of Aluminum Alloy (A356) 78
4.3. Computer Modeling as a Tool to Understand Casting Solidification Pattern 80
4.4. Microstructural Analysis of Magnesium AZ91E 102
4.4.1. SDAS Analysis for Magnesium AZ91E 103
4.4.2. Grain Size Analysis for Magnesium AZ91E 107
4.5. Microstructural Analysis of Aluminum Alloy (A356) 111
4.5.1. SDAS Analysis for Aluminum alloy (A356) 112
4.5.2. Grain Size Analysis for Aluminum Alloy A356 115
4.6. Thermal Analysis of Heat Pipe Permanent Mold casting Process 120
4.6.1. Sample Calculation for a Transient Heat Flux 122
4.7. Estimation of the Local Cooling Rates from the SDAS Measurements 123
4.8. Comparison of a water cooling channel and a heat pipe 125
4.9. The Interfacial Heat Transfer Coefficient, h 130
4.9.1. Sensitivity Analysis for the Interfacial Heat Transfer Coefficient, h 132
4.10. The Importance of Thermocouple Location 134

CHAPTER 5 SUMMARY AND CONCLUSIONS 136
5.1. Design of Permanent Mold and Novel Heat Pipe for Nonferrous Casting Process.136
5.2. Analysis of Permanent Mold Castings of Magnesium and Aluminum Alloys.....139

STATEMENT OF ORIGINALITY 141
REFERENCES 144

LIST OF FIGURES

Figure 2.1. Casting/mold interface 13
Figure 2.2. Heat flow across casting/mold interface 14
Figure 2.3. Illustration of a traditional heat pipe 25
Figure 2.4. The different operating ranges for heat pipe working substances 27
Figure 2.5. Heat pipe cooling Notebook CPU (The Chemical Engineers Resource Page) 30
Figure 2.6. Primary limitations to the heat transport capability of a heat pipe [90] 33
Figure 2.7. Boiling curve for water at 1 atm [92] 36
Figure 2.8. Grains and dendrites of alloy AA 1050 under two different cooling rate (a) Cooled at a rate of 1.2 °C/s; (b) Cooled at a rate of 4.2 °C/s [101] 39
Figure 2.9. Tensile properties versus SDAS for the casting of aluminum alloy A356 [99] 40
Figure 3.1 Configuration of the designed heat pipe 43
Figure 3.2. Basic configuration of the designed heat pipe (solid model) 45
Figure 3.3. The various parts of the condenser section 46
Figure 3.4. The return line designed in the present work 48
Figure 3.5. The flow modifier used in the present work 49
Figure 3.6. The sleeve welded to a connection flange 50
Figure 3.7. Heat pipe extensions and connections 51
Figure 3.8. Return line with vent 52
Figure 3.9. The configuration of the mold developed in the present work 53
Figure 3.10. The engineering drawing of the designed mold 55
Figure 3.11. Design of the permanent mold (solid model) 56
Figure 3.12. The model used to simulate the casting process with heat pipes 57

Figure 3.13. The model used to simulate the casting and the H13 tool steel.....57
permanent mold
Figure 3.14. Temperature distribution results obtained from the model for.....59
a magnesium casting (a) mold without heat pipes (b&c) mold
with heat pipes
Figure 3.15. Temperature distribution results obtained from the model for.....60
an aluminum casting (a) mold without heat pipes (b&c) mold
with heat pipes
Figure 3.16. The effect of heat pipe cooling on the casting and mold temperatures.....62
(modeling)
Figure 3.17. A schematic of the test set-up.....64
Figure 3.18. The heat pipe laboratory test set-up 65
Figure 3.19. Results of a preliminary test 66
Figure 3.20. The heat pipe experimental setup 69
Figure 4.1. Mold and heat pipe industrial test set-up 72
Figure 4.2. Magnesium casting produced without heat pipe cooling (H2) 76
Figure 4.3. Magnesium casting produced with heat pipe cooling (H2) 76
Figure 4.4. Magnesium casting produced without heat pipe cooling (H1) 77
Figure 4.5. Magnesium casting produced with heat pipe cooling (H1) 77
Figure 4.6. The effect of freezing range on shrinkage [106] 78
Figure 4.7. Aluminum casting produced without heat pipe cooling (H2) 79
Figure 4.8. Aluminum casting produced with heat pipe cooling (H2) 79
Figure 4.9. The upper surface of A356 casting (H2) 81
Figure 4.10. Temperature distribution results obtained from the model for one A356 ...83
casting (with no heat pipe cooling)
Figure 4.11. Temperature distribution results obtained from the model for one A356....84
casting (with heat pipe cooling)
Figure 4.12. Temperature distribution results obtained from the model for AZ91E.....85
casting (with no heat pipe cooling)

Figure 4.13. Temperature distribution results obtained from the model for A356.....85
casting (with no heat pipe cooling)
Figure 4.14. Temperature distribution results obtained from the model for both.....86
sides of AZ91E casting (with heat pipe cooling)
Figure 4.15. Temperature distribution results obtained from the model for both.....87
sides of A356 casting (with heat pipe cooling)
Figure 4.16. Temperature distribution obtained from the model for a plane cut.....88
of AZ91E casting (with out heat pipe cooling)
Figure 4.17. Temperature distribution obtained from the model for a plane cut.....88
of A356 casting (with out heat pipe cooling)
Figure 4.18. Temperature distribution obtained from the model for a plane cut.....89
of AZ91E casting (with heat pipe cooling)
Figure 4.19. Temperature distribution obtained from the model for a plane cut.....89
of A356 casting (with heat pipe cooling)
Figure 4.20. Points selected for temperature measurements (H2) 90
Figure 4.21. A plan cut temperature distribution results obtained from the model.....93
for the whole mold (AZ91E casting with heat pipe cooling)
Figure 4.22. A plane cut temperature distribution results obtained from the model.....93
for the whole mold (A356 casting with heat pipe cooling)
Figure 4.23. Micro-shrinkage defect in AZ91E 94
Figure 4.24. Critical fraction solid time results obtained from the model.....95
for AZ91E casting (with no heat pipe cooling)
Figure 4.25. Critical fraction solid time results obtained from the model for.....95
A356 casting (with no heat pipe cooling)
Figure 4.26. Critical fraction solid time results obtained from the model for.....96
AZ91E two casting sides (with heat pipe cooling)
Figure 4.27. Critical fraction solid time results obtained from the model for.....97
A356 two casting sides (with heat pipe cooling)
Figure 4.28. The critical fraction solid time at a plane cut of AZ91E casting.....99

simulated with no heat pipe cooling
Figure 4.29. The critical fraction solid time at a plane cut of A356 casting.....99
simulated with no heat pipe cooling
Figure 4.30. The critical fraction solid time at a plane cut of AZ91E casting.....100
simulated with heat pipe cooling
Figure 4.31. The critical fraction solid time at a plane cut of A356 casting.....100
simulated with heat pipe cooling
Figure 4.32. SDAS measurement specimen 102
Figure 4.33. SDAS results for magnesium AZ91E (casting no. 46&47 H1) 103
Figure 4.34. SDAS results for magnesium AZ91E (casting no. 46&47 H2) 104
Figure 4.35. Microstructure (SDAS) obtained for point number 1.....105
(casting no. 52 H1, without heat pipe cooling)
Figure 4.36. Microstructure (SDAS) obtained for point number 1.....106
(casting no. 53 H1, with heat pipe cooling, reduction of 23%)
Figure 4.37. Grain size results for magnesium AZ91E (casting no. 68&69 H1) 108
Figure 4.38. Grain size results for magnesium AZ91E (casting no. 68&69 H2) 109
Figure 4.39. Microstructure obtained for point number 1 (casting no.68 H1).....110
(without heat pipe)
Figure 4.40. Microstructure obtained for point number 1 (casting no.69 H1).....110
(with heat pipe)
Figure 4.41. SDAS results for aluminum 356 (casting no. 81&83 H1) 113
Figure 4.42. SDAS results for aluminum 356 (casting no. 81&83 H2) 113
Figure 4.43. Microstructure of A356 (point 1, casting no. 81 H1).....114
(without heat pipe cooling)
Figure 4.44. Microstructure of A356 (point 1, casting no. 83 H1).....114
(with heat pipe cooling)
Figure 4.45. The setup used to view the macrostructure of A356 116
Figure 4.46. Grain size results for aluminum alloy, A356 (casting no. 81&83 H1) 117
Figure 4.47. Grain size results for aluminum alloy, A356 (casting no. 81&83 H2) 117

Figure 4.48. Macrostructure obtained for A356 (casting no. 74 H2).....119
(without heat pipe cooling)
Figure 4.49. Macrostructure obtained for A356 (casting no. 76 H2).....119
(with heat pipe cooling)
Figure 4.50. Temperature measurements obtained during.....122
magnesium casting process
Figure 4.51. Mold temperature measurements obtained form AZ91E casting..... 127
process with heat pipe cooling (industrial experiment)
Figure 4.52. Mold temperature measurements obtained form AZ91E casting.....128
process with heat pipe cooling (computer modeling)
Figure 4.53. Mold temperature measurements obtained form AZ91E casting.....128
process with water channel cooling (computer modeling)
Figure 4.54. The locations of the three thermocouples used in the measurements 129
Figure 4.55. Temperature distribution results obtained from the model for.....133
A356 casting (with no heat pipe cooling)
Figure 4.56. Simulation of temperature measurement for thermocouples.....135
located in permanent mold during casting of AZ91E magnesium alloy

LIST OF TABLES

Table 3.1. The results of two tests conducted to evaluate the heat pipe 64

Table 4.1 Details of selected castings used for analysis 74

Table 4.2. Temperature distribution results obtained from the 91
model (H2, 100% solid)

Table 4.3. The critical fraction solid time for AZ91E and A356 (H2) 101

Table 4.4. SDAS results obtained for magnesium castings 107

Table 4.5. Grain size results obtained for magnesium castings 111

Table 4.6. SDAS results obtained for aluminum castings 115

Table 4.7. Grain size results obtained for aluminum A356 castings 120

Table 4.8. Estimated heat fluxes for both heat pips 121

Table 4.9. Estimated cooling rates for magnesium AZ91E castings 124

Table 4.10. Estimated cooling rates for aluminum A356 castings 124

NOMENCLATURE

Symbol	Meaning	Units
h	interfacial heat transfer coefficient	W/m^2-K
t_f	freezing time	s
Mc	modulus coefficient	
S_A	surface area of casting	m^2
Vc	volume of casting	m^3
V_R	volume ratio ($V_{mold}/V_{casting}$)	
q	interfacial heat flux	kW/m^2
A	area across which heat flow occurs	m^2
T	temperature	K
Tc	casting surface temperature	K
Tm	mold surface temperature	K
k	thermal conductivity	W/m-K
t	time	s
Cp	specific heat	J/kg-K
q_R	radiative heat flow	W
A	surface area	m^2
F	view factor for the radiating surface	
$\overline{Nu}_D$	average Nusselt number based on the pipe diameter	
Re_D	Reynolds number of the fluid	
Pr	Prandtl number of the fluid	
v	average velocity of the water flow	m/s
D	internal diameter of the passage	m
Pr	Prandtl number of fluid	

$\dot{m}$	mass flow rate	kg/s

Greek Characters

ρ	Density	kg/ m^3
σ	Stefan-Boltzmann constant, 5.67 x 10^{-8}	W m^{-2} K^{-4}
α	thermal diffusivity	m^2/s
λ	measured SDAS	μm
τ	estimated local cooling rate	$^oC/s$
μ	viscosity	Ns/m^2
ε	emissivity of the radiating surface	

Subscripts

P	point
SDAS	secondary dendrite arm spacing
HP	heat pipe
H1	casting poured into the mold cavity close to heat pipe number 1
H2	casting poured into the mold cavity close to heat pipe number 2

CHAPTER 1 INTRODUCTION

Casting is the most economical industrial process used to transform liquid metals into near net shape components. Permanent mold (PM) casting is a productive and cost-effective method for making a wide range of complex shapes for both nonferrous and ferrous castings. The castings range from small, thin-walled castings to large castings. Mechanical properties such as strength, toughness, ductility, fatigue strength, and stress corrosion resistance can be improved by using grain-refining techniques [1-4]*.

During the last 2 decades, rapid solidification technology has been developed in combination with powder metallurgy technology [5-8] to obtain bulk alloys with finer microstructures.

The thermal conditions during the solidification of a casting influence its properties significantly [1]. A faster rate of solidification can result in finer grain size or smaller dendrite arm spacing with resultant improvement in mechanical properties. Hence a large tonnage of nonferrous alloy castings are produced in permanent metallic molds.

* Numbers in square brackets [ ] refer to references.

In the competitive world of today, it is necessary for the foundryman to use Computer Aided Design (CAD) to produce castings with intricate shapes and to increase profitability. CAD of a casting requires the ability to predict the temperature field in the solidifying casting. While the velocity field and stress field in the casting are important, the effect of the thermal field on the properties is more significant.

The study of heat extraction from a solidifying casting by a metal mold has been a subject of investigation for many researchers [3,9-11]. Both experimental and theoretical methods were used to study this problem.

An important feature of the solidification of a casting in a metal mold is the existence of a thermal resistance at the casting/mold interface. The thermal resistance is usually characterized by the 'interfacial heat transfer coefficient', h. The value of h is influenced by a number of factors like metallostatic pressure, mold surface conditions, mold coatings, presence of oxide layers on casting surface, casting geometry, cooling method [12-14], etc. For Computer Aided Design of castings, knowledge of the value of h is necessary for the calculation of the temperature field in the solidifying casting.

The optimum mold temperature is the temperature that will produce a sound casting in the shortest time. Mold temperature control is largely achieved through the use of auxiliary cooling or heating and through the control of mold coating thickness and/or properties.

There is variety of permanent mold cooling methods available. The most commonly used are air or water-cooled systems and combinations thereof. With each method of cooling, there are definite advantages and disadvantages, which should be evaluated.

An alternative cooling method for the permanent mold casting process involves the use of heat pipes. This technique is the focus of a research group at McGill University, and the current work is a part of an overall effort in this area.

A heat pipe is a heat transfer device that utilizes the vaporization and condensation of a working substance contained within to move energy from the evaporator section to the condenser section. A heat pipe can be as effective in transporting energy as 1,000 times the equivalent quantity of copper under similar heat transfer conditions. This places heat pipe cooling ahead of some of the other cooling processes.

1.1. SCOPE OF THE PRESENT WORK

With the increasing growth of magnesium and aluminum permanent mold castings, more research has to be directed to develop the production process. Cooling is the key technique in producing sound castings, which can fulfill the high industrial standard required in industries such as aerospace and automotive. In addition, cooling techniques can assist in maximizing productivity. The aim of this work is to design, model and construct a permanent mold and heat pipes for the magnesium and aluminum casting processes. The mold is designed to produce shrinkage defects and the heat pipes are designed to demonstrate that it is possible to force the shrinkage away from desired locations and hence, improve the casting quality. In general, the objectives can be stated as the following:

1) Design and model a permanent mold that will produce shrinkage defects in the casting of light metals.
2) Develop a novel, water-based, heat pipe of improved design and high efficiency.
3) Perform experiments and analysis of permanent mold cooling for magnesium and aluminum castings.

4) Conduct analysis of the microstructures of magnesium and aluminum castings to evaluate the cooling effect using heat pipes. The analysis includes an evaluation of the shrinkage distribution in the castings, an evaluation of the secondary dendrite arm spacing (SDAS), and an evaluation of the grain sizes.
5) Investigate the metallurgical differences and the solidification behavior of magnesium AZ91E and aluminum A356.

CHAPTER 2 LITERATURE SURVEY

2.1 Introduction

The thermal conditions during the freezing of a casting influence the casting soundness significantly [15]. The thermal conditions are influenced by the rate of heat extraction from the casting by the mold and the latter depends on the type of mold material. In the case of insulating sand molds, the rate of heat extraction is controlled by the thermal resistance of the mold material. In the case of metallic molds, it is now well established that the heat flow rate from the casting to the mold is controlled by the thermal resistance at the casting/mold interface [11]. This thermal resistance arises due to imperfect contact between the casting and the mold, and in some cases an air gap may form between the casting and the mold in the later stages of solidification. The presence of mold coatings on the mold surface and oxide films on the casting surface also influence the thermal resistance of the casting/mold interface.

The presence of an air gap increases the freezing time of the casting. The rate of heat extraction from the casting by the mold can be related to the freezing time, t_f of the

casting. Since casting soundness is related to the rate of heat extraction, early investigators developed relations between casting soundness and freezing time [10].

In terms of casting quality, mold temperature control is important to ensure that desirable thermal gradients in the mold are established, and thus regulate the casting solidification. In terms of mold life, hot or cold spots in the mold must be controlled. Uniform cooling will eliminate localized areas that may be subjected to thermal shock or liquid metal erosion.

One of the key techniques for producing sound permanent mold castings is to use controlled mold cooling such as air cooling, water cooling and heat pipe cooling. Air-cooling has limited applications in permanent mold casting due to its low cooling capability and high cost. Water-cooling is widely used in permanent mold casting, but has some disadvantages such as safety issues and the facilities required. The early applications of heat pipes in a permanent mold casting have shown tremendous results due to their high cooling rates, low cost and safety [16].

In this chapter, an overview on casting parameters, mold design and cooling is presented. Heat pipe development, applications and problems are also presented.

2.2. Air Gap Formation

The studies carried out on solidification of castings in metal molds show that an air gap forms in the initial stages of solidification and the size of the air gap increases with time [12]. The formation of an air gap at the casting/mold interface is important in the case of large castings like steel ingots and many early investigators studied the time, location and other factors relating to the air gap formation at the casting/mold interface [12-15, 17-19].

Matuschka [20] concluded that due to the expansion of the mold when it absorbs heat and contraction of the casting due to cooling, an air gap forms along the casting/mold interface in the case of steel ingots. Henzel and Keverian [12] concluded that the time and the magnitude of air gap formation are determined by casting size, mold wall thickness, mold surface roughness, mold wall temperature, superheat, rate of pouring and the coefficient of expansion, density, thermal conductivity, and specific heat of mold and casting materials. Paschkis [21] explained that as a result of air gap formation, the casting skin may be reheated, and this can cause the metal to break through the skin resulting in fresh metal freezing against the mold wall and thereby leading to a cyclic process referred to as "breathing" [21]. The methods for the determination of the time for air gap formation, and width of air gap are discussed below. Factors affecting the time for air gap formation are also presented.

2.2.1. Time for Air Gap Initiation

Some of the methods developed by various investigators to determine the time of initiation of air gap at the casting/mold interface are given below:

a. Temperature measurements

Rapid temperature changes occur at the casting and mold surfaces at the time of air gap formation [12]. By monitoring the interface temperatures, the time of air gap formation can be determined [22,23]. Bishop et al [22] concluded that the air gap formation between the casting and its metal mold is associated with a sharp change in the surface temperature of the permanent mold. Their experiments were carried out using steel solidifying in metallic molds of different alloys. Thermocouples of sheathed type having a small mass were used to measure the surface temperature. Some investigators [15,16] concluded that temperature measurement is not a reliable method for determining

the time of air gap formation, especially in the case of thin molds with insulating mold coats, because sharp changes in temperature are not always noticed in this case.

b. Heat flow Method

From the temperature measurements in the casting and the mold, the heat flow across the casting/mold interface can be determined. Mackenzie and Donald [24] concluded that the heat transfer rate increases rapidly from a low value to reach a maximum value and then decreases subsequently. The air gap formation starts at the time of occurrence of the maximum value of the heat transfer rate. Henzel and Keverian [12] used the data of Bishop et al [25] to calculate the rate of heat transfer and arrived at similar results. Very often, instead of a well defined peak, wide fluctuations are observed in the heat transfer rate in the initial stages of solidification [26].

c. Electrical probe Method

In some early investigations, the air gap formation was studied by inserting electrical probes in the casting and the mold, and connecting them to an electrical circuit with an electric light and a battery in series. At the time of air gap formation, the electrical contact is broken and this causes the light to be switched off, thus indicating the onset of air gap formation.

2.3. Freezing Time of Castings Solidifying in Metallic Molds

When liquid metal is poured in a metallic mold, solidification begins near the mold wall and progresses towards the center. The freezing time of the casting, t_f is the time at which the last point to solidify in the casting reaches the solidus temperature. When an air gap forms at the casting/mold interface, the heat extraction rate will decrease because of the insulating nature of the gases present in the air gap. This will increase the

freezing time of the casting. The factors affecting t_f and the relation between t_f and casting parameters are discussed below.

2.3.1. Factors Affecting Freezing Time, t_f

Many experiments were performed by a number of investigators [13,14,27-34] to study the factors affecting the freezing time. They found that the freezing time depends on the thermal properties of the mold and the casting, conditions at the casting/mold interface and also application of pressure on the liquid metal during solidification. The factors affecting t_f are mold material, volume ratio, modulus coefficient, mold preheat, mold surface roughness, mold coatings, type of alloy, pouring temperature, casting geometry, and pressure. These factors are discussed below.

Mold material

The freezing time, t_f of a casting depends on the thermal conductivity of the mold material - higher conductivity gives lower t_f due to the faster heat extraction. Srinivasan et al [13] found that t_f is lower in copper molds when compared to cast iron molds or anodized aluminum molds and this was attributed to the higher conductivity of copper.

Volume ratio and modules coefficient

Volume ratio, V_R (i.e. the ratio of mold volume to casting volume) affects freezing time, t_f, when V_R is below 5.0 [13]. Similar results were obtained by Nehru and Seshadri [15] using gunmetal castings. It was found that t_f is proportional to the modulus coefficient, Mc [15, 17-19,27-37] i.e.

$$Mc = (Vc/S_A)^{1.5} (V_R)^{-0.5} \quad .....(2.1)$$

Where

S_A = surface area of casting

Vc = volume of casting

V_R = volume ratio ($V_{mold}/V_{casting}$)

Mold Preheat

Ayyamperumal [36] found that t_f increases with increase in mold preheat temperature in the case of aluminum alloy castings. In the case of cast iron solidifying in a cast iron mold, t_f is found to increases marginally with increase in mold preheat [18].

Mold surface roughness

According to Morales et al [38] increase in mold surface roughness results in an increase in t_f. Similar results were reported by Sharma and Mythily [26].

Mold coatings

Mold coatings may increase or decrease t_f depending on the conductivity of the coating material [18,26]. Nehru and Seshadri [15] observed that in the case of silica based mold coats, there is an optimum coating thickness at which t_f is maximum.

Type of alloy

Srinivasan et al [13] found that aluminum - 12% silicon alloy has a higher freezing time, t_f, compared to pure aluminum and long freezing range alloys like aluminum - 4.5% Copper and aluminum - 10% magnesium for similar casting conditions.

Pouring temperature

The freezing time, t_f increases with an increase in pouring temperature [39,40].

Casting geometry

Geometry of the casting affects the freezing time t_f, and Mohan and Shenoy [18] found that in the case of cast iron solidifying in a metal mold, at a constant mold wall thickness, the following relationship is observed:

$$t_f \text{ (cylinder)} < t_f \text{ (square)} < t_f \text{ (plate)}$$

Pressure

Applying a pressure on the molten metal can decrease the freezing time. Application of pressure results in a better contact between the casting and the mold, and hence the heat extraction will be higher [41,42].

2.4 The Interfacial Heat Transfer Coefficient

In the solidification of a casting in a metal mold, the heat flow from the casting to the mold is controlled by the casting/mold interface as mentioned earlier and this is primarily due to the imperfect contact between the casting and the mold. If the contact were perfect, (this may happen in the case of an ideally smooth mold surface) the casting and mold surfaces would attain a common temperature at the interface as shown in figure 2.1(a). If the contact is imperfect (as in the case of real mold surface with some surface imperfection or roughness) with a non-wetting liquid metal, the temperature on the casting and mold surfaces would vary from point to point and the mean values for the

mold and casting surface temperatures would not be the same. It is customary to represent this situation by an air gap of finite width as shown in figure 2.1(b).
The heat flow across the casting/mold interface with imperfect contact can be determined using the expression:

$$q = h A (Tc - Tm) \quad .....(2.2)$$

where

q = rate of heat flow across the interface
A = area across which heat flow occurs
h = interfacial heat transfer coefficient
Tc = temperature of the casting surface
Tm = temperature of the mold surface

and the situation is shown in figure 2.2.

The value of h can be calculated if all the other terms in equation (2.2) are known. h characterizes the thermal behavior of the interface completely [26]. If it is assumed that the heat flow across the interface is by conduction through the gas layer of thickness y in the interface, then the heat flow rate is given by the relation [43]

$$q = (k/y) A (Tc- Tm) \quad .....(2.3)$$

where

k = thermal conductivity of the gas film in the interface.
y = thickness of the gas film.

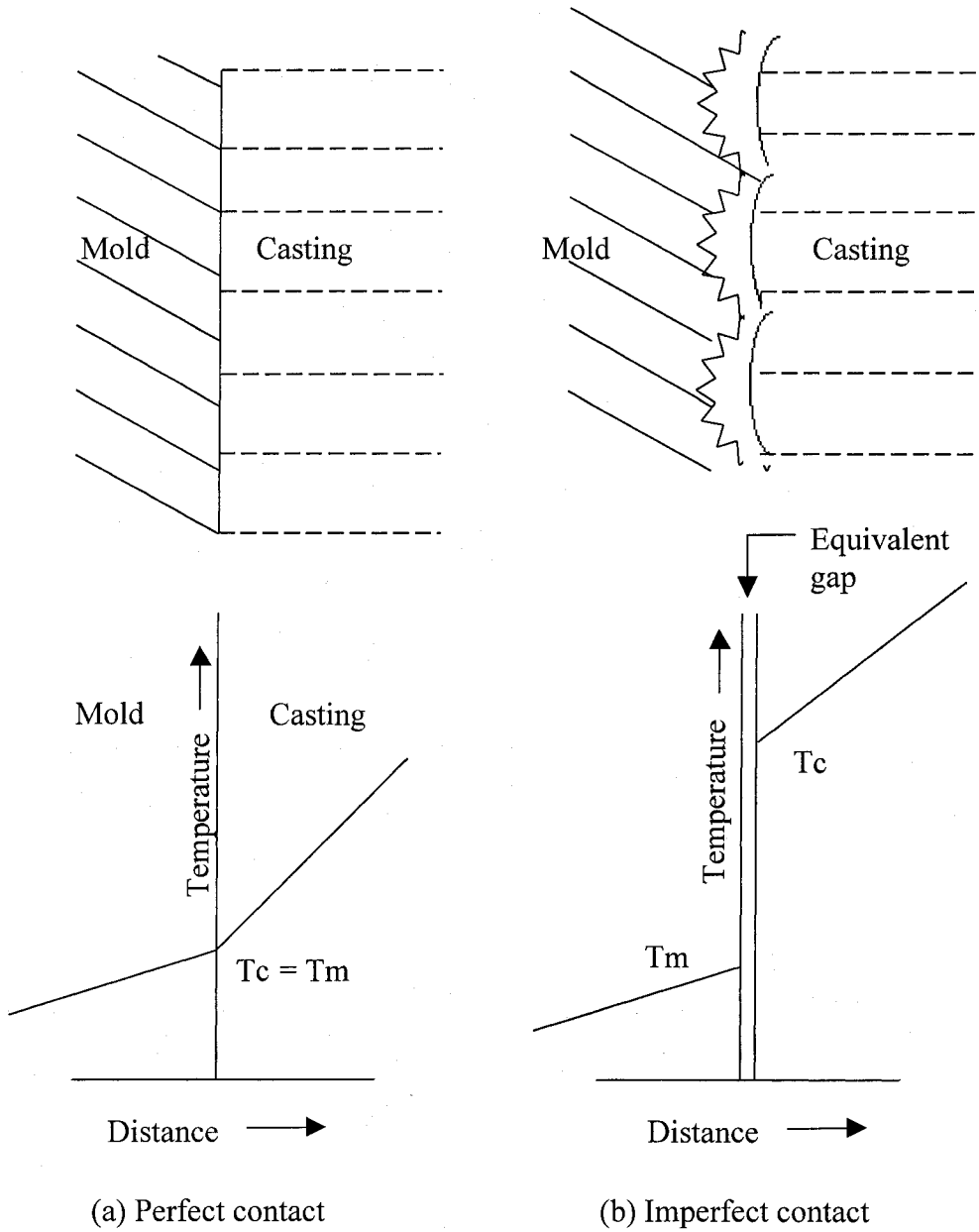

Figure 2.1. Casting/mold interface

From equations (2.2) and (2.3) we can obtain the relation:

$$h = k / y \quad .....(2.4)$$

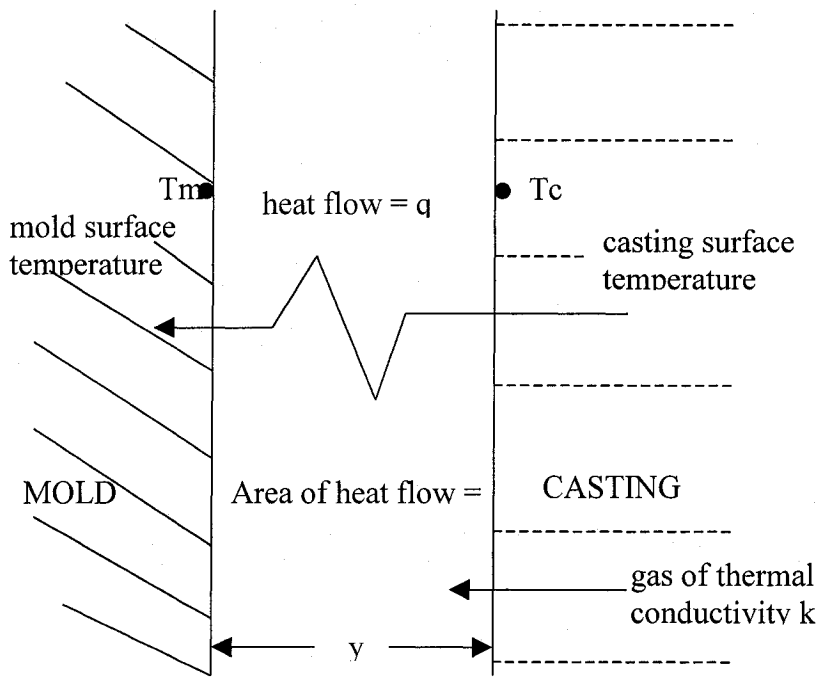

Figure 2.2. Heat flow across casting/mold interface

In the case of alloys, which solidify at low temperatures, heat transfer by radiation between the mold and the casting surfaces at the interface is very low when compared to that by conduction through the gas film, and convection in the gas film and hence these may be neglected [15]. The heat storage in the gap can also be neglected [44]. Hence h can be given by equation (2.4). The introduction of thermocouples of finite mass at the interface can cause distortion in the temperature field and hence Tc and Tm cannot be measured directly. Also, the region close to the interface may not have a heat flow pattern predicted by theory due to the non-uniform surface conditions. Hence using equation (2.2) to determine h by measurement of Tc, Tm and q is difficult [9], and indirect methods should be used.

Determination of h at the casting/mold interface requires the solution of the Inverse Heat Conduction problem (IHCP), which refers to the determination of the boundary condition using the measured values of temperatures at some internal locations in the casting and/or mold. Some theoretical and empirical models have also been developed to determine the value of h [26,44-46].

Many investigators have reported different methods to determine the value of h. Sully [47], in his work, obtained the value of h between the casting and the mold for three different shapes of castings by measuring the temperatures at appropriate locations in the casting and the mold. The first case of a casting solidifying around a water cooled copper or steel pipe was analyzed by a simple analytical procedure. In the second case, the implicit finite difference method was used to find the value of h in case of steel solidifying against a horizontal chill. The variation of h as a function of time could be obtained over the entire duration of solidification. In the third case, a permanent mold plate casting solidification problem was studied by FDM. Using the known values of temperatures, the transient heat transfer coefficient could be obtained.

Sun [48] found the value of h between cylindrical slugs used as cores with the molten metal solidifying around them. Slugs of cast iron, graphite, copper and molybdenum were used with insulating end covers to ensure radial heat flow. Different surface coatings were given to the slugs and then immersed into molten aluminum. The temperature rise of the slugs was noted and from these temperature values, the value of h was determined by appropriate calculations based on explicit FDM. Variation in the properties of the slug with temperature was incorporated in the computations. From here it is found that h increases linearly with time, i.e.

$$h = a_0 + b\,t \quad \text{.....(2.5)}$$

The increase in h is explained in terms of increased contact pressure due to expansion of the slug, contraction of the solidified metal and increase in the thermal conductivity of the coating layer at the elevated temperature.

Nishida and Matsubara [49] used a cylindrical casting solidifying in a metallic die under pressure. Assuming a radial heat flow in their calculations, they found the interfacial heat transfer coefficient by an iterative procedure by matching the temperature at a point closest to the interface in the mold. The differences between calculated and measured values of temperature at other points in the set up were attributed to axial heat flow.

2.5 Latent Heat Liberation

Consideration of latent heat liberation is very important for the calculations of thermal profiles during casting solidification. The thermal profile in a conducting body is obtained by solving the heat conduction equation.

$$\alpha\, \partial^2 T/\partial x^2 = (\partial T/\partial t) \quad .....(2.6)$$

where

α = thermal diffusivity (m^2/s)

T = temperature (^oC)

t = time (s)

Equation (2.6) is for 1-D heat flow and is non-linear due to the liberation of the latent heat and temperature dependant properties. There are many numerical methods for solving the above equation taking the liberation of latent heat into account. Simulation of solidification of congruent melting materials does not pose any serious problem and some of the methods available for solution are mentioned below. However, solidification of an alloy with freezing over a temperature range is difficult to model due to the uncertainty in the value of properties in the solidification range.

Usually, the above equation is solved by numerical methods like FDM or FEM to account for the complicated geometry of real castings and the associated boundary conditions, which are difficult to solve analytically. The variation of properties with

temperature can also be accounted for by suitable algorithms incorporated in the numerical solution procedure.
The liberation of latent heat, on the other hand is usually solved by employing one of the few standard methods available [50-53].

2.6. Mold Design

In early days, the art of mold design was based on design practice and a long experience of failures and successes. Now the development of efficient computer aided design packages and high-speed computers is transforming this art of mold design into a complete science. There are numerous advantages from computer-aided analysis and design, which help to:

-Select the optimum location of cooling channels.
-Produce defect-free castings.
-Design the mold before the drawings are finalized.
-Increase productivity.
-Reduce casting design time.
-Provide the production rate in advance, which help in the machine planning and scheduling.
-Eliminate the time wasted in modifying the mold when the production is not up to standard.

These advantages can be transformed into tremendous savings to the manufacturer because of the reduction in the overall cost of the part. The time saved from part design to actual production can sometimes mean the success of the project.

Computer software for the mold design has to account for the heat transfer from the hot casting into the mold and, further, from the mold into the coolant, which flows

under pressure in the cooling lines. The faster the heat is removed from the casting, the sooner the mold can be opened to eject the part and, therefore, make it available for the next shot of molten metal. The duration of the cycle is consequently dependent upon the efficiency of the cooling system.

Usually, the location and sizing of the cooling lines in the mold are based on the experience of the designer since designing a permanent mold with optimum production capabilities is not an easy task. The designer sometimes is unaware of the relative advantages of different sizes and locations of the cooling lines. If a computer program is available to the designer for optimizing these cooling line parameters, experience and analysis can then go side by side in increasing the productivity and the quality of the part.

2.7. Heat Transfer in Molds

Understanding heat transfer principles is a key issue in designing permanent molds since the design includes controlling the mold temperature by using mold cooling methods. There are three heat transfer modes in a permanent mold casting process. A brief description of these heat transfer modes is given in the following sections.

2.7.1. Conduction

One mode of heat transfer is the process of molecular transport of heat in a body or between bodies due to temperature variation in the domain considered. The conduction can be steady state, where the temperature of a body remains constant in time, or it can be in the transient state, in which case the temperature in the domain not only varies from point to point but also with time. Transient conduction takes place in plastic- and glass-parts manufacturing, rubber vulcanizing, and metal casting.

For unidirectional conduction of heat, Fourier [54] derived the law

$$dq/dt = kA\ (-\ dT\ /dx).....(2.7)$$

where dq/dt is the instantaneous rate of heat flow, k is the thermal conductivity of the material , A is the section area and –dT/dx is the temperature gradient. For a steady-state case, dq/dt is independent of time and is normally referred to as q. Equation (2.7) can then be written as

$$q^{\cdot} = -kA\ \partial T/\partial x.....(2.8)$$

The rate of heat flow by conduction is directly proportional to the thermal conductivity of the material. Use of a mold material with higher thermal conductivity does not necessarily mean the casting will cool faster since the cooling of the casting is also a function of its own thermal properties. Thermal diffusivity, the property of a material, which determines the rate at which it will gain or lose heat, is the limiting factor in determining the cooling time of a part. Thermal diffusivity, α, is given by the relation

$$\alpha = k/\rho Cp.....(2.9)$$

where ρ is the density, Cp is the specific heat, and k is the thermal conductivity of the material. From this it follows that the larger the value of α, the higher will be the rate of change of temperature at any point in the body.

2.7.2. Convection

Another mode of heat transfer in molds is heat transport occurring through movement of the macro-particles of the coolant flowing in the cooling lines. There is a combined action of convection and conduction taking place in the fluid. The convection between the coolant and the surrounding mold will be referred to here as heat transfer by convection.

The calculation of convective heat transfer is based on Newton's law

$$q^{\cdot} = h(Tm-Tc)A.....(2.10)$$

where $q^{\cdot}$ is the heat flow rate, h is the convective heat transfer coefficient, Tm is the temperature of the mold, Tc is the temperature of the coolant, and A is the area over which the convective heat transfer takes place.

The heat transfer coefficient, h, is a variable dependent upon the physical properties, velocity, and temperature of the fluid, shape and size of the surface, and the nature of fluid flow. There are two kinds of convective heat transfer: free or natural, and forced.

Natural convection is created by motions due to heterogeneity of the mass forces acting upon the fluid, whereas forced convection takes place due to motion from external kinetic energy, as from pumps or fans. Natural convection takes place on the external surface of the mold where the surface is cooled by the ambient air. On the other hand, the flow of coolant in the cooling lines provides the forced-convection cooling of the mold.

2.7.3. Radiation

The phenomena of conduction and convection, as seen earlier, are affected primarily by temperature difference and very little by temperature level. In radiation the heat transfer increases rapidly with increase in temperature level. It is immediately obvious that for low temperatures, conduction and convection are dominant; for high temperatures radiation is the controlling factor. In the case of plastics, radiation from the external surface of the mold to the atmosphere is not significant because the temperature of the mold surface is not very high.

The rate of heat transfer from a surface to the ambient by radiation is described by the following equation:

$$q^{\cdot}_R = \sigma A F \varepsilon (T_1^4 - T_2^4).....(2.11)$$

where q_R is the radiative heat flow (W), σ is the Stefan-Boltzmann constant (5.67×10^{-8} W $m^{-2} K^{-4}$), A is the surface area (m^2), T_1 is the temperature of the surface (K), T_2 is the temperature of the surrounding medium (K), F is the view factor for the radiating surface (unitless), and ε is the emissivity of the radiating surface (unitless).

2.8. Mold Cooling General Approach

Temperature control in permanent mold castings is an important factor in mold design. The cooling system should regulate heat flow, ensure production of sound castings, and prolong mold life.

Careful technical and economic analysis should be performed before choosing the suitable cooling system design. In selecting the most cost-effective system, the total number of castings to be made must be considered as a major economic factor. Several technical factors must be taken into account such as the weight, modulus and section thickness of the casting, its production cycle times and quality, and mold life. In addition to that, the cooling method chosen should be reliable and easy to be conducted.

The removal of heat during the solidification process is the very important issue in order to produce sound castings and to lengthen the mold life [55]. A great percentage of the molds used in industry are water-cooled. However, difficulties are sometimes experienced in taking water-cooling channels to inaccessible parts of the die. In such cases, inserts made of more highly conducting material such as molybdenum are used to conduct the heat away to more remote water-cooling channels. Furthermore, it is often inconvenient to take water-cooling to movable or removable parts such as sprues and cores.

Mold cooling is an important aspect to minimize thermal shock, thus lengthening the mold life [56]. In the case of using water cooling, with quite large temperature differences between the molten material and the cooling water, which must be tolerated by the intervening mold, the life of the die can be shortened. The solution in this case is using a means of rapidly abstracting heat from the mold working surfaces at a temperature more nearly approaching that of the molten metal.
Generally in casting processes using metallic molds, it is necessary to heat parts of the mold to ensure continuous flow of the molten material to the more inaccessible regions remote to the pouring point. To obtain the subsequent rapid solidification, cooling is required in a minimum amount of time to keep cycle times as short as possible.

In summery, the purpose of using cooling in permanent molds is to reduce the production time cycle, control of mold temperature, lengthen mold life, and improve casting quality

2.8.1. Control of Mold Temperature

Optimum mold temperature is the temperature that will produce a sound casting in the shortest time. For an established process cycle, temperature control is largely achieved through the use of auxiliary cooling or heating and through control of coating thickness.

Auxiliary Cooling is often achieved by forcing air or water through passages in mold sections adjacent to the heavy sections of the casting. Water is more effective but over a period of time scale can coat the passages, thus necessitating frequent adjustments in water flow rates. Without cleaning, the flow of water eventually stops. Water passages should be checked and cleaned each time the mold is put into use [57].

The problem of scale formation has been solved in some plants by the use of re-circulating systems containing either de-mineralized water or another fluid such as ethylene glycol. However, such systems are rarely used. Water flow is regulated manually or automatically to each mold section with the aid of flow meters. A main shutoff valve is used to stop the water flow when the casting process is interrupted. Adjusting the rate of water flow to control the solidification rate of a heavy section permits some leeway in the variation of wall thickness that can be designed into a single casting. In addition to the control of water flow, the temperature of the inlet water (or any other coolant that might be used) affects the performance of the mold cooling system.

If water or another liquid coolant is used, it must never be allowed to contact the metal being poured, or a steam explosion will result. The intensity of a steam explosion increases as metal temperature increases. In addition, water will react chemically with molten metal (e.g. in the case of magnesium casting).

Mold coating of controlling thickness can equalize solidification rates between thin and heavy sections. Chills and anti-chills can be used to adjust solidification rates further, so that freezing proceeds rapidly from thin to intermediate sections and then into heavy sections, and finally into the feeding system. Coatings applied to the mold's inner surface improve casting quality by providing appropriate thermal resistance at the metal/mold interface, as well as by promoting directional solidification [58-60].

Chills are used to accelerate solidification in a segment of a mold [61]. This can be done by directing cooling air jets against a chill inserted in the mold or, more simply, by using a metal insert without auxiliary cooling. Chilling can also be achieved by removing some or the entire mold coating in a specific area to increase thermal conductivity. Chills can be used to increase production rate, improve metal soundness, and increase mechanical properties.

2.9. Heat Pipe Technology

A new alternative for cooling a permanent mold is to incorporate heat pipe cooling elements in the mold at the desired locations.

2.9.1. Heat Pipe Concept

A heat pipe is a heat transfer device that utilizes the vaporization and condensation of a working substance contained within to move energy from the evaporator section to the condenser section. A heat pipe can be as effective in transporting energy as 1,000 times the equivalent quantity of copper under similar heat transfer conditions. As a working substance, many fluids can be used, depending on the temperature range of the application. Some common fluids are water, ammonia, freon, or acetone. The tube has a wick, which transports the fluid in the liquid state from the condenser end towards the evaporator end where the liquid evaporates, due to the heat, and changes into a gaseous state. It travels back to the condenser end to repeat the cycle and thus continuously transports heat from one end to the other. At the condenser end the heat is transferred to the coolant flowing in the cooling lines and the gas condenses back to the liquid state [62]. Figure 2.3 shows an illustration of a traditional heat pipe.

Heat pipes have no moving parts. However, care must be taken when designing and manufacturing the heat pipe. Heat is absorbed in the evaporator section and liquid is converted to the vapor state. Heat is dissipated from the upper part of the heat pipe to the environment as vapor condenses to the liquid phase. Liquid returns by gravity to the lower part of the heat pipe (evaporator section).

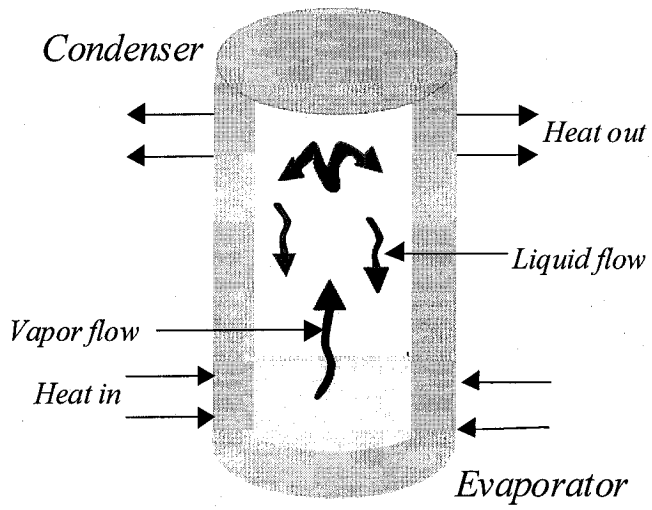

Figure 2.3. Illustration of a traditional heat pipe.

2.9.2. Development of Heat Pipe Technology

Developing a procedure to transfer heat from one point to another was the focus of research of many investigators. The principles of a heat pipe design were set by Gaugler in the year 1944 [63]. No significant work in the field of heat pipes appeared until late 1963 when Grover and his co-workers of the Los Alamos Scientific Laboratory gave their description of the current heat pipe device [64]. Grover wrote the following: "Heat transfer via capillary movement of fluids. The "pumping" action of surface tension forces may be sufficient to move liquids from a cold temperature zone to a high temperature zone (with subsequent return in vapor form using as the driving force, the difference in vapor pressure at the two temperatures) to be of interest in transferring heat from the hot to the cold zone. Such a closed system, requiring no external pumps, may be of particular interest in space reactors in moving heat from the reactor core to a radiating system. In the absence of gravity, the forces must only be such as to overcome the capillary and the drag of the returning vapor through its channels."

In 1964 Grover published his heat pipe experimental results [65]. The working substances were water and potassium.

In the subsequent years, many researchers have noted the potential of heat pipes in different applications and the possibility of bringing the heat transfer device development to a new unexpected level. A significant amount of research has been directed to heat pipe research since then [66-68].

The working substance of a heat pipe can vary from polar molecules such as water to liquid metals such as alkali metals. The working substance is selected depending on the environment temperature the heat pipe is intended to work in. In general the working substances are classified into "Cryogenic" (0-150 K), "low temperature" (150-750 K), and "high temperature" (750-3000 K). In the cryogenic range, elemental or simple gases are used. For low temperature range, polar molecules such as water or other hydrocarbons are used. In the high temperature range, liquid metals such as alkali metals are used. Figure 2.4 shows the different operating ranges for heat pipe working substances.

Remarkable applications for heat pipes in metallurgy have been reported by Mucciardi et al. from McGill University [69-78]. Mucciardi developed and succeeded in incorporating the high temperature heat pipe technology into lance making technology used in steel making applications. Sodium based heat pipe cooled lances have been developed in cooperation with several industrial partners.

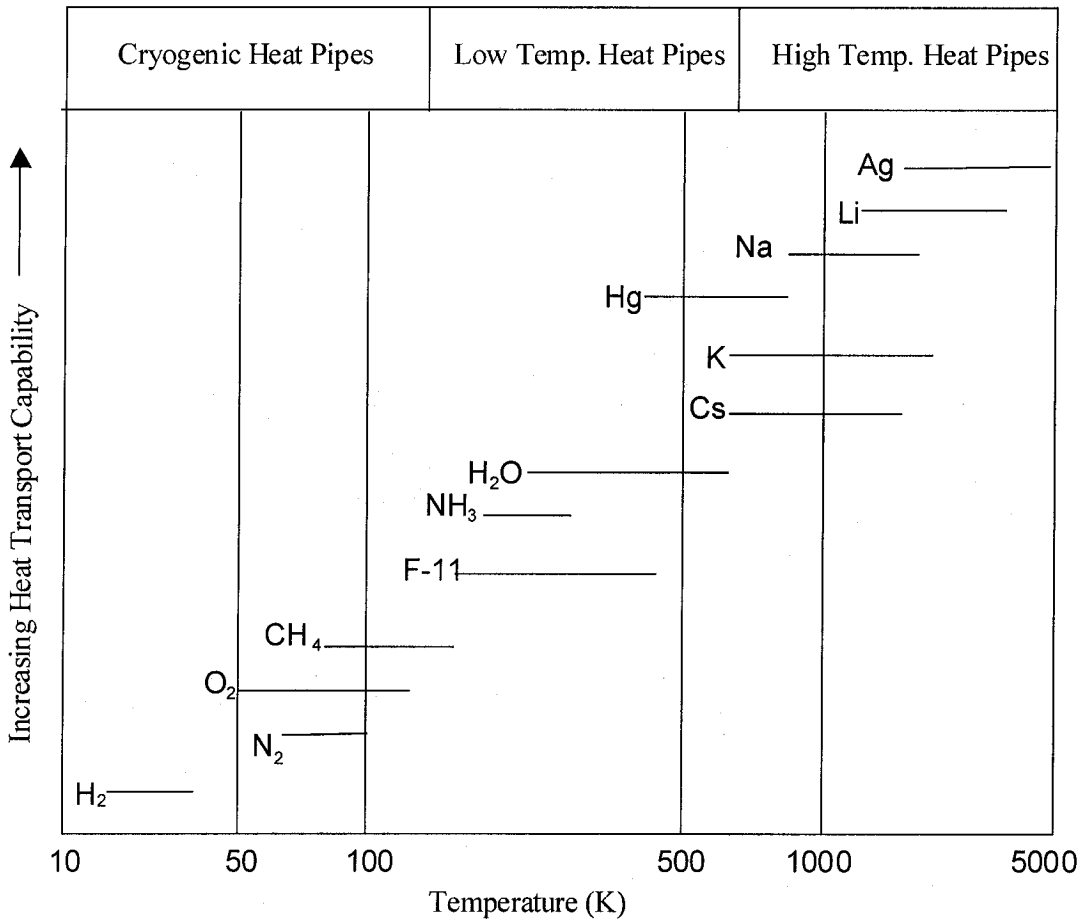

Figure 2.4. The different operating ranges for heat pipe working substances [91]

Heat pipe technology developed at McGill University has been applied into various metallurgical applications such as RH degassing and twin roll casting [70-72]. The field of thermal analysis was part of McGill's heat pipe application where Mahfoud, Gruzleski, and Mucciardi developed a unique method for conducting thermal analysis of aluminum based melts [74,75].

2.9.3. Applications of the Heat Pipe

Heat pipes are studied for a wide variety of applications, covering almost the complete spectrum of temperatures encountered in heat transfer processes. In general, the applications of heat pipes cover many areas in engineering such as heat flux transformation, temperature control, temperature flattening, separation of heat source and sink, and thermal diodes and switches. Each application used a natural property of the heat pipe.

The property of heat flux transformation has attractions in reactor technology and in other technologies such as casting. In thermionics, for example, a comparatively low heat flux as generated by radioactive isotopes can be transformed into sufficiently high heat fluxes capable of being utilized effectively in thermionic generators [79]. Heat pipes are used to control accurately the temperature of devices mounted on the heat pipe evaporator section. Its applications are successfully used in temperature control of many different devices varying from electronics equipment to ovens and furnaces, and many other devices.

Temperature flattening is closely related to source – sink separation. Since the heat pipe is an isothermal device, it is used to reduce thermal gradients between unevenly heated areas of a body. Such applications are applied into spaceships or satellites. For example, the side of the satellite which is facing the sun is hot, the cooler section being in the shade. Hence, the heat pipe will distribute the heat evenly through the satellite body. Alternatively, an electronic device connected to single pipe would tend to be subjected to feedback from the heat pipe, creating temperature equalization. The high effective thermal conductivity of a heat pipe enables heat to be transferred at high efficiency over considerable distances. One other advantage of a heat pipe is that it can be used to remove heat from certain components surrounded by other temperature-sensitive components. The heat can be dissipated away from the temperature sensitive area by

using heat pipe intermediate sections and thermal insulation, which can minimize heat losses from intermediate sections of the heat pipe.

There are a number of criteria the heat pipe must fulfill before being accepted in industry. Each different industrial application has it is own criteria. Obviously, each application must be studied in its own right, and the criteria vary considerably. In general the heat pipe has to be: a) reliable and safe, b) satisfy a required performance, c) cost – effective, and d) easy to install and remove.

- Die casting and Injection Molding

Cooling is an important procedure used in die casting and injection molding processes, in which molten metal alloys or plastics are introduced into a die or mold and rapidly cooled to produce a component, often of considerable size and complexity. There is a great necessity for mold cooling in such casting processes to eliminate casting and mold defects, such as hot spots and poor mechanical properties. In addition to that, the mold life can be improved by reducing the potential of having hot spots. This also reduces the production cycle.

Heat pipes are used in die casting and in injection molding casting process [80]. The cooling capability, reliability, low cost and the safety issues put it in competition with the water cooling procedure traditionally used in industry.

The simple configuration of the heat pipe makes it attractive in two areas of application in dies and molds. It can be used to even out temperature gradients in the die by inserting it into the main body of the die, without connecting it to the water-cooling circuits. Also, it can be used to assist the heat transfer between the die face and the water circuits by connecting them with a heat pipe to reduce the risk of having areas with hot spots.

-Cooling of Electronic Components

Heat pipes have wide applications in cooling technology of electronic components such as transistors, other semiconductor devices, integrated circuit packages, and computer processors [81,82]. The electronic component can be directly mounted on the heat pipe or it can be mounted onto a plate into which heat pipes are inserted.

Heat pipes have great applications in computers especially in notebooks. The year 1994 witnessed the first use of a heat pipe in a notebook computer [83,84]. The limited space in the notebook provided the necessity of using an alternative cooling device to the fan. The heat pipe is used to remove the heat from the CPU and dissipate it in another location in the notebook (heat sink) as shown in figure 2.5. Currently, most of the notebooks rely on heat pipe technology in their cooling circuits. Heat pipes with their flexibility and reliability have provided the system designers with tools to improve

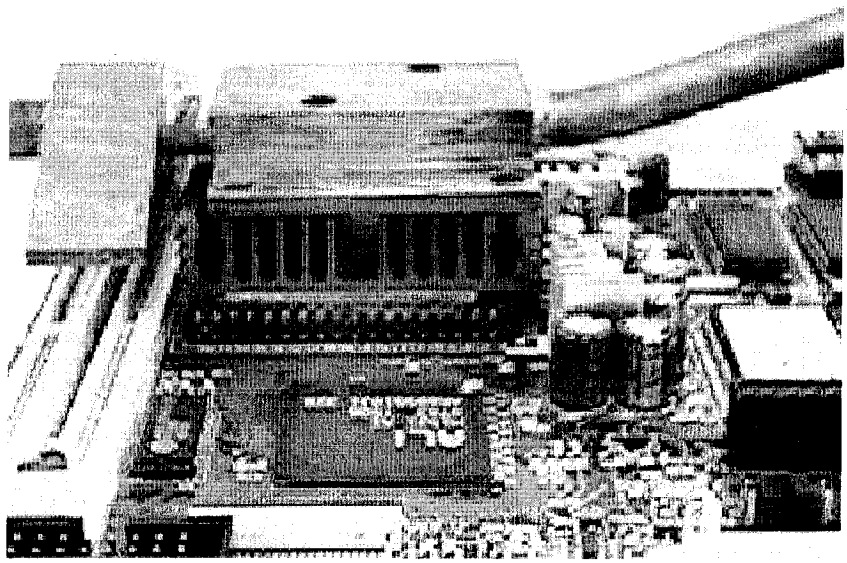

Figure 2.5. Heat pipe cooling Notebook CPU (The Chemical Engineers' Resource Page)

the thermal performance [85].

There are many different applications for heat pipes in different forms. The following are a few applications in brief:

a) In space: where heat pipes have been used for:

- Spacecraft temperature equalization
- Component cooling, temperature control and radiator design
- Space nuclear power sources

b) Energy Conservation: The heat pipe with its effectiveness in heat transfer, is used in applications involving the conservation of energy, and has been used to advantage in heat recovery systems, and energy conversion devices.

c) Preservation of Permafrost: 100,000 heat pipes were placed by McDonnell Douglas Corporation for the Trans – Alaska pipeline [86].

These units are used to prevent thawing of the permafrost around the pipe supports for elevated sections of the pipeline. Those heat pipes use ammonia as the working fluid, heat from the ground being transmitted upwards to a radiator located above ground level.

d) Snow Melting and Deicing: This idea was developed in Japan where the heat pipe snow melting (or deicing) system is based upon the use of ground heat as the heat input to the evaporators of the heat pipes.

2.9.4. Problems with Heat Pipe Technology

In a traditional heat pipe, a few problems might occur and limit the maximum heat transfer rate it can achieve [87]. A detailed discussion of these limitations is given

in many heat pipes books [88-91]. There are six general limitations, which include the viscous, sonic, capillary, entrainment, flooding, and boiling limitations. Figure 2.6 show the limits to maximum axial heat transfer capability as a function of operating temperature of the heat pipe [90].

1) Viscous limit

This limitation is present when the pressure gradient between the evaporator and the condenser is very small at low operating temperature. In this case, the pressure gradient might be smaller than viscous forces, and the viscous forces tend to prevent vapor flow in the heat pipe. The heat pipe requires a pressure gradient to overcome the viscous forces and to sustain the flow. Such a condition is called the viscous limit. Heat pipes which operate at moderate temperature normally don't experience such a limitation.

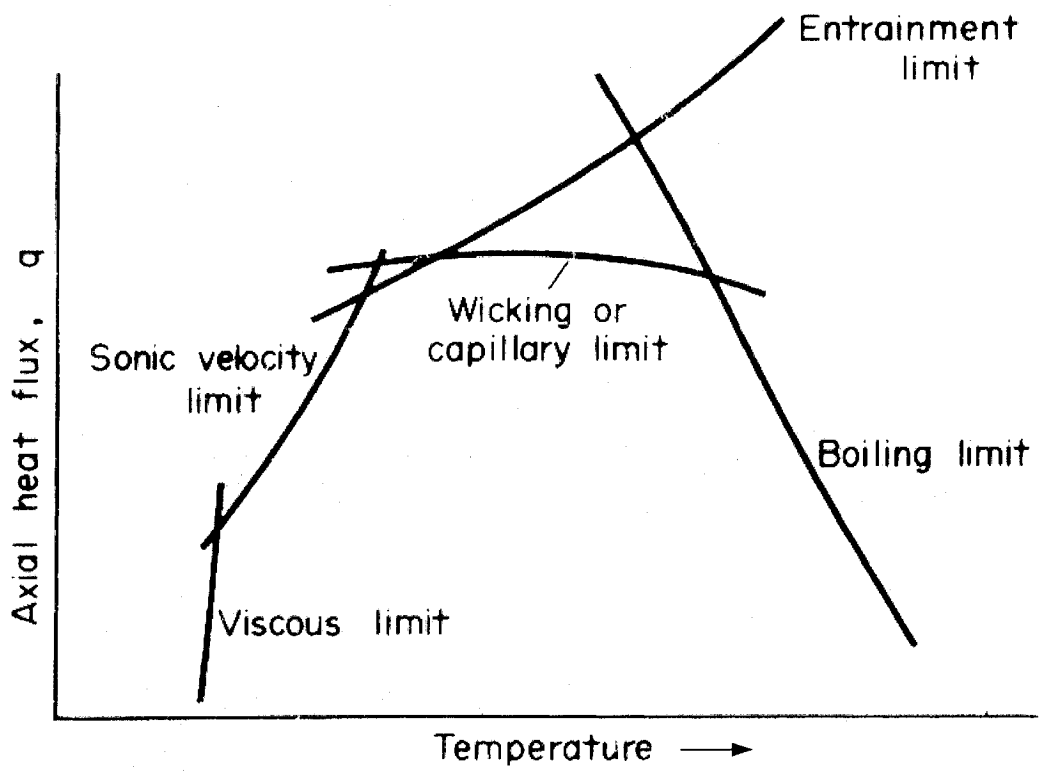

Figure 2.6. Primary limitations to the heat transport capability of a heat pipe [90]

2) Sonic Limit

At a certain temperature and when the velocity of the vapor at the evaporator exit approaches sonic velocity, a choked flow condition will eventually arise. At this point, the vapor velocities cannot increase and a maximum heat transport limitation is achieved. The heat flux that results in choked flow is considered the sonic limit.

3) Capillary Limit

The heat pipe wick has a limited pumping ability to return the working substance from the condenser to the evaporator. The wick capillary pressure depends on wick structure, wick material, working substance, evaporator heat flux, and the operating temperature. This limit is referred to as the capillary limit. For horizontal or against

gravity (evaporator at a higher elevation than the condenser) heat pipes, the capillary limit is an important heat pipe limit.

4) Entrainment Limit

The vapor and the liquid in a heat pipe are moving in countercurrent directions and that leads to a shear force at the liquid-vapor interface. When the vapor velocity is sufficiently high, a limit can be reached at which the liquid will be torn from the pores of the wick and entrained in the vapor and this will stop the condensate flow, which will lead to dry-out of the wick at the evaporator. The corresponding heat flux that results in this phenomenon is called the entrainment limit.

5) Boiling Limit

The film boiling phenomena (boiling limit) is an important problem, which might occur in a heat pipe. Water based heat pipes are safe and easy to handle and expected to function at high heat systems. Film boiling might limit the performance of water based heat pipes in high temperature applications such as permanent mold casting where the temperature of the mold normally varies from 200-400 ^{o}C. In the mean time, water based heat pipes have been used successfully in many industrial applications especially in systems with a low heat flux.

To understand the film boiling phenomena, knowledge of boiling heat transfer is essential. The following is an over view on boiling heat transfer [92].

Boiling heat transfer is a phenomenon onto itself. A simple experiment can be conducted to demonstrate the boiling heat transfer. The experimental setup is such that a 1 mm diameter wire is electrically heated in a water bath at its normal boiling point (i.e. 100 ^{o}C). In the early stages of boiling before discrete vapor bubbles are formed and released, free convection plays an important role. However, once discrete bubbles are

formed and released from the device, the mixing action of the bubbles is of much greater importance.

The bubbles become transporters of large quantities of energy from the boiling surface. The vapor bubbles move away from the interface by virtue of their buoyancy. Since it takes a substantial quantity of energy to vaporize a liquid, this implies that the greater the vigor of the boiling action, the larger the rate of heat transfer. A classical boiling curve for water at 1 atm is shown in figure 2.7. As the surface temperature of the wire increases, the heat flux from the wire increases. The corresponding boiling heat transfer coefficients are also plotted in figure 2.7. From figure 2.7, one can see that the heat flux increases as the temperature difference between the wire and the bulk liquid increases. During this stage of the boiling phenomenon the system is in the nucleate or pool boiling regime. Eventually, the heat flux is so high that the rate of vapor generation begins to exceed the rate at which vapor can leave the heated surface. At this point the surface becomes blanketed by a vapor film. This vapor film can reduce the heat transfer dramatically.

Thus, further increases in the temperature driving force result in a reduction of the heat flux, and a dropping off of the curves. As the temperature driving force increases further, radiation across the vapor film is able to transfer large quantities of energy with the result that the heat flux eventually begins to increase again.

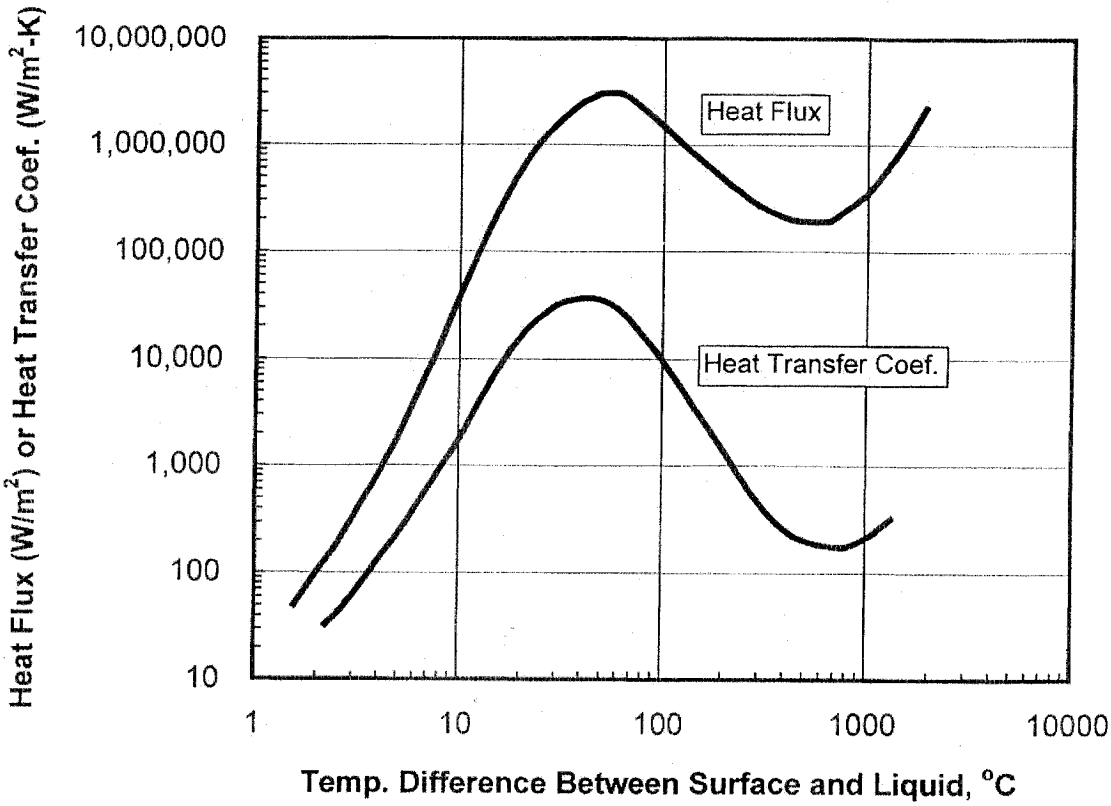

Figure 2.7. Boiling curve for water at 1 atm [92]

While the curves shown in figure 2.7 are for the case of water at 1 atm on a surface with no imposed external velocity, it is worth noting that the curves can be shifted upward by increasing the operating pressure of the system and by imposing an external velocity on the fluid. Substantial increase in the peak heat flux before film boiling occurs can be achieved in this manner. Thus, a system that is prone to experience film boiling can be made to operate in the nucleate boiling regime by adjusting the operating pressure and fluid velocity. This concept is used in continuous casting molds where heat fluxes can be extremely large.

In a traditional heat pipe, the film boiling phenomenon described above can limit its ability to extract high heat fluxes from a high temperature system such as the permanent mold casting process.

2.10. Thermal Modeling of Permanent Mold Casting of Nonferrous Alloys

The use of computer modeling and simulation packages in the design of metal casting molds brought mold designers to a new level of excellence. Powerful computer modeling techniques have been developed and applied to metal casting processes [93-96]. The cost of the products is reduced and the quality is improved by using computer modeling since the casting defects can be spotted and the design modified before actual casting production.

Numerical methods are used for the simulation of mold filing and the solidification process in permanent mold casting. The simulation is well developed based on solving the coupled Navier-Stokes equations for Newtonian flow, and energy equations for heat transfer. The simulated resulted are widely verified and recognized.

The modeling software includes pre-processor, calculation module, and post processor. The solid model, meshing model, materials properties and boundary conditions are built up in the pre-processor. The simulation of the casting process is done in the calculation module. The simulation results are analyzed and visualized in the post processor.

2.11. The Relationship between Microstructure and Mechanical Properties vs. Cooling Rate

The rate of cooling of a molten alloy influences the grain size of the solidified material. Rapid cooling results in a finer microstructure, which leads to better

mechanical properties [97]. Slow cooling usually gives a coarser structure with reduced mechanical properties. Different casting processes have different cooling rates.
Metal mold casting processes produce castings with good mechanical properties. Properly cast, the product is sound, and requires only a minimum clean up from nominal cast size to give a finished shape.

The grain density for a casting produced under rapid cooling is found to be high [98]. Higher cooling reduces the solidification time and the grain size. The Secondary Dendrite Arm Spacing (SDAS) and the size of second-phase particles are reduced with higher cooling rates. Figure 2.8 shows the grains and the dendrites under two different cooling rates. The mechanical properties improve because of the change in dendrite formation controlled by the solidification rate as shown in figure 2.9 [99].

Equations have been developed to correlate the average measurements of the secondary dendrite arm spacing, SDAS, and the cooling rate. Equation (2.12) was developed for magnesium AZ91 alloy [100]:

$$\lambda = 39.8 \, . \, \tau^{-0.32} \quad \ldots\ldots\ldots (2.12)$$

where

λ = the measured SDAS (μm)

τ = the estimated local cooling rate (^{o}C/s)

Equation (2.13) was developed to estimate the cooling rate for A356 alloy [101]

$$\tau \ (^{o}\text{C/s}) = 3.57*10^{4} * \text{SDAS} \ (\mu\text{m})^{-2.56} \quad \ldots\ldots\ldots (2.13)$$

where

τ = the estimated local cooling rate (^{o}C/s)

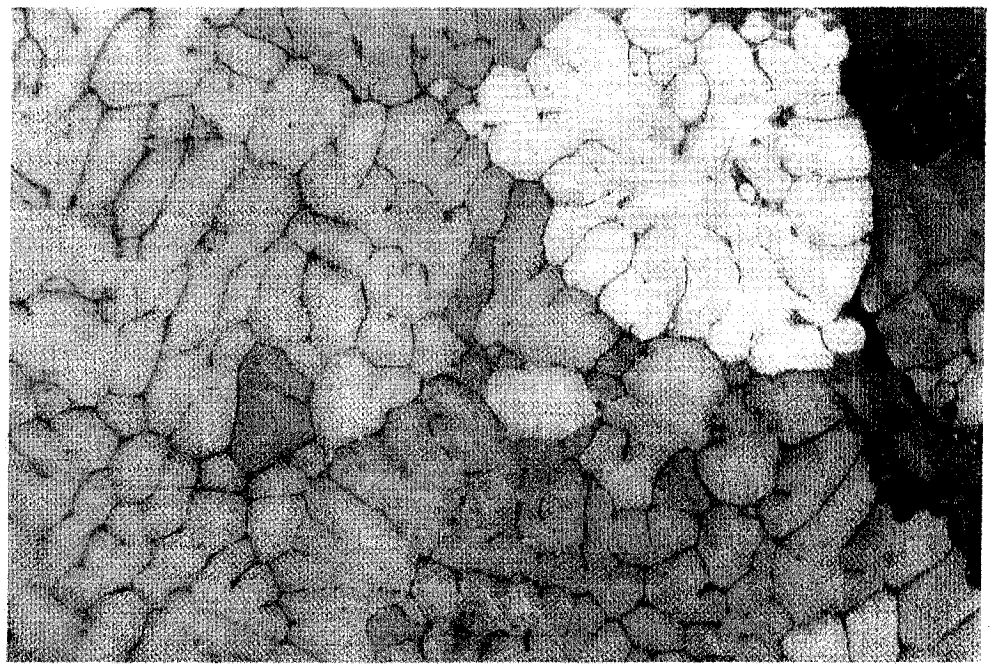

(a)

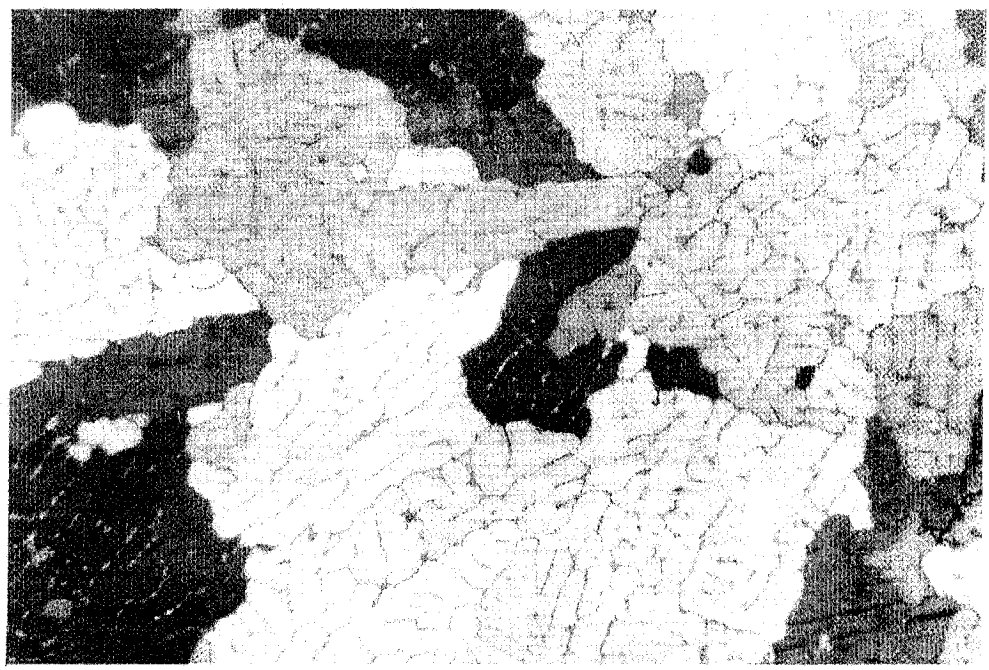

(b)

Figure 2.8. Grains and dendrites of alloy AA 1050 under two different cooling rates (a) Cooled at a rate of 1.2 °C/s; (b) Cooled at a rate of 4.2 °C/s [101]

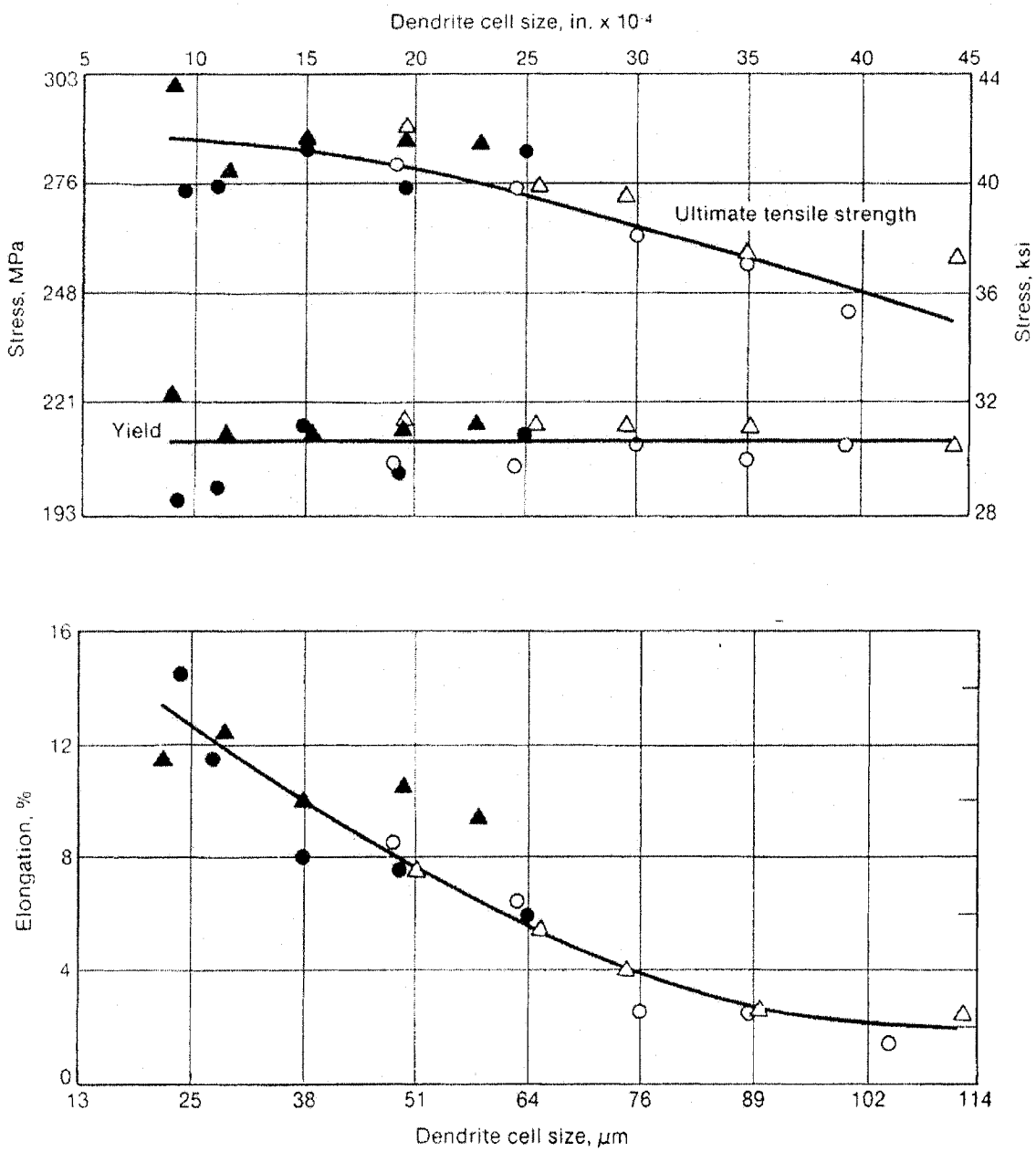

Figure 2.9. Tensile properties versus SDAS for the casting of aluminum alloy A356 [99]

CHAPTER 3 DESIGN AND TESTING OF A WATER-BASED HEAT PIPE AND A PERMANENT MOLD

3.1. Heat Pipe Design

3.1.1. Introduction

The heat pipe, which was used in the present study, was the product of a novel design that was developed at McGill to overcome several problems associated with classical heat pipes. In the case of the permanent mold casting process, there are several problems, which arise when a regular heat pipe is used for cooling purposes. Some of these are due to; 1) high operating temperatures, 2) high heat fluxes, 3) film boiling in the heat pipe, 4) entrapment of liquid by the vapor flow in the heat pipe, and 5) the contact thermal resistance between the heat pipe and the mold. These problems have been discussed in detail in chapter 2.

3.1.2. Design Guidelines

Before designing the water-based heat pipes presented in this work, a few guidelines and

specifications were formulated as desirable for the heat pipe unit that was to be built. The specifications include:

- The heat pipe has to be reliable and safe.
- The cooling rates aimed for are as high as the rates obtained with water-cooling passages.
- The condenser should be located away from the evaporator to make it easier to handle and to make the system safer.
- The heat pipe extracts heat only at desired locations (local extraction technique).
- Heat extracted from the mold is buffered by an external chill.
- The heat pipe can be turned on/off at any time with quick response.
- The heat pipe should deliver the required cooling for permanent mold nonferrous casting.
- The heat pipe is air-cooled.
- The heat pipe has to be of low cost, and environmentally friendly.

3.1.3. Heat Pipe Configuration

The configuration of the heat pipe that was developed is shown in Figure 3.1. As discussed is chapter 2, the selection of the working substance is an important issue to ensure safe and effective performance. According to the typical industrial working temperature for the permanent mold casting of magnesium and aluminum alloys, water was chosen as the working substance in the heat pipe.

In this heat pipe, the liquid water is released from the reservoir to flow through the return line flexible hose to the evaporator by opening the valve. Dish washing machine soap was added to the water (4%) to reduce the surface tension and this led to better flow in the return line. In the evaporator, the liquid is converted into vapor, which flows through the flexible hose connected to the condenser.

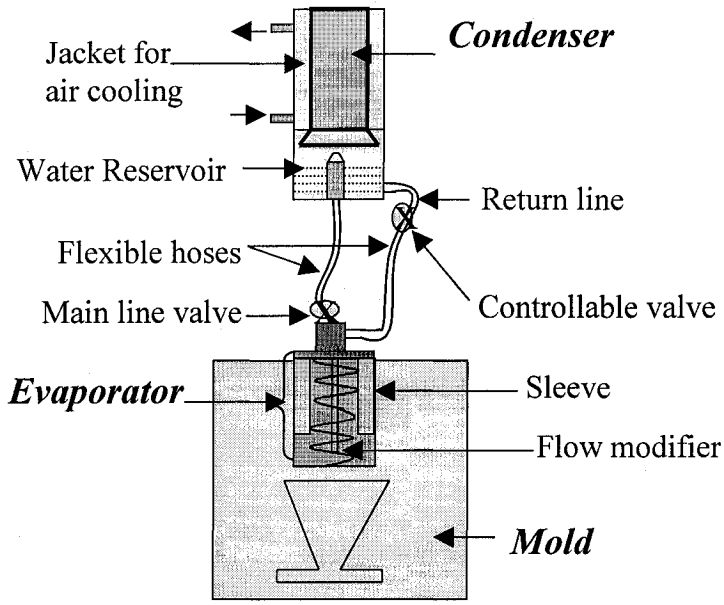

Figure 3.1 Configuration of the designed heat pipe

A 14.5 kg external chill was incorporated in the condenser. The condenser is a hollow stainless steel pipe with thick walls. The vapor is liquified on the inner walls of the condenser. The chill, with its large mass, absorbs the heat from the condensing vapor and dissipates it into the air blown on the outer walls of the chill. Such a technique made it possible to absorb the heat when required and to continuously dissipate the heat into the cooling air stream that comprises the cooling circuit during the entire casting cycle. The chill in effect is acting as an energy buffer. It absorbs heat from the evaporator as required and continuously dissipates it to the cooling air. The internal surface area of the hollow chill is about 10 times larger than that of the evaporator to ensure easy handling of the high heat fluxes.

The condensate from the condenser and the liquid, which might be lifted by the vapor is collected in the reservoir, which sits under the condenser. The reservoir

continuously returns the liquid back to the bottom of the evaporator through the return line. The valve on the return line allows one to turn on/off the heat pipe by controlling the flow in the return line. This on/off feature allows for mold cooling by the heat pipe to be applied during only the desired time period of the casting cycle. As shown in figure 3.1 another valve is installed on the main line to prevent any water remaining in the main line from falling into the evaporator during the off mode.

Stainless steel 304 has been used to construct the heat pipe because of its corrosion resistance and weld-ability properties. Figure 3.2 presents a solid model of the designed heat pipe. Using flexible hoses is a desirable development especially in an industrial environment, since it allows placing the condenser at any suitable location. Three smooth teflon tubes with stainless steel outer braid flexible hoses of 152 cm in length, 1.03 cm internal diameter and 1.35 cm outer diameter are used as the heat pipe flexible hoses.

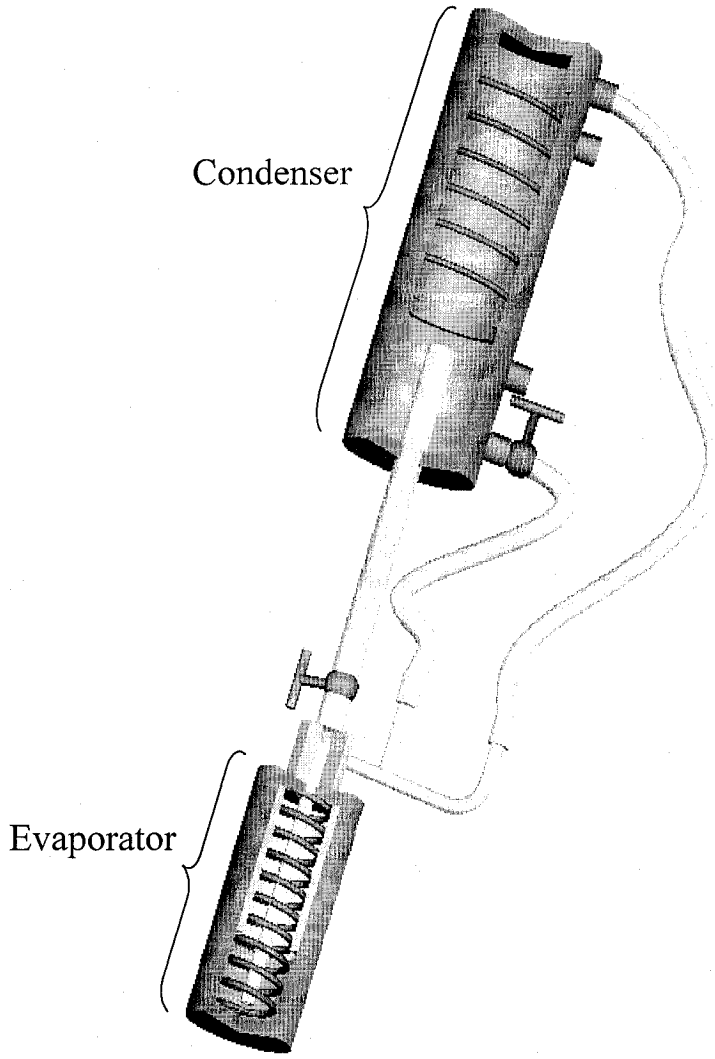

Figure 3.2. Basic configuration of the designed heat pipe (solid model)

3.1.3.1. The condenser section

The condenser section consists of a water reservoir, a steel chill, a flow modifier, a cooling jacket, and an on/off valve. The cooling jacket is built up around the chill. The steel chill is fitted with a flow modifier to mix the flowing cooling air in the jacket. This arrangement leads to better heat transfer from the chill to the cooling air. Figure 3.3 shows the various parts of the condenser section.

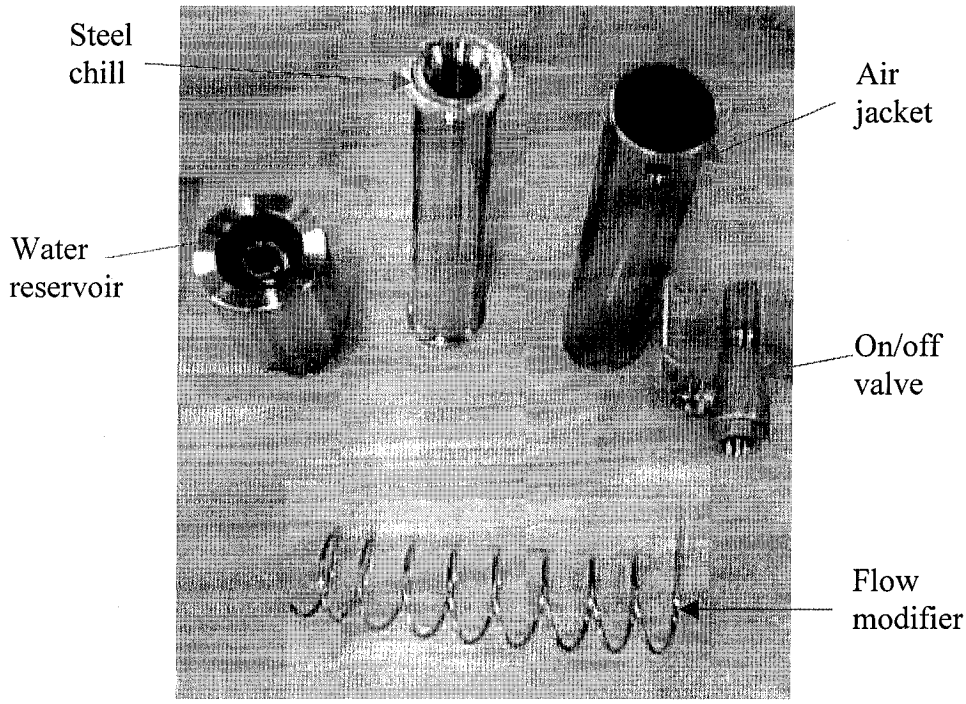

Figure 3.3. The various parts of the condenser section

3.1.3.2. The evaporator section

The heat pipe parts packaged inside the mold, (evaporator, return line, flow modifier, and sleeve), form the other section of the heat pipe (the evaporator section).

This section of the heat pipe takes advantage of a novel design to overcome the limitations due to high mold temperature and high heat fluxes, which prevent using a traditional heat pipe in cooling permanent molds as mentioned earlier.

Eliminating thermal resistance limitation

In the present novel heat pipe design, the evaporator is part of the mold in the form of a hole drilled in the mold as shown in figure 3.1, which reaches close to the area to be cooled. This technique was developed to cut the thermal resistance, which will occur if a traditional heat pipe is inserted directly into a hole to cool a certain internal location. This thermal resistance is the result of the imperfect contact between the mold wall and the heat pipe.

Eliminating liquid entrapment limitation

The difficulty in returning the water to the bottom of the evaporator is one of the key limitations. In the case of a traditional heat pipe, the stream of vapor moving upwards from the evaporator to the condenser tends to entrap the liquid on the inner wall of the heat pipe.

This liquid entrapment will prevent the liquid from falling back into the evaporator and this will result in disabling the heat pipe. To overcome this limitation in the current design, a separate 5mm diameter stainless steel pipe is passed inside to return the water to the bottom of the evaporator as shown in figure 3.1. Figure 3.4 shows the actual return line used to return the water into the evaporator in the present heat pipe. The 5mm diameter is experimentally found to be a good diameter to deliver enough water into the evaporator to achieve high cooling rates for our laboratory setup.

Eliminating of film boiling limitation

To overcome film boiling, which is the main limitation preventing one from using a traditional heat pipe in the permanent mold casting process, a flow modifier (swirl) has been introduced into the evaporator as shown in figure 3.1. The flow modifier is a spring

used to generate an upward centrifugal force inside the evaporator. This technique will force the vapor to move up with high velocities and in the meantime to sweep the inner evaporator wall to remove any film, which might form on the wall. The centrifugal force will cause mixing and thus improve the convective heat transfer coefficient and provide better wetting of the evaporator walls. Such a technique greatly enhances the heat transfer inside the evaporator.

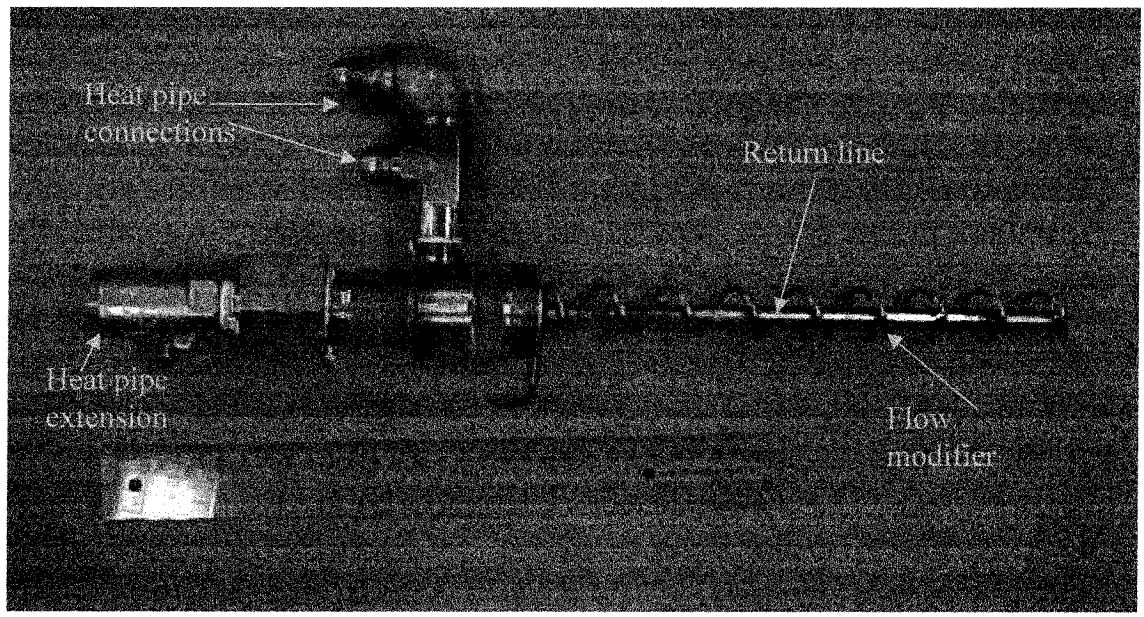

Figure 3.4. The return line designed in the present work

Heat transfer enhancement by generating swirl flow has been reported by many investigations [102-104]; however the use of such a technique in a heat pipe is a new idea.

Figure 3.5 shows the flow modifier used in the present work. A number of flow modifiers were tried and the one which gave the optimum cooling rate was selected. The selection was based on experimental trials.

Local Heat Extraction technique

An effective technique has been developed in the present work to cool only the desired location. As seen in figure 3.1, the evaporator is part of the mold as a hole drilled in the mold close to the casting cavity, which must be cooled. As seen in figure 3.1, only the part of the evaporator close to the casting cavity needs to be cooled and not the whole evaporator area. A sleeve has been inserted into the upper part of the evaporator. The sleeve is a metal insert (stainless steel) which is inserted into the evaporator and covers its upper part. The diameter of the sleeve is 0.5 mm smaller than that of the evaporator. This diameter difference forms a small gap, which naturally cuts the heat transfer from the mold towards the evaporator. Figure 3.6 shows the sleeve designed in the present work.

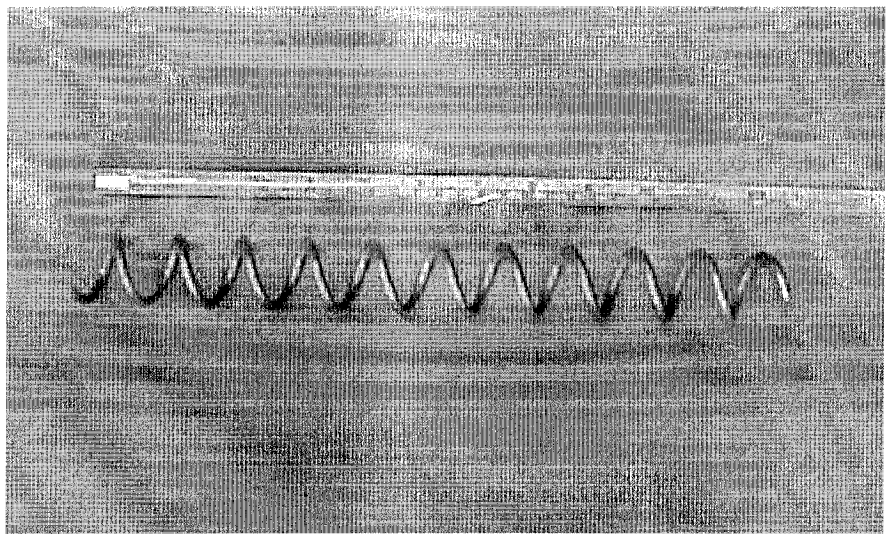

Figure 3.5. The flow modifier used in the present work.

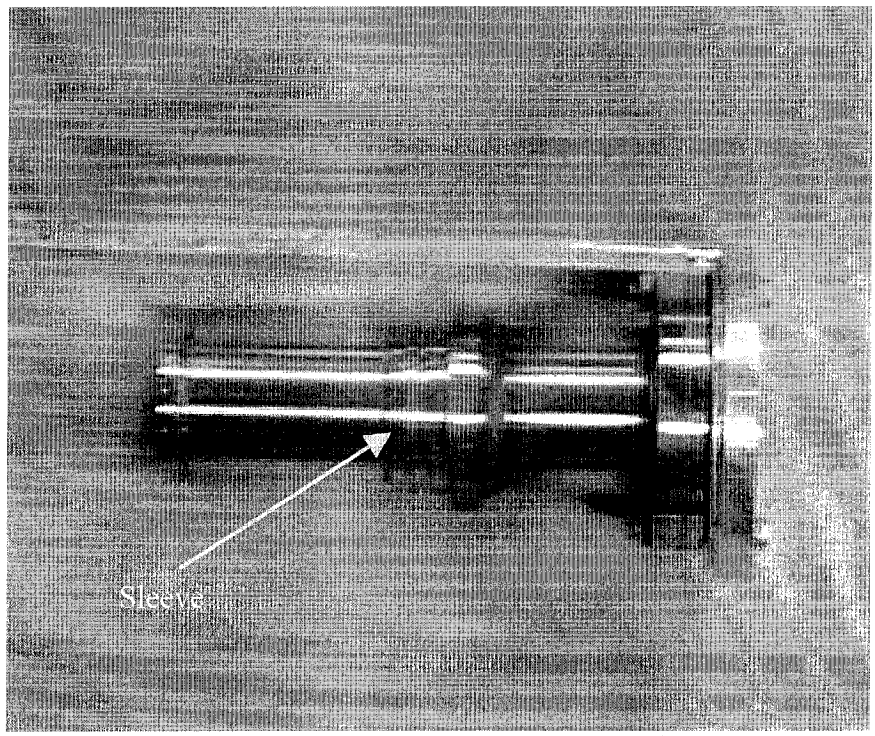

Figure 3.6. The sleeve welded to a connection flange

An extension was welded on the evaporator section as shown in figure 3.7. This extension allows the vapor to escape via a flexible hose into the condenser section of the heat pipe, and it also connects the return line to the water reservoir in the condenser section via a flexible hose.

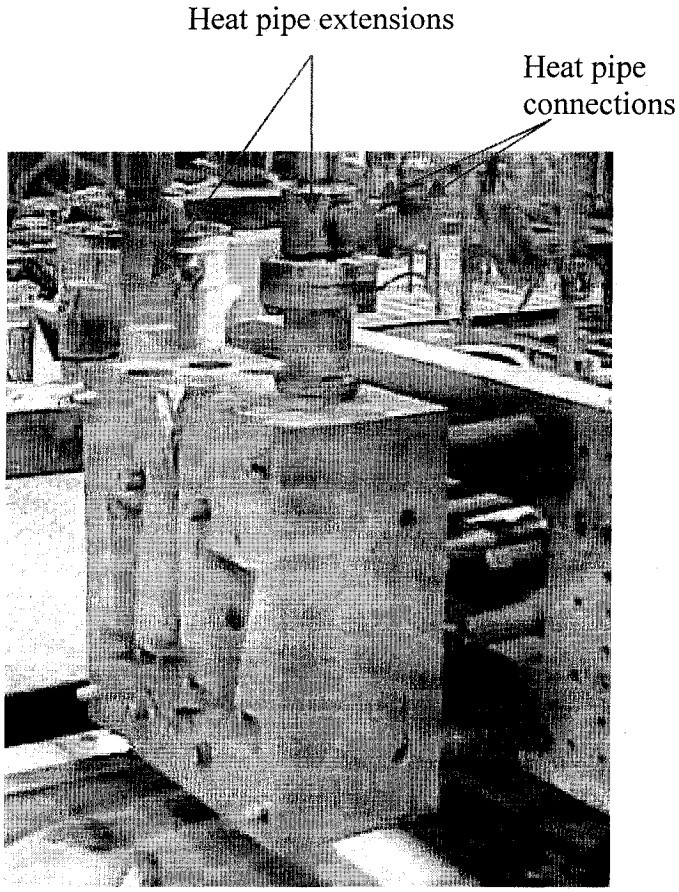

Figure 3.7. Heat pipe extensions and connections

A thermocouple was inserted into the condenser to measure the heat pipe temperature. To conduct the temperature measurement inside the sealed condenser, a 2 mm diameter tube with one closed end was welded inside the condenser and the thermocouple was inserted inside the tube.

3.1.3.3. Vent necessity in McGill heat pipe

Introducing a vent to the McGill heat pipe was a necessity. The vent connects the return line and the condenser. When the heat pipe is off, the part of the return line inside the

evaporator is heated by the mold. When the heat pipe is turned on, the first packet of liquid (water) traveling from the reservoir to the evaporator will transform to vapor. This will cause counter current flow between the vapor moving upward and the water moving down the return line resulting in a dry evaporator. A vent on the return line will allow the vapor to escape and have a short cut to the condenser. Figure 3.8 shows a return line with a vent.

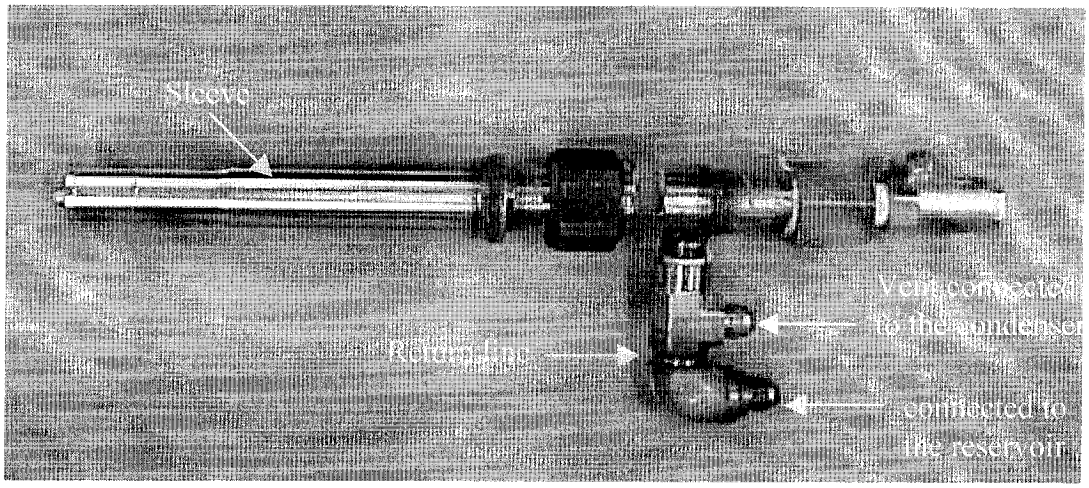

Figure 3.8. Return line with vent

3.2. Design and Construction of a Permanent Mold for Nonferrous Casting

3.2.1. Mold Design

A mold was designed to produce permanent mold castings for magnesium and aluminum. The mold was designed with the intention of creating shrinkage defects in two castings when cooling is not used, and to eliminate or reduce these defects when heat pipe cooling is used.

The mold was made of H13 steel, which is widely used in permanent mold casting. Two cavities with different dimensions were machined into the bulk material as shown in Figure 3.9. The two cavities have the shape of inverted triangles.

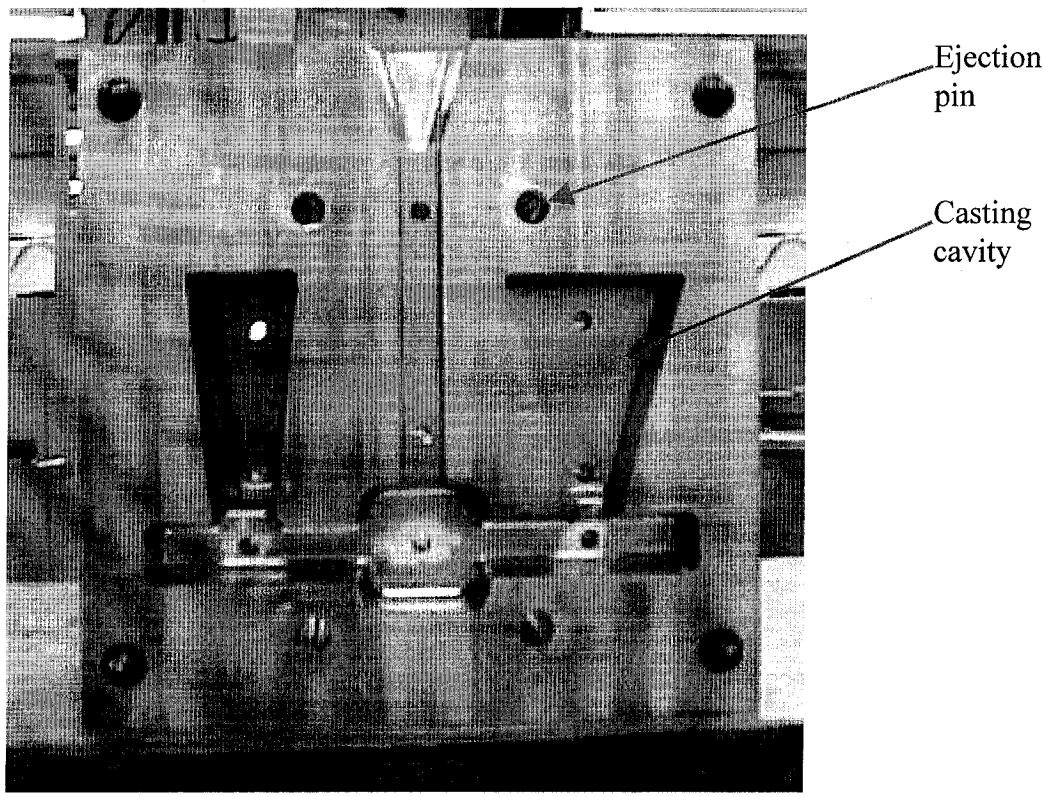

Figure 3.9. The configuration of the mold developed in the present work

The gate for feeding each cavity is at the lower shorter side of the cavity. Such a design will ensure that shrinkage is present at the center of the castings since it will take a longer time for this location to solidify due to its large mass and the shortage of the molten metal supply from the bottom. A number of holes for the ejection pins were drilled in the mold. These holes are used to allow the sliding of the casting machine ejection pins to open the mold and extract the casting. The purpose of using heat pipes on this mold is to

cool the side of the casting from the middle to the upper part and to direct the solidification towards the other side of the casting. Two holes were drilled into the mold from the top to a distance of one centimeter from the cavities. These holes are the evaporators of the heat pipes and are connected to the condensers using flexible hoses. The reason behind having the evaporators of the heat pipes as part of the mold is to cut the interfacial resistance, which occurs when two solid surfaces are in contact. As mentioned earlier, a sleeve was inserted in each hole to cut the heat extraction inside the evaporator at areas away from the upper faces of the cavities by forming a tiny gap with the mold walls. The engineering drawing with all the dimensions of the designed mold is given in figure 3.10.

K-type thermocouples were inserted into a few selected locations in the mold to monitor the temperature distributions during the casting process. The thermocouple positions are shown in figure 3.10. A solid model of the mold is shown in figure 3.11. One can see the cavities as well as see the heat pipes positioned at the side of the castings. The mold has been used to produce a series of castings with and without heat pipe cooling. The mold is designed to be fixed on a casting machine and to be used for a series of actual industrial trials at the plant.

Computer modeling was used in designing the heat pipes and the mold. The details are given in the following section.

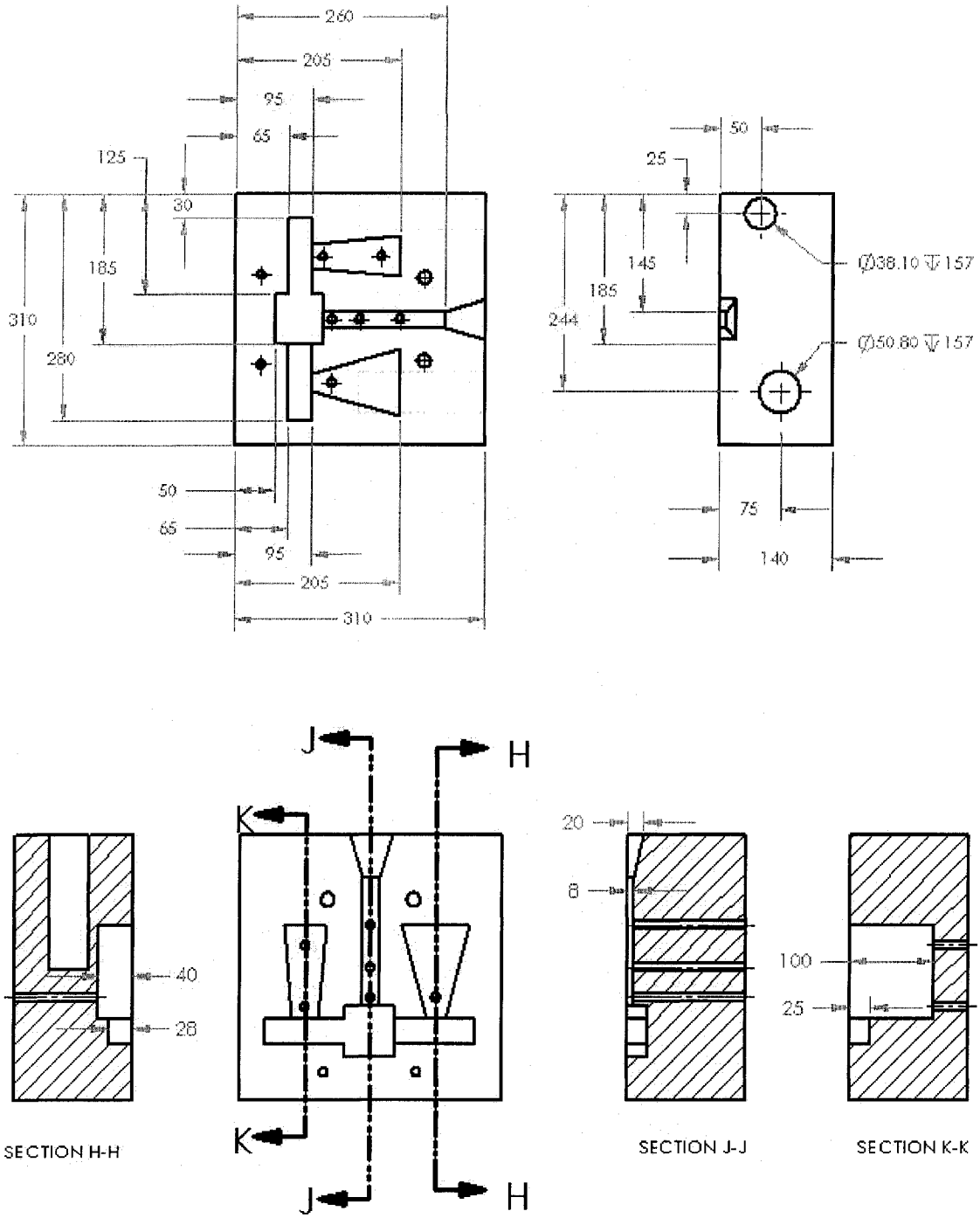

Figure 3.10. The engineering drawing of the designed mold

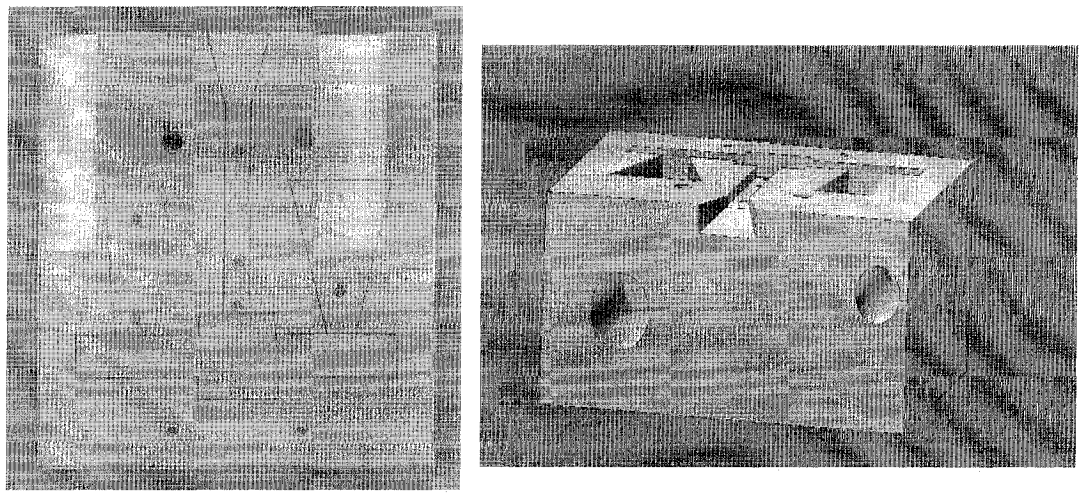

Figure 3.11. Design of the permanent mold (solid model)

3.3. Computer modeling of the casting process

Before starting to machine the mold, a computer model of the mold and the casting process was developed using AFS-SolidCast to confirm the design. The modeling shows shrinkage present in the castings and also shows that heat pipes can be used to reduce and redistribute the shrinkage. Figure 3.12 shows the model developed in the present work to simulate the mold with heat pipes. In this figure both the casting and the heat pipes are shown. Figure 3.13 shows the complete model where the mold and the casting can be seen.

The physical and the thermal properties of the casting and mold were selected from the AFS-SolidCast built-in library. The values of the interfacial heat transfer coefficient, h, between the casting and the mold, and the mold and the ambient were selected as 4000 W/m^2-K and 40 W/m^2-K respectively as recommended by the AFS-SoildCast guidebook [105].

The heat pipes were simulated as a mold material with constant temperature to act

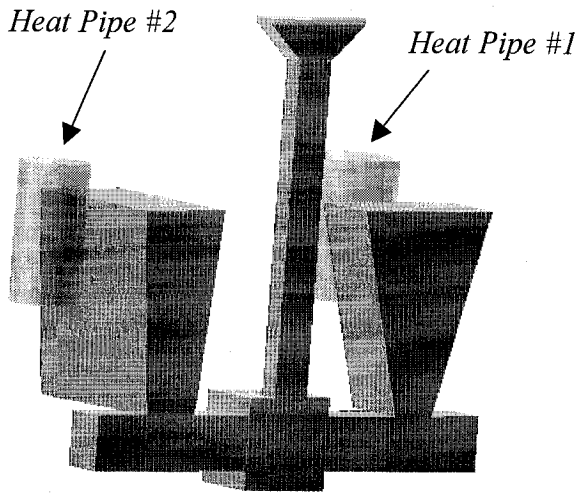

Figure 3.12. The model used to simulate the casting process with heat pipes

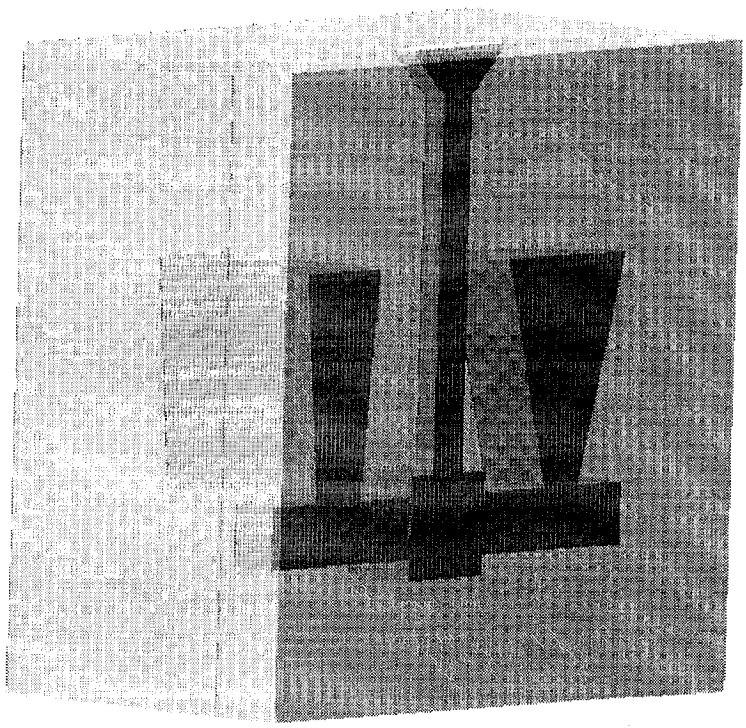

Figure 3.13. The model used to simulate the casting and the H13 tool steel permanent mold

as a heat sink. The constant heat pipe temperature was chosen as 70 °C, which is a suitable average heat pipe temperature. The value of the heat transfer coefficient between the mold and the heat pipe was set to 20,000 W/m^2-K, which is a conservative h value for boiling heat transfer.

Figure 3.14(a) shows the temperature distribution results obtained from the model of the mold for magnesium casting produced without heat pipes. Figure 3.14(b) shows the temperature distribution results of the mold for magnesium casting produced with heat pipes. Figure 3.14(c) shows the other side of the casting shown in figure 3.14(b).

Figure 3.14(a) shows clearly that the central parts of the castings are the hottest sections and they are the last locations to solidify because they are away from the mold walls and contain more metal than the lower sections. The lower parts have smaller volumes so they will freeze faster. This indicates clearly that shrinkage will be present in the upper hot areas. Figures 3.14(b&c) show clearly that the heat pipe managed to push the shrinkage to the lower part of the casting, and also to the other side of the casting.

If we now turn to the aluminum system, figure 3.15(a) shows the temperature distribution results obtained from the model of the mold for aluminum casting produced without heat pipes. Figure 3.15(b) shows the temperature distribution results of the mold for aluminum casting produced with heat pipes, and figure 3.15(c) shows the other side of the casting illustrated in figure 3.15(b).

From figures 3.15(a, b&c), one can see that the results obtained for aluminum casting exhibit the same trend as those of magnesium casting and hence the same observations can be obtained. The modeling also showed reduction in the freezing time when a heat pipe is used for all castings simulated. The modeling results will be discussed in more detail in chapter 4.

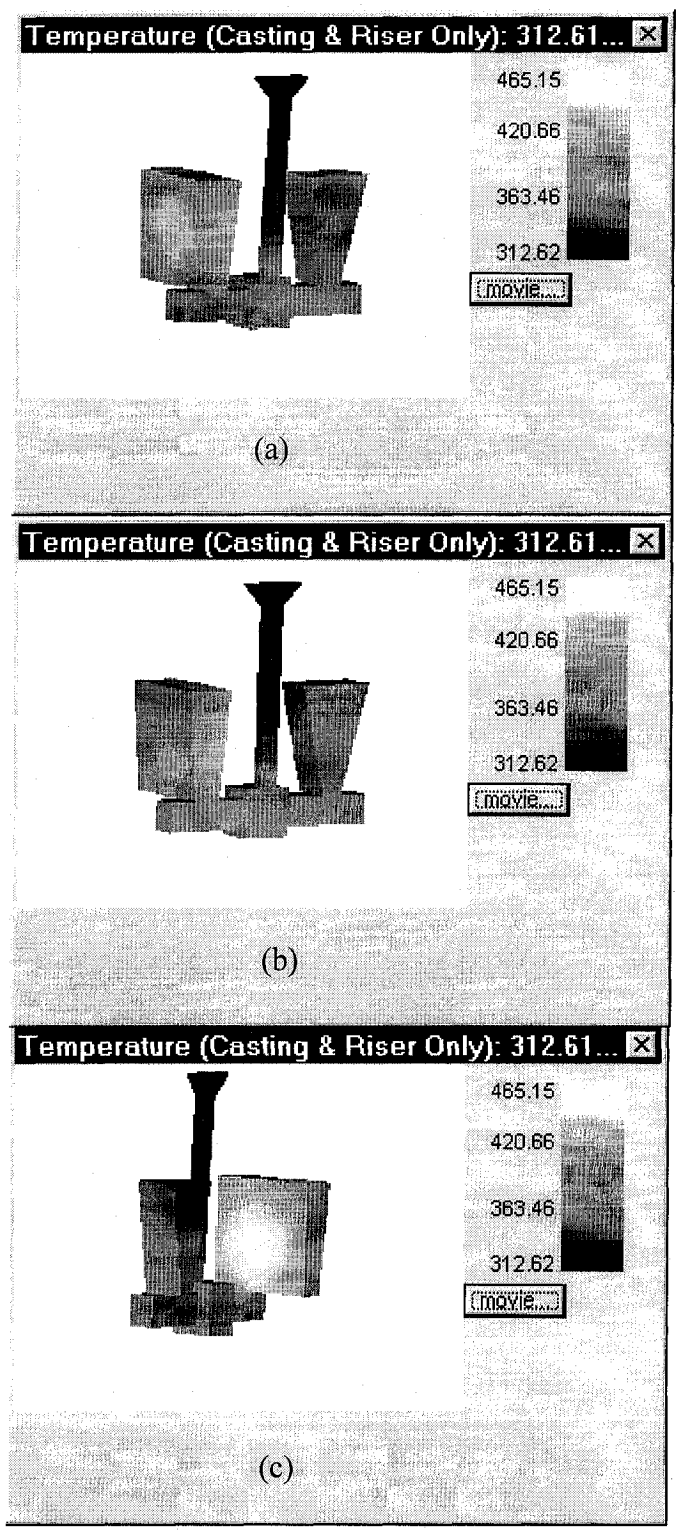

Figure 3.14. Temperature distribution results obtained from the model for a magnesium casting (a) mold without heat pipes (b&c) mold with heat pipes

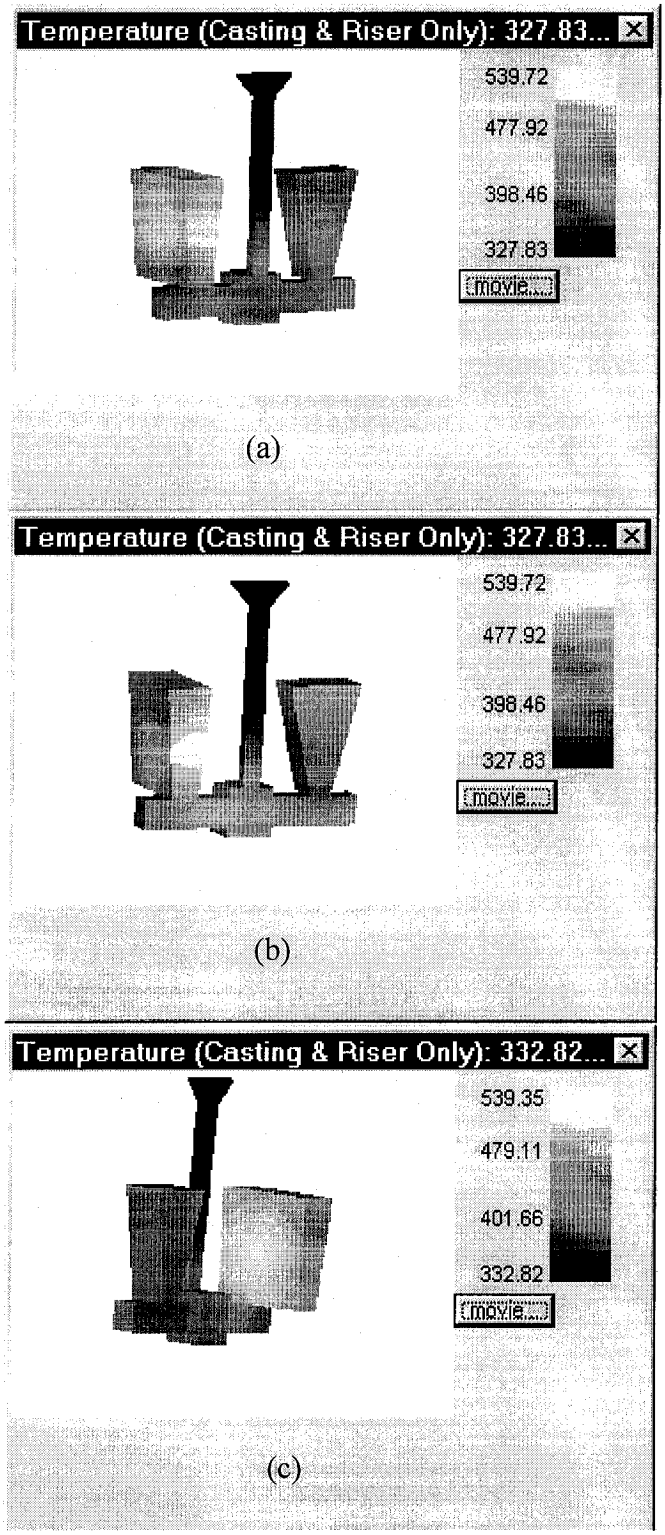

Figure 3.15. Temperature distribution results obtained from the model for an aluminum casting (a) mold without heat pipes (b&c) mold with heat pipes

3.3.1. Computer modeling of cooling curves

Computer modeling was used to determine the cooling curves at four thermocouple locations (Tc1 to Tc4) in the casting and the mold as donated in figure 3.16. The results of the modeling showed the effect of the heat pipes on casting solidification. Figure 3.16(a) shows two sets of temperature curves for one of the inverted magnesium castings. Two conditions were analyzed. In one case, the mold was not cooled; in the other case heat pipe cooling was applied to the mold (i.e. temperature curves denoted with the label 'HP'). Curves denoted with the label 'HP' were obtained from simulations that included heat pipe cooling. One can clearly see from the results the expected effect of heat pipe cooling on the magnesium casting and also on the temperature of the mold.

The same exercise was repeated for the other inverted casting. The results are shown in figure 3.16(b). Once again one sees how heat pipe cooling affects the casting and the mold in the vicinity of the casting. The locations of the thermocouples used in the modeling are shown in the figures. Curves obtained from the simulation that included heat pipe cooling are denoted with the label 'HP'. Curves without this label were obtained from reference simulations that did not involve cooling.

From figure 3.16, the effect of the heat pipes on the mold and the casting is obvious. Comparing the casting temperatures on the cooling curves for both castings with no heat pipe cooling and with heat pipe cooling, it is clear that the temperature of the casting is lower in the case of castings produced with heat pipe cooling. Also, the mold temperature is lower for the case of the heat pipe cooling, casting process. Further explanation will be given in chapter 4.

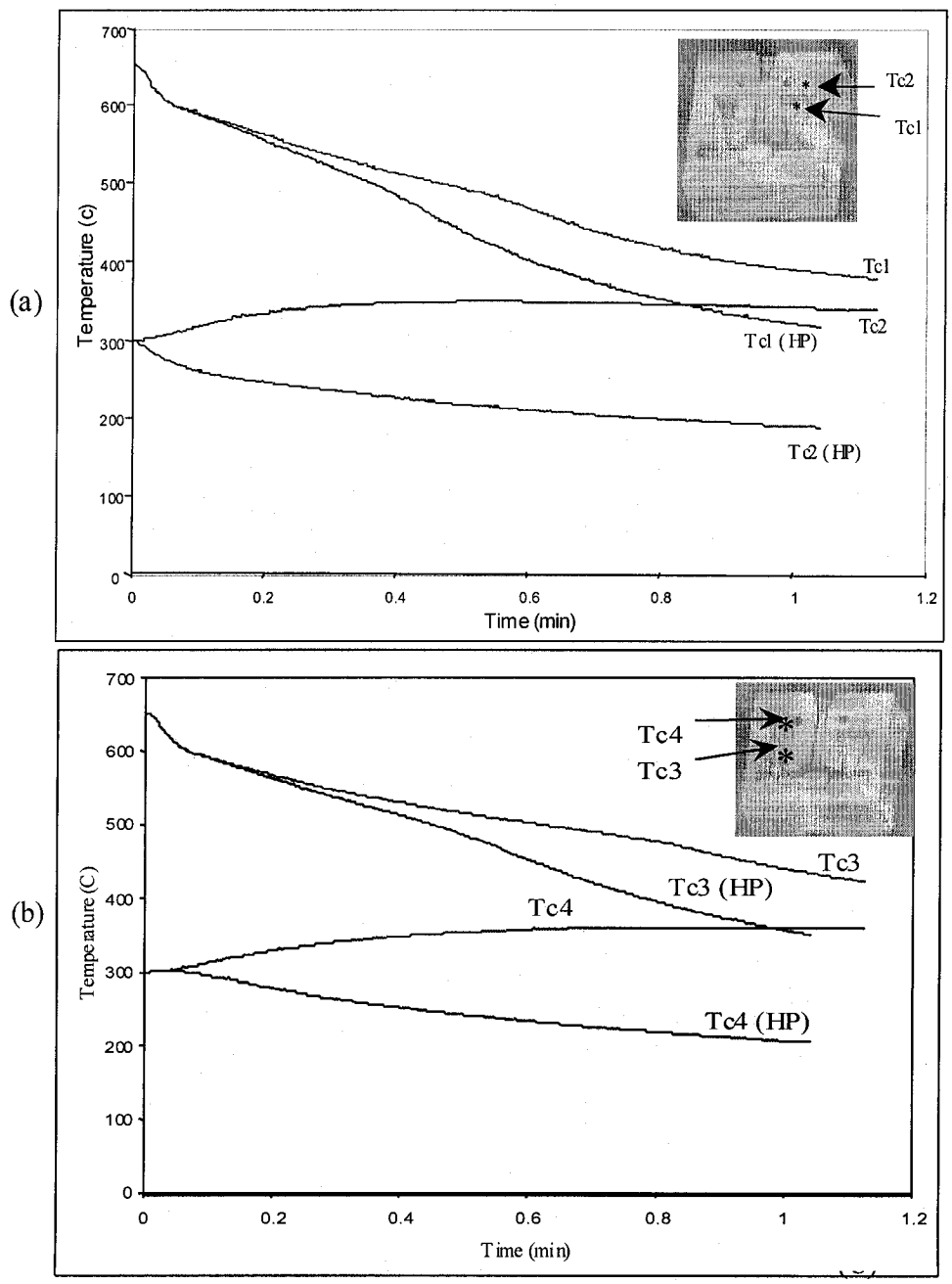

Figure 3.16. The effect of heat pipe cooling on the casting and mold temperatures (modeling)

3.4. Laboratory Testing of the Novel Heat Pipe

After designing and constructing the heat pipe, preliminary laboratory testing was an important task before connecting the heat pipe into the permanent mold.

A stainless steel pipe was connected to the condenser via a flexible hose at one end and sealed from the other end. This pipe was used as the evaporator. A schematic of the test set-up is shown in figure 3.17. The evaporator was inserted into a gas furnace running at a high temperature. The water was released from the reservoir and the heat pipe responded immediately to extract heat. The temperature of the heat pipe and the cooling air were recorded by a data acquisition system. The same test was repeated with a higher temperature of the furnace. The heat fluxes extracted were calculated and found to be as high as expected. The results from the test are given in table 3.1. The heat pipe components were examined throughout the test and found to be functioning properly. The test set-up is shown in figure 3.18.

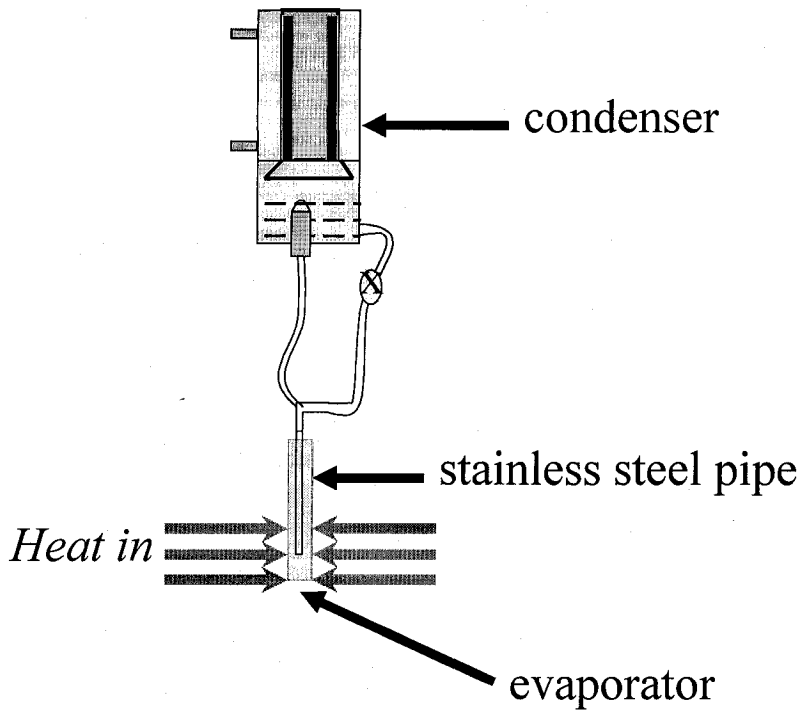

Figure 3.17. A schematic of the test set-up

Table 3.1. The results of two tests conducted to evaluate the heat pipe

	Condenser			Heat pipe	
	Air flow rate (Nl/s)	Inlet air T (°C)	Outlet air T (°C)	T (°C)	Max. transient heat flux (kW/m^2)
1 (low T)	22	20.5	42.8	66.5	388.7
2 (high T)	31	20.9	61.9	104.2	789.5

T= Temperature

The heat fluxes were estimated based on the heat pipe, air inlet and air outlet temperatures, where 70% of the heat was assumed to be absorbed by the chill and 30% dissipated by the condenser cooling air.

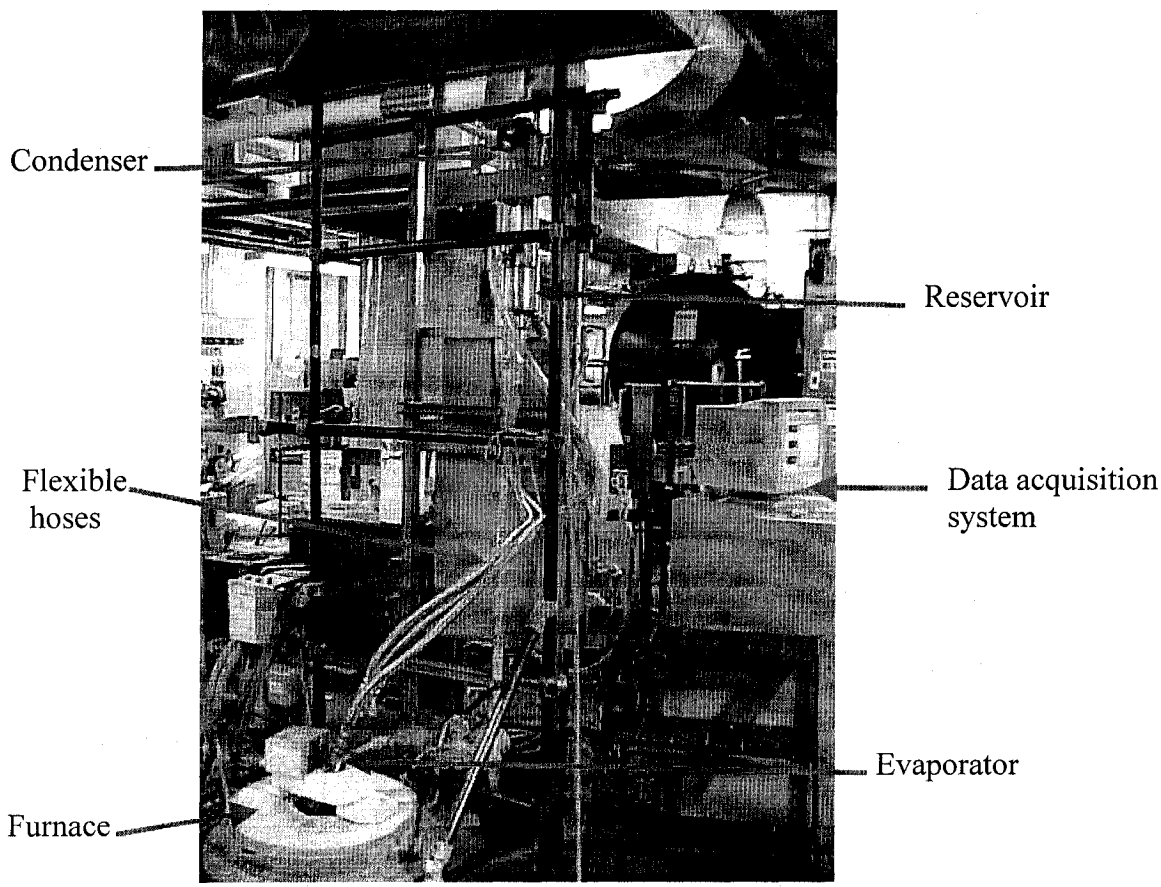

Figure 3.18. The heat pipe laboratory test set-up

The aim of this test was to make sure that the heat pipe functions in the proper way i. e. the water circulates from the reservoir all the way down to the bottom of the evaporator and is converted to vapor. The vapor is then driven by a pressure gradient up through the main hose to the condenser where it condenses and the liquid falls into the reservoir. It is important that the heat pipe can operate at high heat fluxes as well as lower ones. This was achieved by adjusting the temperature of the furnace. The results obtained were close to what was expected.

The performance of the heat pipes developed in the present work was tested again before conducting actual industrial trials by heating the mold to about 325 °C. Thermocouples were inserted at two locations in the mold to monitor its temperature using the data acquisition system. Location number 1 was 2 cm away from the first heat pipe and location number 2 was 0.5 cm away from the second heat pipe. The two heat pipes were switched on and their quick response was noticed by the sharp drop in the temperature of the mold at the two thermocouple locations. The result of this test is shown in figure 3.19. From the figure, one can see the dramatic drop in the mold temperature caused by heat pipe cooling. In location number 1, a drop of about 100 °C is obtained over a period of time of 250 seconds. In the case of the other thermocouple location, which is closer to the heat pipe, a sharp drop in the mold temperature is observed. A temperature drop of about 150 °C is obtained in about 50 seconds. Such a

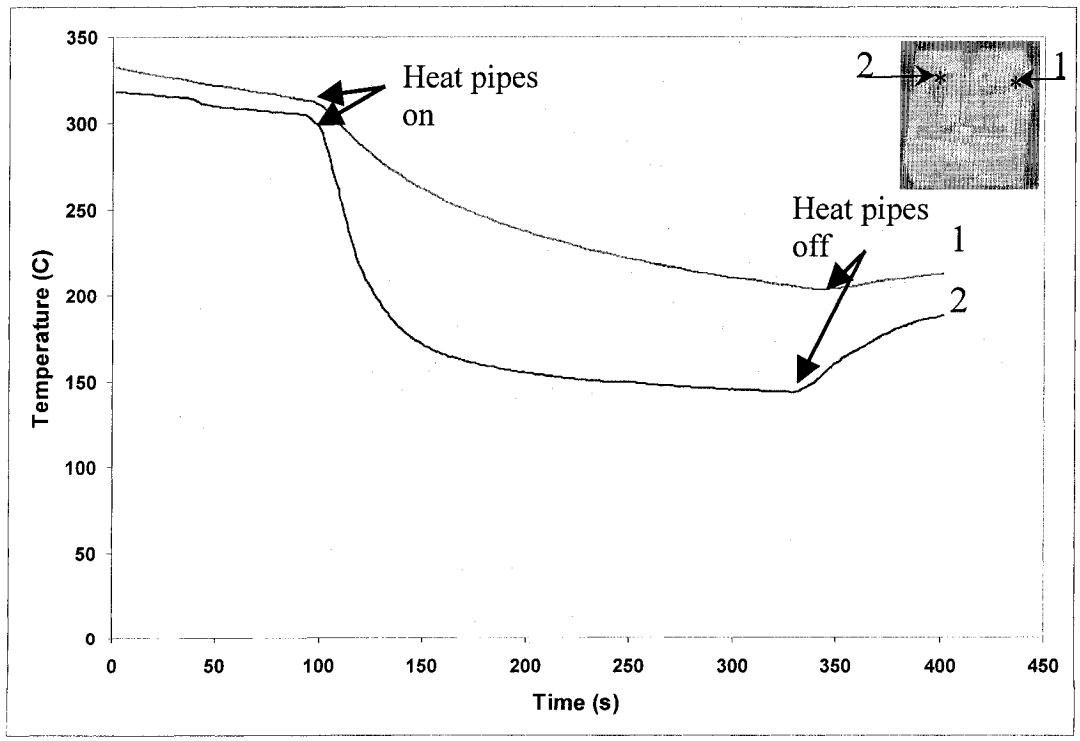

Figure 3.19. Results of a preliminary test

test demonstrated the cooling capabilities of the novel heat pipes developed in the present work. After passing this test, confidence in the performance of the heat pipes was established and the preparations for the next stage of the research, the industrial trials, were started.

3.5. Heat pipe Experimental Studies

As mentioned earlier, the flow modifier was incorporated in the design to produce swirling motion, which in turn creates a centrifugal force that forces liquid onto the evaporator wall. As a result, the vapor film on the walls become insatiable and film boiling is eliminated, thus improving the convective heat transfer coefficient and providing better wetting of the evaporator walls while minimizing vapor films. This technique is one of the key elements, which has made the McGill heat pipe suitable to be used in high temperature systems such as the casting process. The total amount of working substance (water) contained in the heat pipe unit is a small fraction of the total evaporator space. When the heat pipe is operating, water is flowing from the reservoir to the evaporator thorough the return line. Some of this return water is transformed into vapor and the rest is carried towards the condenser by the vapor. The above mechanism was considered in the design of the current novel heat pipe.

After the completion of this work, primary heat pipe experimental studies have been conducted at McGill University to study the role of the flow modifier in enhancing the heat pipe cooling capabilities. The setup is shown in figure 3.20. The setup was made of a transparent material and consisted of a water reservoir, return line, evaporator, and flow modifier. The bottom of the evaporator has small holes and was connected to a compressed air outlet.

The air passed through the bottom of the evaporator simulates the vapor produced in the evaporator. This first experiment was conducted without using a flow modifier in

the evaporator. The water was released from the reservoir to reach to the bottom of the evaporator. The water was then carried up by the air towards the upper part of the setup. No generation of a centrifugal force inside the evaporator was observed. A flow modifier was introduced in the evaporator and the same experiment was conducted. A centrifugal force inside the evaporator was observed and a vortex was generated inside the evaporator. The air was inside the vortex and the water was pushed to the circumference of the pipe and wetted the entire evaporator wall.

When the return line and the air were turned off, the amount of water sitting in the evaporator was measured. This amount of water was found to be only 5% to 10% of the total evaporator space.

The above observations confirmed the heat pipe design principles used in the present work. It proved that the developed novel heat pipe is using only a small amount of water to reach a remarkable high cooling rate. Also it shows the importance of the novel element used in the current heat pipe (flow modifier) that allows the heat pipes to be used in high temperature systems.

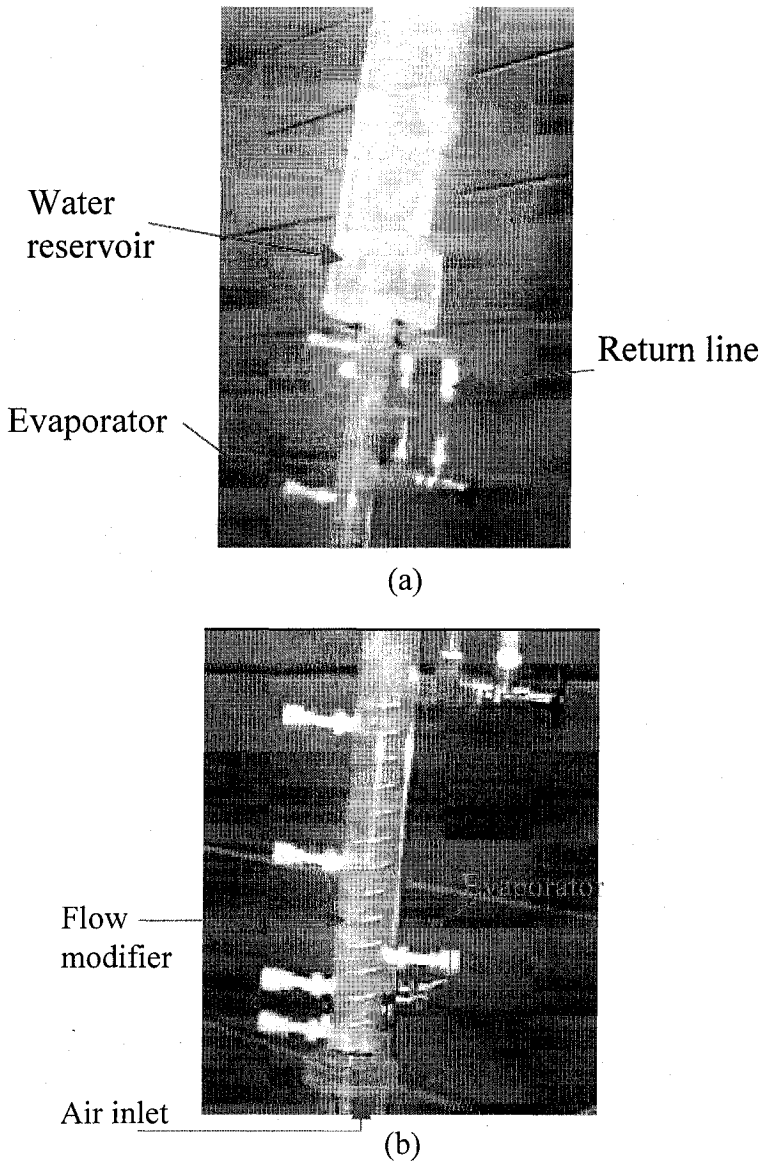

Figure 3.20. The heat pipe experimental setup

CHAPTER 4 RESULTS AND DISCUSSION

4.1. Industrial Trials for Nonferrous Permanent Mold Casting

After designing and manufacturing the mold and the heat pipes, as mentioned earlier, the heat pipes were tested in the laboratory and in the plant. The results of the laboratory tests have been given in chapter 3. After the satisfactory results obtained in the laboratory, the setup was sent to InterMag Technologies which is a foundry specializing in magnesium casting.

Industrial trials were conducted to produce both commercial magnesium (AZ91E) and aluminum 356 castings. Magnesium (AZ91E) is widely used in the automobile industry and aluminum 356 has a variety of applications in industry. Many castings were produced with and without heat pipe cooling.

4.1.1. Industrial Setup

The industrial setup used in this work is seen in figure 4.1. In this figure one can see the casting machine, the mold mounted on the machine and the heat pipes. As mentioned earlier in chapter 3, consideration of the industrial environment space limitation has been taken into account in the heat pipe design. Flexible hoses were used

to connect the evaporator to the condenser. By using the flexible hoses, it was possible to locate the condensers at any desired locations. As seen in figure 4.1, the condensers are located above the mold. A steel frame was specially made to hold the condensers in position.

The amount of working substance (water) inside both heat pipes was 300 ml. The heat pipes were evacuated using a vacuum pump. Thermocouples were located to monitor and record the heat pipe temperature, the temperatures of the inlet cooling air and outlet cooling air for each pipe. In addition to that, the mold temperature was monitored in a few locations (one thermocouple was inserted from the upper face of the mold to reach 7mm away from the middle of each heat pipe evaporator, and one thermocouple inserted 3 cm inside the center of each side of the mold). Data acquisition was used in temperature measurement. The thermocouples were calibrated using boiling water and its response for high temperature was tested using a flame torch.

The casting machine was automatically operated (open and close). The opening time could be set automatically. A solidification time of two minutes was allowed before opening the mold automatically.

The permanent mold was preheated with a burner that impinged on only one side of the mold. In the permanent mold casting process, the mold has to be preheated to a certain temperature range (normally 200-400 ^{o}C for magnesium and aluminum alloys).

It is important to mention that it was impossible to obtain a uniform preheating mold temperature because of the procedure used in the plant to preheat the mold. This was due to the facilities available. Because of this limitation, effects were noted on the final microstructure comparison and on other results.

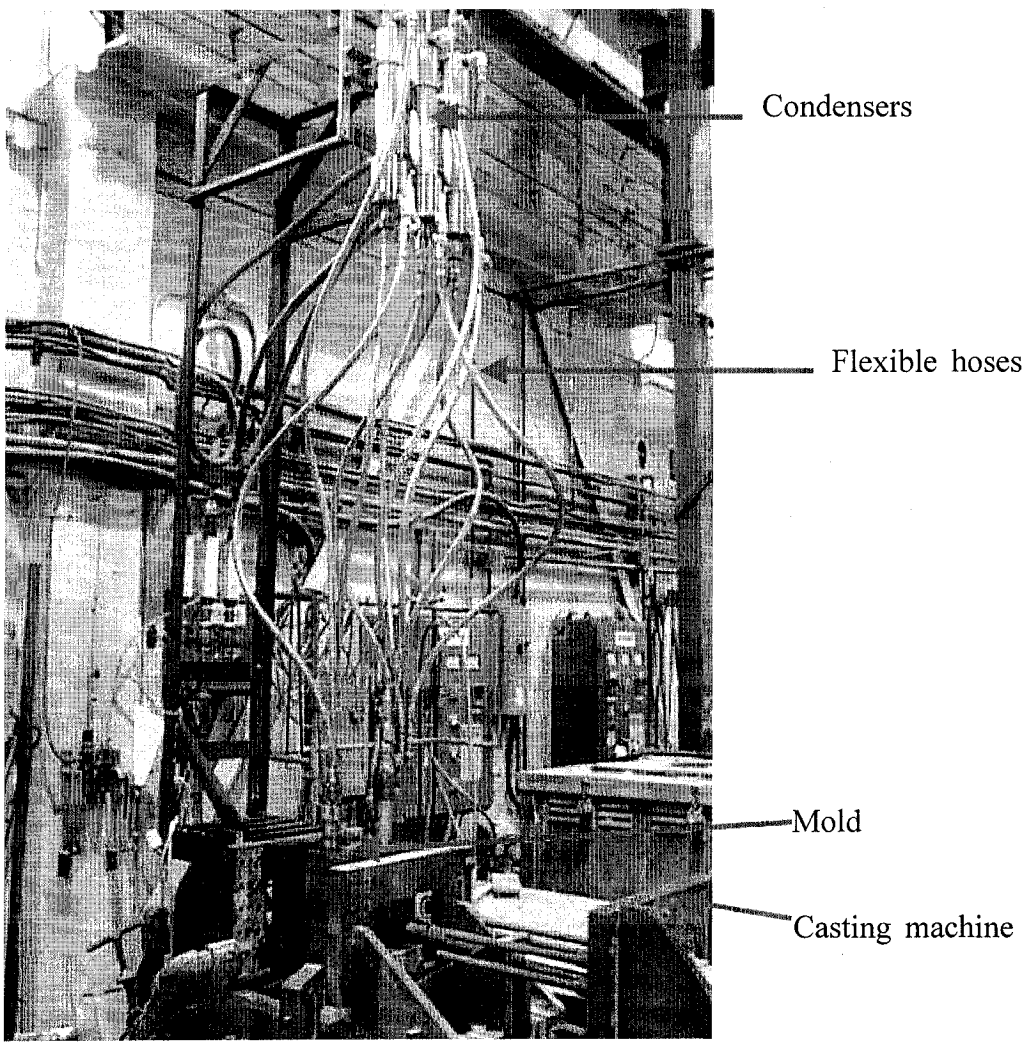

Figure 4.1. Mold and heat pipe industrial test set-up

The capacity of the crucible was 180 kg. Two types of coatings were tested for the magnesium castings. The first coating tried was boron nitride and the second was graphite. In the case of the aluminum castings, only the graphite coating was used. Both coatings were used and made available by InterMag company.

Hexachloroethane, C_2Cl_6, 200g tablets were used as a degasser for the magnesium AZ91E melts. Recent research has shown that C_2Cl_6 has a grain refining effect on AZ91E [108]. It would be expected that this effect should be the same in all the casting

produced. Argon gas was used as a degasser for the aluminum A356 melts (rotary degasser at 40 rpm, gas pressure 20 psi for 25 minutes). In the case of AZ91E magnesium castings, a protective layer of CO_2+1% SF_6 (sulphur hexafluoride) is used to prevent reaction with the atmosphere.

Many magnesium and aluminum castings were produced during the course of this work. Table 4.1 shows the details of casting conditions for selected castings chosen for analysis. These castings were chosen to represent different casting parameters namely, mold temperature, mold coating, melt temperature, and mold cooling. In order to evaluate the effect of heat pipe cooling on the castings, the castings are divided into groups of two castings each, and in some cases into three castings to check for the reproducibility of the experiments under an industrial environment. The castings in the same group are produced under similar casting conditions except for the fact that one of them was cast without heat pipe cooling and the other with cooling as seen in the table and marked by "N" and "Y". It is worth mentioning that each casting number seen in the table represents two castings with different configurations poured at the same time (as seen in figure 3.10, the mold contains two cavities to produce two castings in one cycle). Microstructural analysis was conducted at a total of 108 points for the 36 selected castings. The code "H1" is used to refer to castings poured into the mold cavity close to heat pipe number 1 and "H2" is used to refer to those poured into the mold cavity close to heat pipe number 2.

Table 4.1 Details of selected castings used for analysis

Casting No.	Melt Temp.	Mold Temp.	Coating	Heat Pipe Cooling
Magnesium Castings				
46	704	370	boron nitride	N
47	704	365	boron nitride	Y
52	704	340	boron nitride	N
53	704	310	boron nitride	Y
56	704	275	boron nitride	N
49	704	265	boron nitride	Y
57	704	290	boron nitride	Y
62	704	260	graphite	N
66	704	270	graphite	Y
68	747	370	graphite	N
69	747	350	graphite	Y
Aluminum Castings				
74	728	370	graphite	N
75	728	360	graphite	N
76	728	360	graphite	Y
79	728	300	graphite	N
80	728	310	graphite	Y
81	722	260	graphite	N
83	722	245	graphite	Y

N= no heat pipe cooling

Y= Heat pipe cooling

4.2. Casting Analysis

Both visual and microstructural analysis were performed on the castings. The procedure used in the analysis, the results obtained and its discussions are given in the next sections.

4.2.1. Visual Analysis of Magnesium AZ91E

The first analysis method conducted was by looking visually at the castings to see the effect of heat pipe cooling. As mentioned earlier, the castings are grouped in pairs to represent castings cast under similar conditions except for the mold cooling.

Figures 4.2 and 4.3 show two side faces of one pair of magnesium castings produced under the same conditions. One casting has been produced without heat pipe cooling and the other with heat pipe cooling. Figures 4.4 and 4.5 show the other pair of magnesium castings.

By visually looking at the castings, one finds that the casting produced with no heat pipe cooling has no shrinkage voids appearing on the surface. This makes it difficult to evaluate visually the effect of heat pipe cooling on the casting. The reason behind no obvious visual concentrated shrinkage voids on the casting was because of the long freezing range of magnesium AZ91E (128 ^{o}C), where in alloys with long freezing ranges, a mushy solid plus liquid region develops before solidification is complete. Liquid metal does not easily flow through this region to compensate for solidification shrinkage. Consequently, widespread interdendritic shrinkage is typically found. On the other hand, short freezing range alloys tend to produce little or no mushy region; consequently, concentrated shrinkage voids are found [106]. Figure 4.6 shows the effect of freezing range on shrinkage.

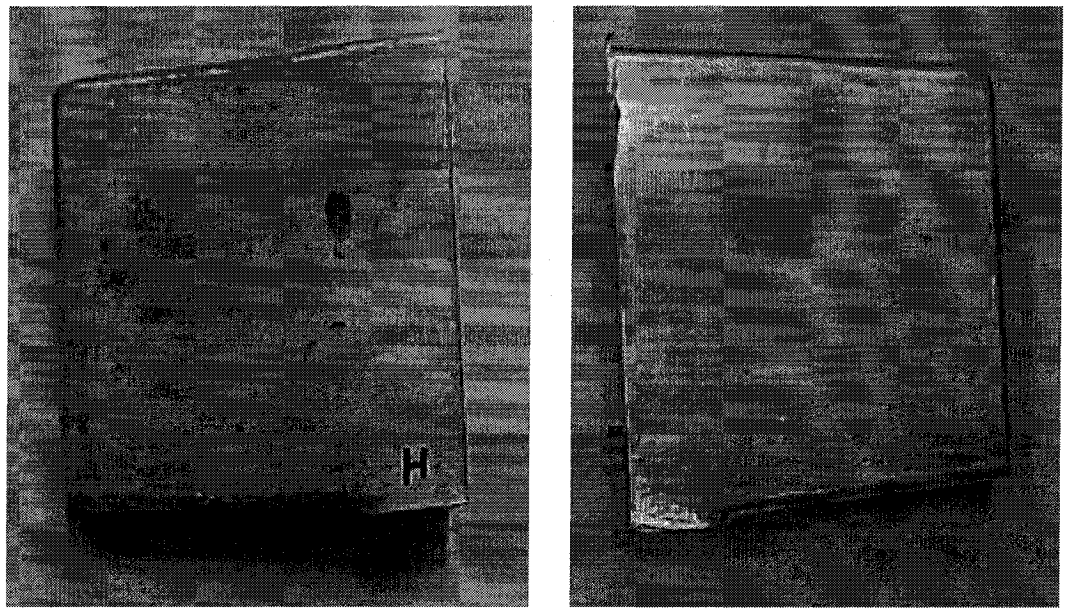

Figure 4.2. Magnesium casting produced without heat pipe cooling (H2)

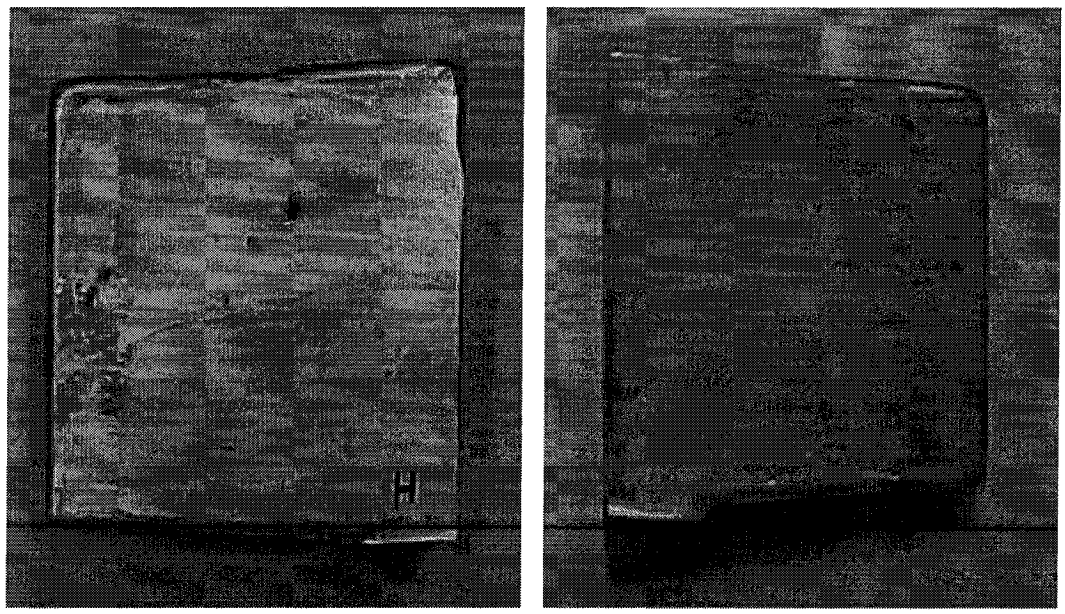

Figure 4.3. Magnesium casting produced with heat pipe cooling (H2)

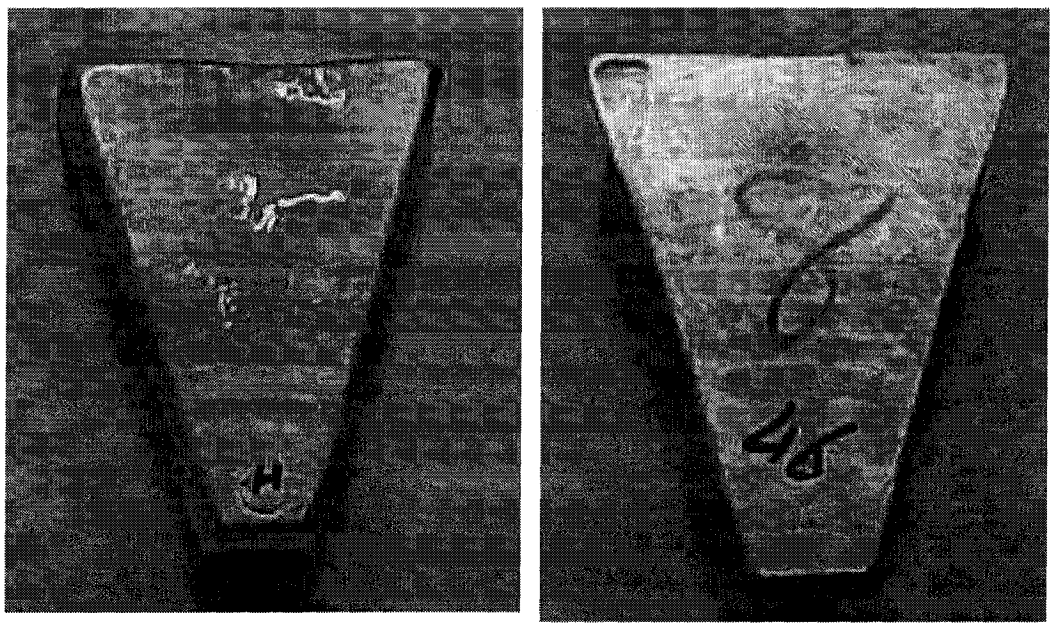

Figure 4.4. Magnesium casting produced without heat pipe cooling (H1)

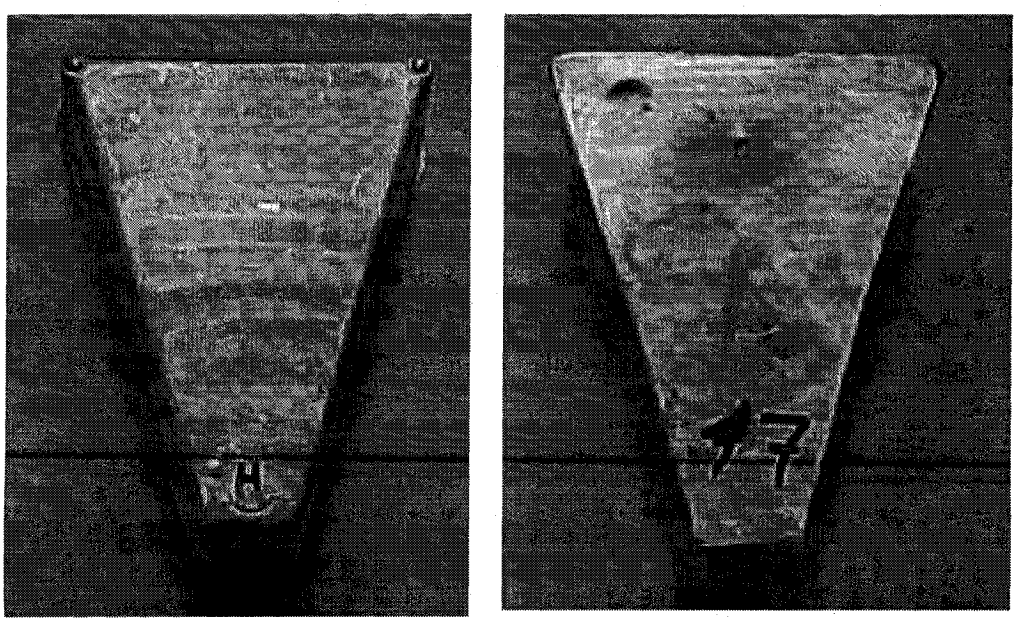

Figure 4.5. Magnesium casting produced with heat pipe cooling (H1)

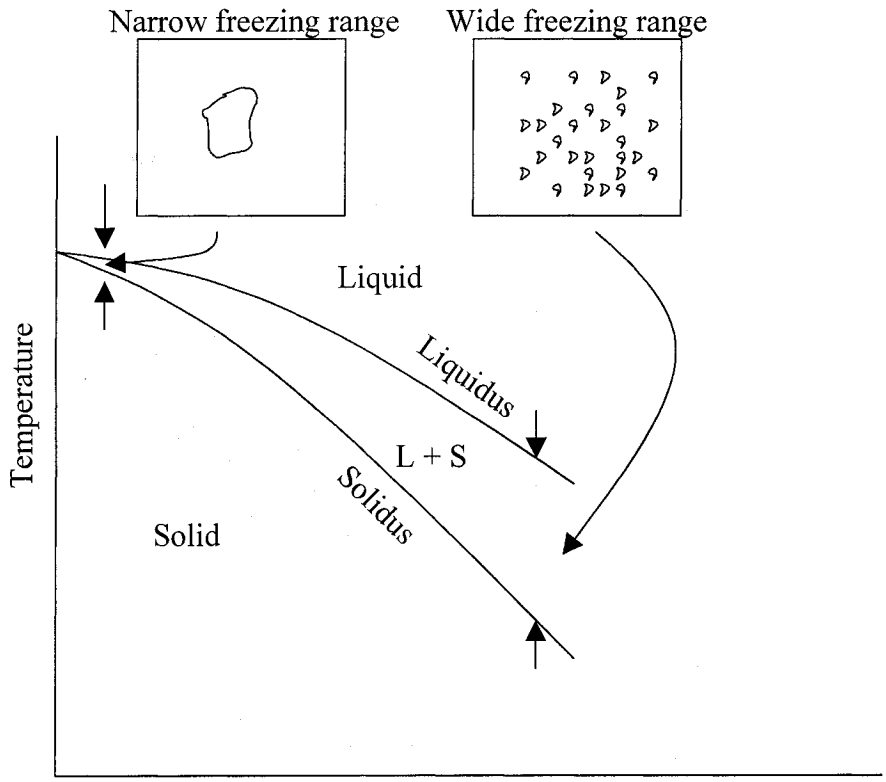

Figure 4.6. The effect of freezing range on shrinkage [106]

4.2.2. Visual Analysis of Aluminum Alloy (A356)

The same experiments were conducted for the shorter freezing range aluminum alloy (A356 with a freezing range of 70 °C). The results obtained demonstrate the effect of freezing range on alloy solidification.

Figure 4.7 shows the two sides of an A356 casting produced without cooling and figure 4.8 shows the same two faces of the A356 casting produced with heat pipe cooling.

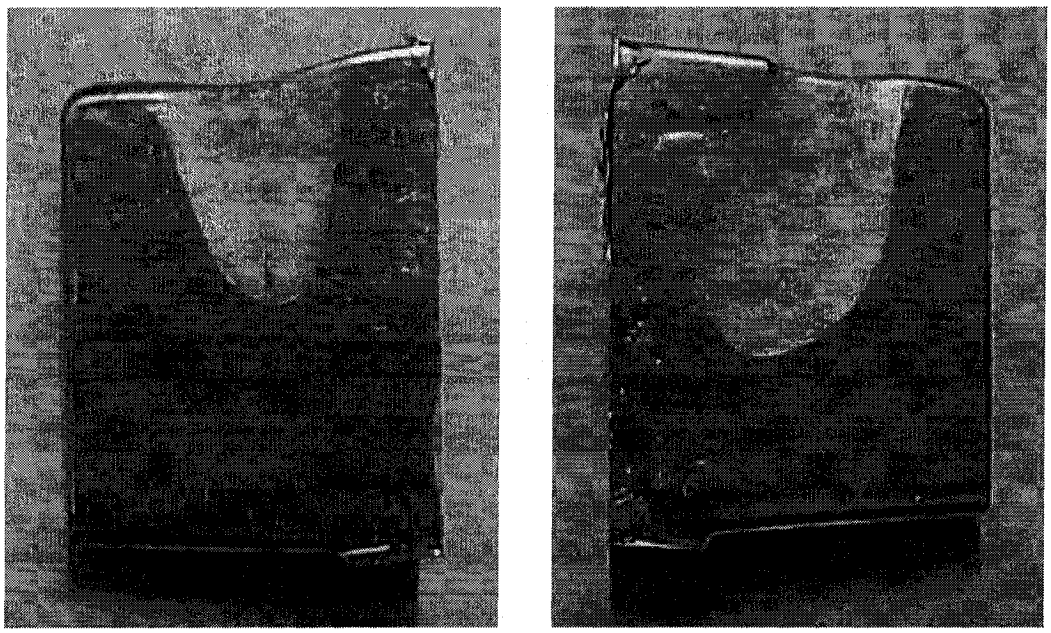

Figure 4.7. Aluminum casting produced without heat pipe cooling (H2)

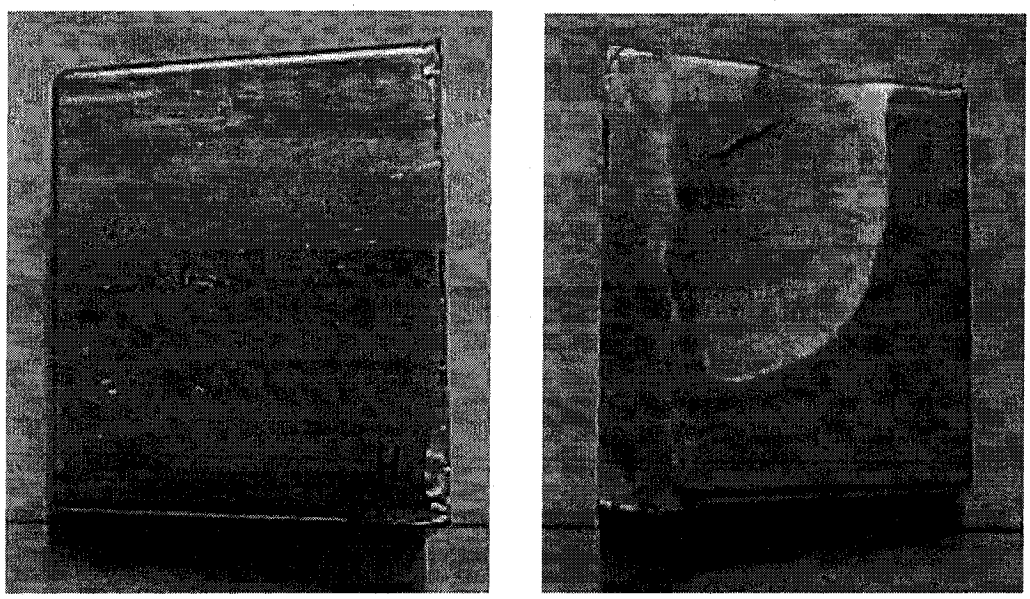

Figure 4.8. Aluminum casting produced with heat pipe cooling (H2)

From figure 4.7, one can see that the casting produced with no HP cooling developed a concentrated shrinkage void that can be seen visually on both sides. This is due to the shorter freezing range of A356 (70 ^{o}C) as explained earlier. Now looking at figure 4.8, where the A356 casting has been produced using heat pipe cooling, one can see

the improvement of casting quality on the casting side (face) adjacent to the heat pipe, where the big shrinkage void disappeared because of the rapid cooling provided by the heat pipe. On the other hand, a large shrinkage void developed on the other casting face (away from the HP). This shrinkage void is even larger than the one noted on the casting produced with no heat pipe cooling. This is an understandable phenomenon because the heat pipe succeeded in pushing the shrinkage from the side it faced to the other side. From these A356 casting analysis results, the effect of HP cooling is visually observed.

4.3. Computer Modeling as a Tool to Understand Casting Solidification Patterns

As mentioned earlier in chapter 3, the mold was designed with an intention to introduce shrinking in the castings produced from the magnesium and aluminum alloys. The temperature distribution results obtained by the computer modeling, as shown in figures 3.14 and 3.15, suggested shrinkage should appear in the center of both the magnesium and aluminum castings. When the theoretical results were compared with the actual castings of the magnesium and aluminum alloys, a difference in shrinkage type and location was observed. In other words, the expected shrinkage void predicted by the model for the magnesium casting did not appear on the actual casting, and the shrinkage void expected on the center of the aluminum casting by the computer modeling appeared with different shape and position on the actual casting.

An explanation of the different shrinkage type of the magnesium alloy is given in section 4.2.1 and further discussion will be given later in the present section.

The disagreement between the modeling and the actual aluminum castings in terms of shrinkage location led to a second look at the casting boundary conditions used in modeling.

As one can see, the two castings produced by the mold were fed from the bottom. Also the castings had greater metal mass in their upper parts. Because of this configuration, the upper edge of the casting will lose contact with the mold due to gravity, which tends to pull the casting downward. In addition to that, a force will tend to pull the casting downward when the casting starts to solidify first at the lower section (less metal compared to the upper section) where the molten metal from the upper part will flow to compensate for solidification shrinkage. The two forces (gravity and pulling force) will prevent the upper edge of the casting to have contact with the mold and this will lead to poor heat transfer at the edge and will effect the overall modeling results. Figure 4.9 shows the upper surface of the A356 casting where the shrinkage was severe due to the imperfect contact between the casting and the mold.

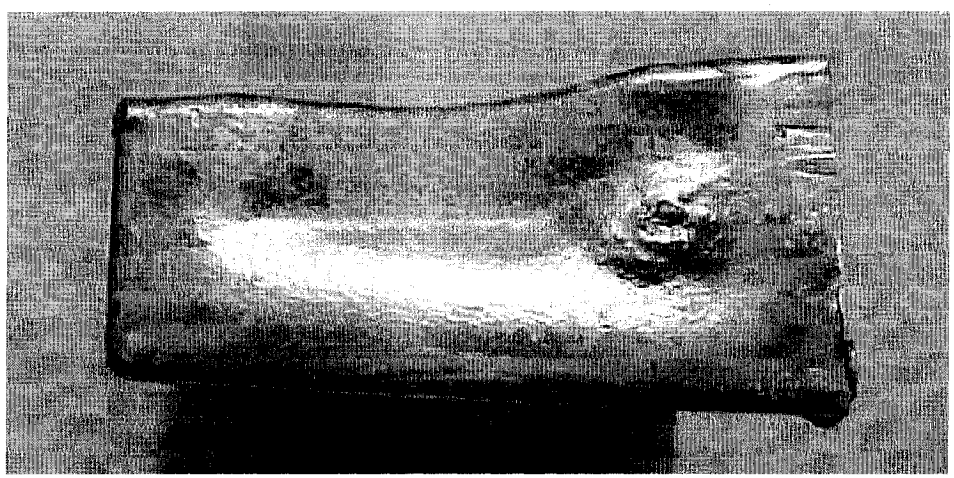

Figure 4.9. The upper surface of the A356 casting (H2)

A new computer modeling was conducted for the aluminum A356. The boundary conditions used in this modeling were the same as the first modeling except that the value

of the interfacial heat transfer coefficient, h, at the upper edge of the casting was lowered to 100 W/m^2-K to make the modeling results align with the experimental observations. The temperature distribution results obtained from the model for both casting sides (facing the heat pipe and far from the heat pipe) of one A356 casting produced without and with heat pipe cooling are given in figures 4.10 and 4.11 respectively.

When looking at figures 4.10 and 4.11, one can see that the shape and location of the shrinkage predicted by modeling are similar to the ones observed on the real castings seen in figures 4.7 and 4.8.

The previous observation is important evidence that shows the casting boundary conditions used in the computer modeling approximate reality well; thus, one can rely on the results produced by the model. In addition to that, one can see also the importance of understanding the casting conditions in order to obtain reliable casting modeling. The computer modeling for the magnesium AZ91E was repeated based on the new corrected boundary condition.

Figures 4.12 and 4.13 show the computer modeling results for the temperature distribution for the AZ91E and A356 castings respectively produced with no heat pipe cooling. The figures show one side of the castings. The other side of each casting looks the same due to the casting symmetry along its centerline. From these figures one can clearly see the hot regions where shrinkage is expected to appear in real castings. Figures 4.14 and 4.15 show the computer modeling results for the temperature distribution for the AZ91E and A356 castings respectively produced with heat pipe cooling. The figures show both casting sides. From these figures, one can see that the heat pipe cooling managed to force the hot regions to the other side of the castings for both alloys. This demonstrates the effectiveness of using heat pipe cooling to reduce shrinkage defects in castings. Figures 4.16 and 4.17 show the computer modeling results for the temperature distribution for a plane cut through the AZ91E and A356 castings respectively produced without heat pipe cooling. The cut was taken at the middle of the hot region of the

casting. Figures 4.18 and 4.19 show the computer modeling results for the temperature distribution for a plane cut of AZ91E and A356 castings respectively produced with heat pipe cooling.

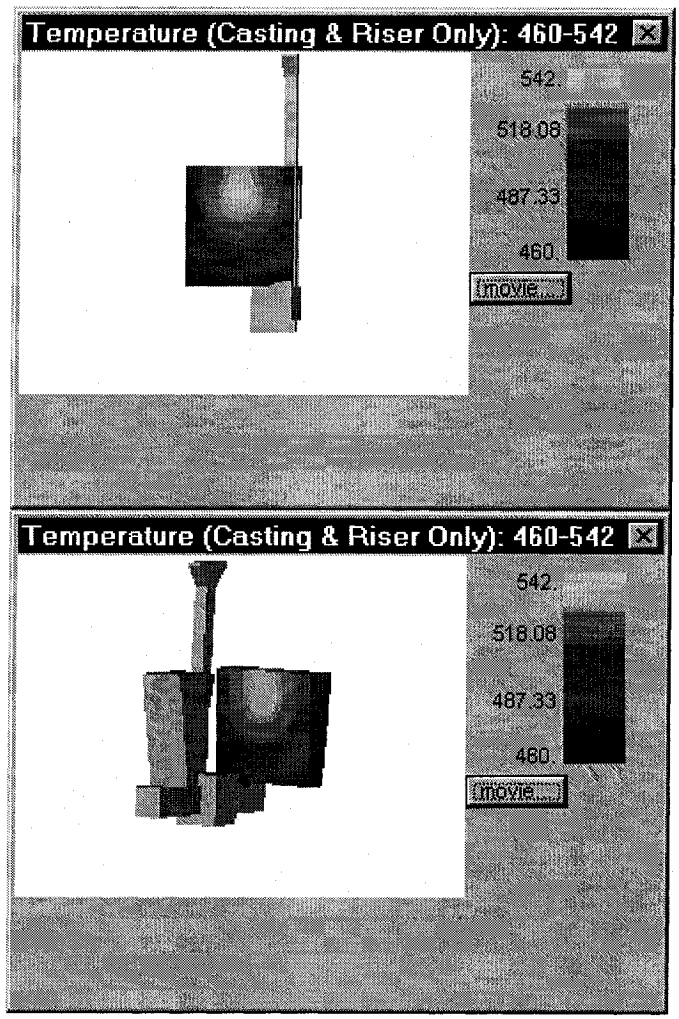

Figure 4.10. Temperature distribution results obtained from the model for one A356 casting (with no heat pipe cooling)

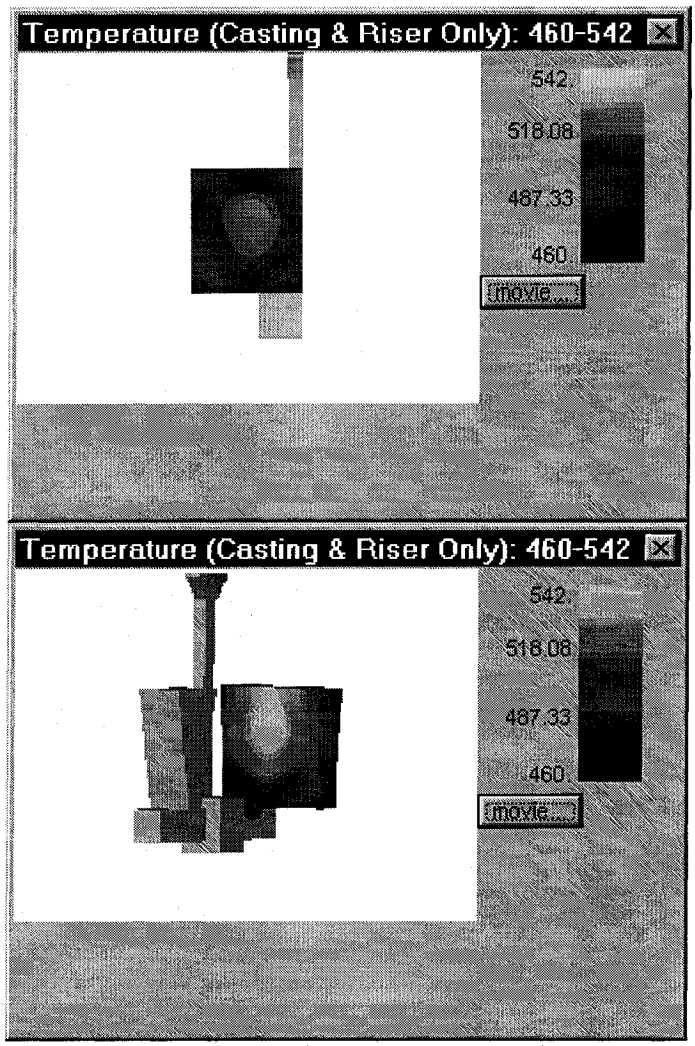

Figure 4.11. Temperature distribution results obtained from the model for one A356 casting (with heat pipe cooling)

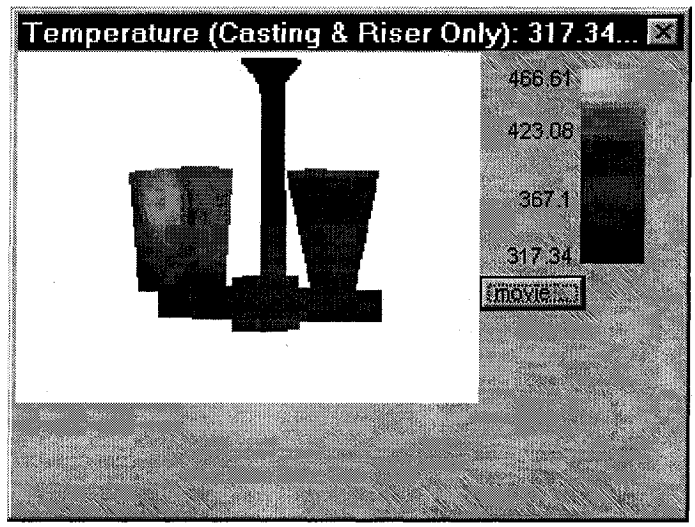

Figure 4.12. Temperature distribution results obtained from the model for AZ91E casting (with no heat pipe cooling)

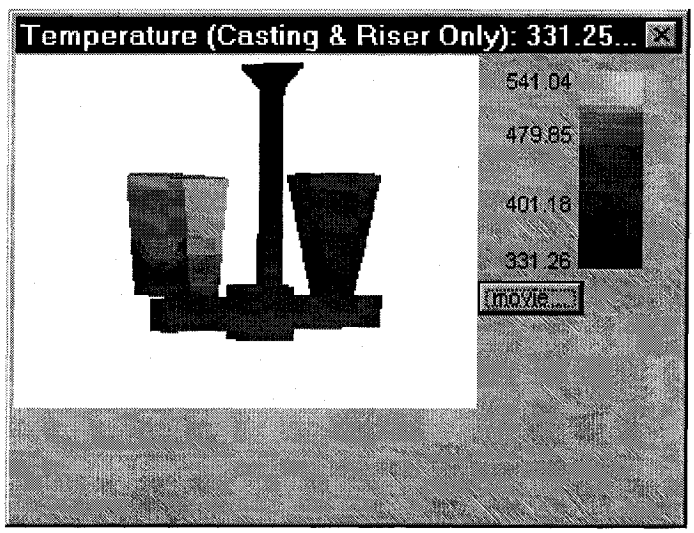

Figure 4.13. Temperature distribution results obtained from the model for A356 casting (with no heat pipe cooling)

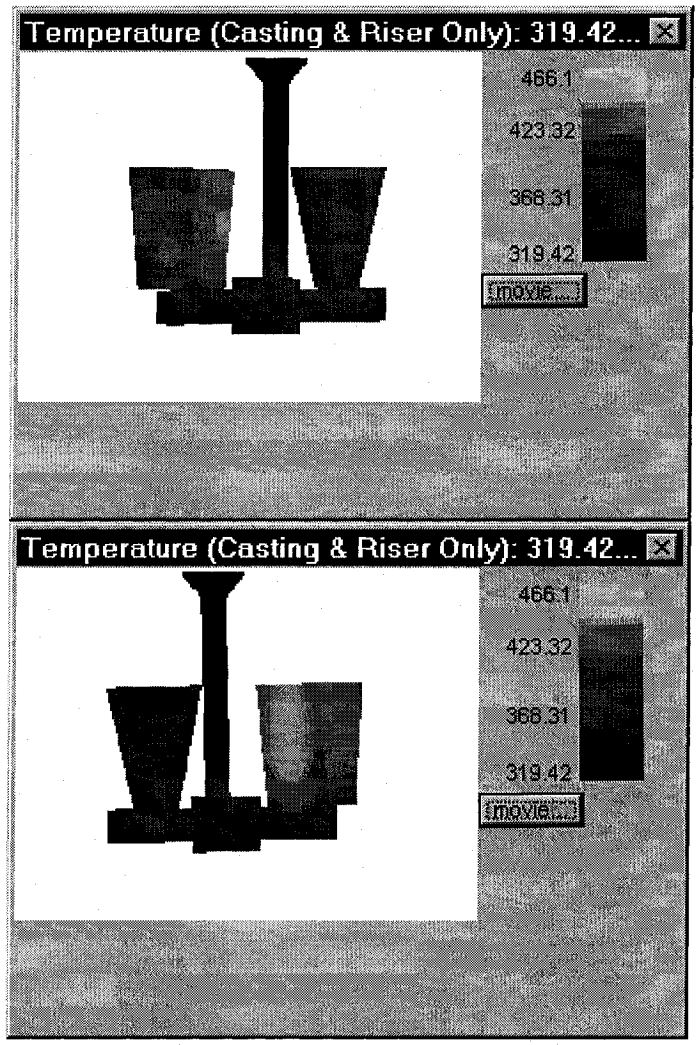

Figure 4.14. Temperature distribution results obtained from the model for both sides of AZ91E casting (with heat pipe cooling)

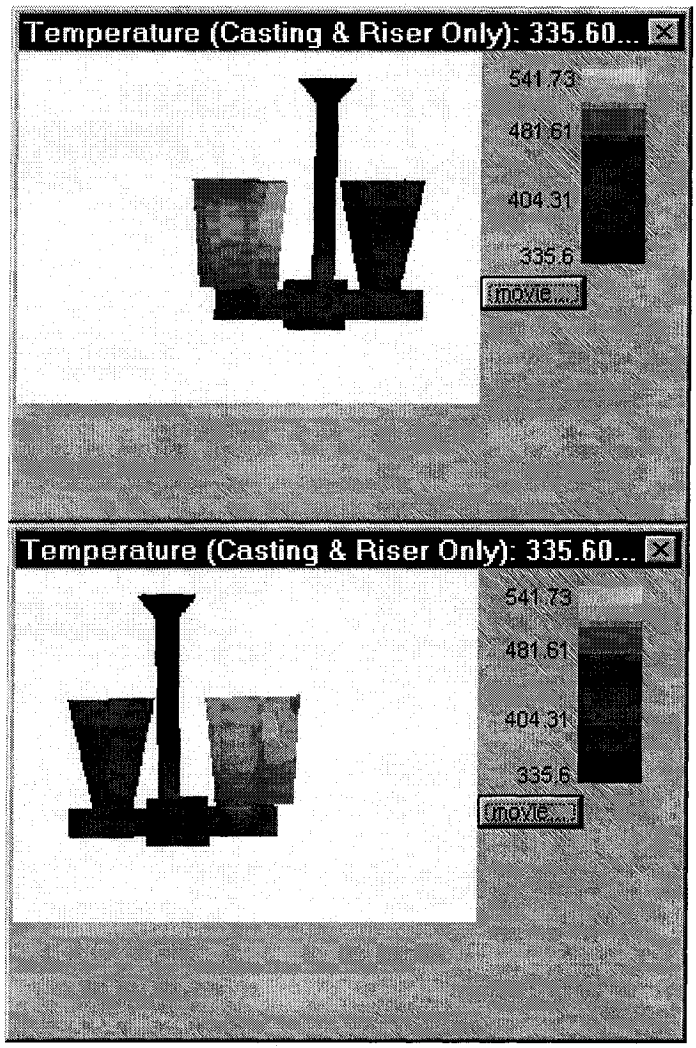

Figure 4.15. Temperature distribution results obtained from the model for both sides of A356 casting (with heat pipe cooling)

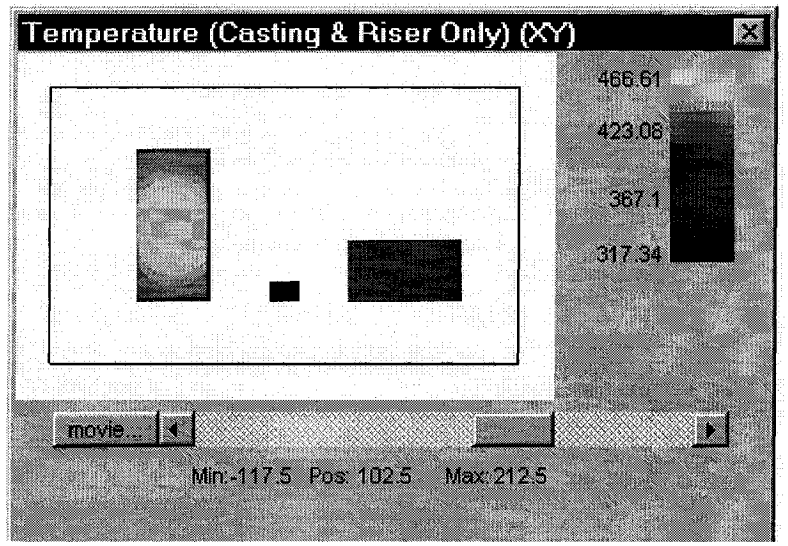

Figure 4.16. Temperature distribution obtained from the model for a plane cut of AZ91E casting (without heat pipe cooling)

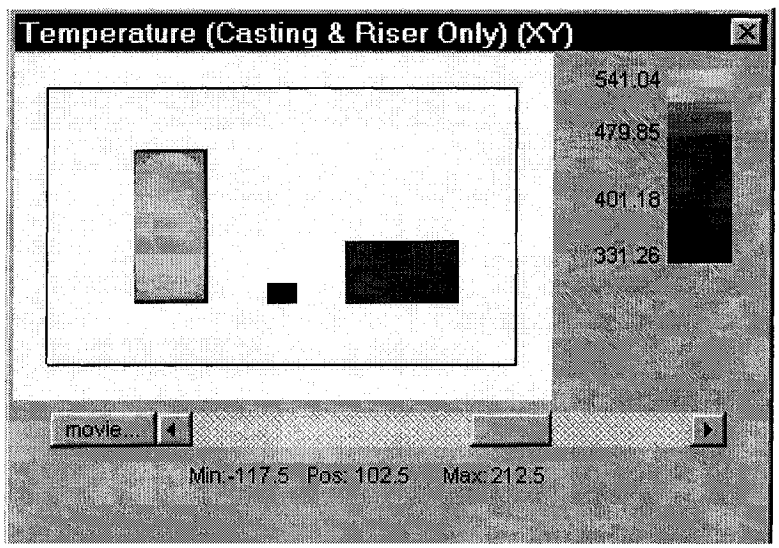

Figure 4.17. Temperature distribution obtained from the model for a plane cut of A356 casting (without heat pipe cooling)

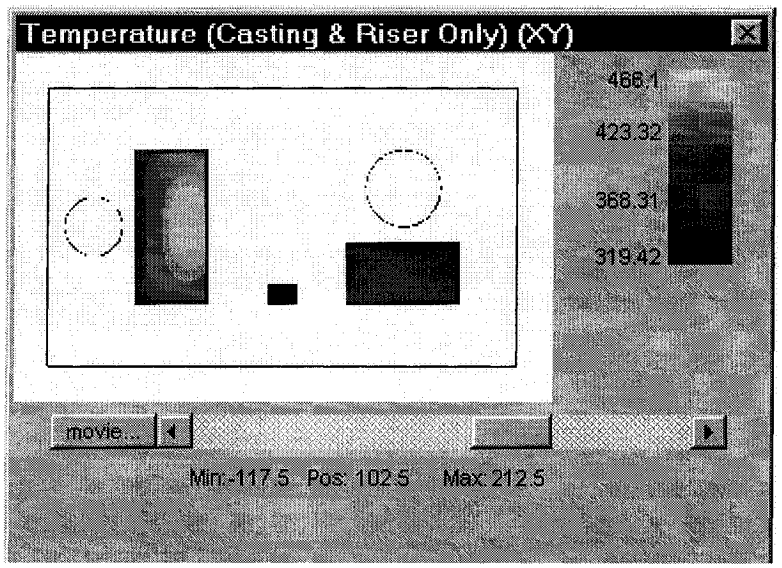

Figure 4.18. Temperature distribution obtained from the model for a plane cut of AZ91E casting (with heat pipe cooling)

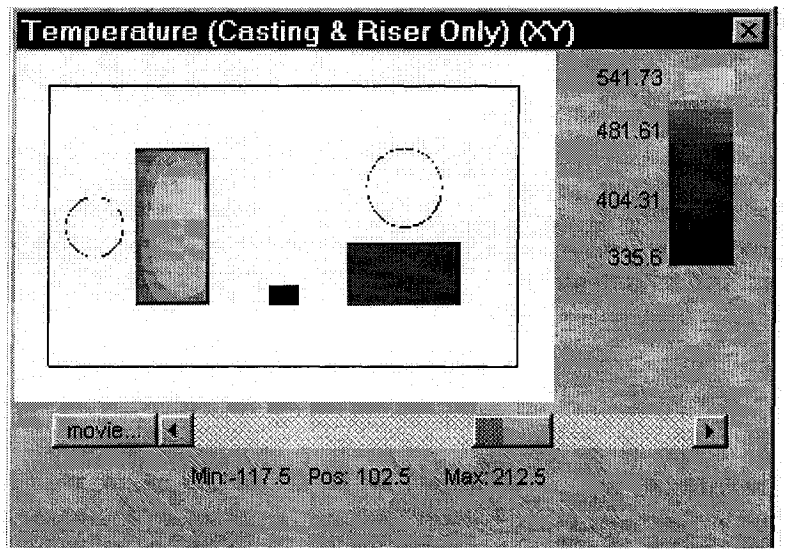

Figure 4.19. Temperature distribution obtained from the model for a plane cut of A356 casting (with heat pipe cooling)

From figures 4.16 to 4.19, one can clearly see the effect of heat pipe cooling on the castings and how the heat pipes managed to reduce the hot spot from the casting faces closest to the heat pipes.

For a better understanding of the above temperature distribution results obtained by the model, seven points in the casting have been selected and their temperatures have been determined by the model. Figure 4.20 show the points selected. The time at which the temperatures at these points were analyzed corresponds to the time when the casting has just completely solidified.

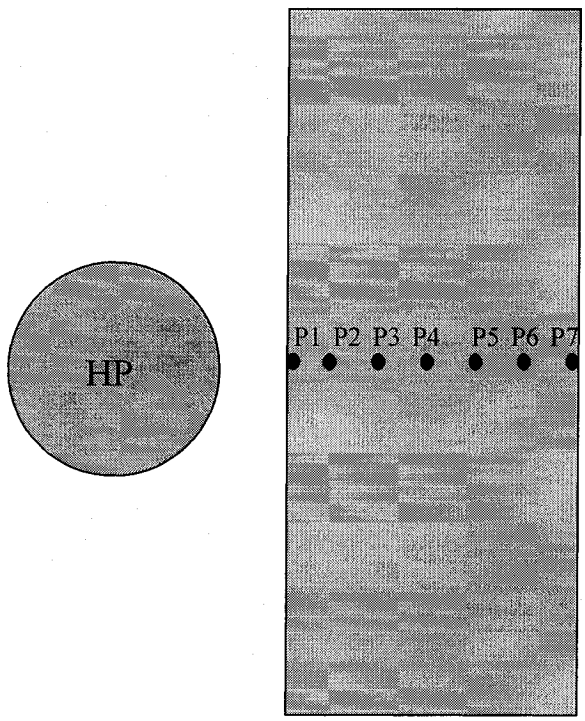

Figure 4.20. Points selected for temperature measurements (H2)

The model was used to obtain the temperature at these seven points for AZ91E casting with no heat pipe cooling, A356 with no heat pipe cooling, AZ91E casting with heat pipe cooling, and A356 with heat pipe cooling respectively. The results obtained from the model are shown in table 4.2.

Table 4.2. Temperature distribution results obtained from the model (H2, 100% solid)

Casting	Temperature (°C)						
	P1	P2	P3	P4	P5	P6	P7
AZ91E	451.4	458.7	461	461.5	461	458.7	451.4
A356	530	535.3	537	537.4	537	535.3	530
AZ91E (HP)	385.5	403.6	430.5	440	451.5	453.7	451.2
A356 (HP)	488.8	500.2	517.2	523.1	530.1	531.2	529

P = Point, HP = heat pipe cooling

From the above table, one can see the effect of heat pipe cooling on the casting by comparing the temperature at each location with and without heat pipe operation. The effect reached little more than half of the casting (reaches point 5). The heat pipe has pushed the hot spot to the other side.

Figures 4.21 and 4.22 show the temperature distribution at a plane cut through the whole mold obtained by the model for the AZ91E and A356 casting processes with heat pipe cooling.

From figures 4.21, and 4.22, one can see the effect of heat pipes on the mold and the castings. The figures show heat pipes at a low temperature, which managed to redistribute the heat in a wide region of the mold. The regions close to the heat pipes have lower temperatures compared to other regions of the mold.

As mentioned earlier, by examining the castings produced with no heat pipe cooling during the industrial trials of the aluminum A356 alloy, one can see huge shrinkage voids in both sides of the castings as seen in figure 4.7, and this agrees very well with the computer modeling results seen in figure 4.10.

As seen in figure 4.8, the heat pipe was successful in forcing the shrinkage void from the side facing the heat pipe to the other side far from the heat pipe as expected by the computer modeling results seen in figure 4.11. The casting side closer to the heat pipe started to solidify sooner compared to the other side of the casting far from the heat

pipe and that was due to the rapid cooling provided by the heat pipe. In such cases, liquid metal flows towards the solidifying side to compensate for the solidification shrinkage. This leads to greater shrinkage voids at the casting side far from the heat pipe as seen in figures 4.8 and 4.11.

As mentioned earlier, when the magnesium AZ91E castings were examined, the expected shrinkage voids on both casting sides were not observed even though the computer modeling results showed hot regions on both sides of the casting as seen in figure 4.12, which leads to shrinkage void presence. As seen from figures 4.2 and 4.4, no concentrated shrinkage voids were seen on either casting face. Instead, widely distributed micro-shrinkage voids were observed in the AZ91E castings as seen in figure 4.23.

The above observation (different shrinkage types between the AZ91E and A356) has raised a flag and a further investigation was conducted to reveal the difference in solidification behavior between magnesium AZ91E and aluminum A356. Another look at the computer results was needed to further understand the solidification behaviors of these alloys.

The modeling results of the critical fraction solid time for both alloys were obtained. The critical fraction solid time records the time, in minutes, for each part of the casting to reach the critical fraction solid point. This is the point at which the alloy is solid enough that liquid feed metal can no longer flow. Therefore, for judging directionality of solidification, and whether any isolated areas have formed within the casting that cannot be fed by risers, the critical fraction solid time is generally a better measure than the solidification time [105]. Figures 4.24 and 4.25 show the modeling results of the critical fraction solid time for the AZ91E and A356 castings respectively with no heat pipe cooling. In these two figures, the time scale is in minutes and time = 0 indicates the time when the mold cavities were completely full with the liquid metal.

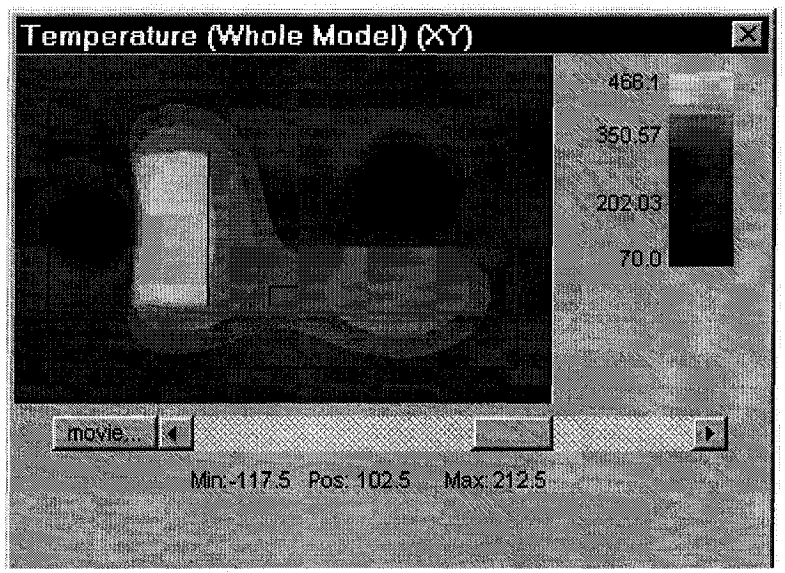

Figure 4.21. A plane cut temperature distribution results obtained from the model for the whole mold (AZ91E casting with heat pipe cooling)

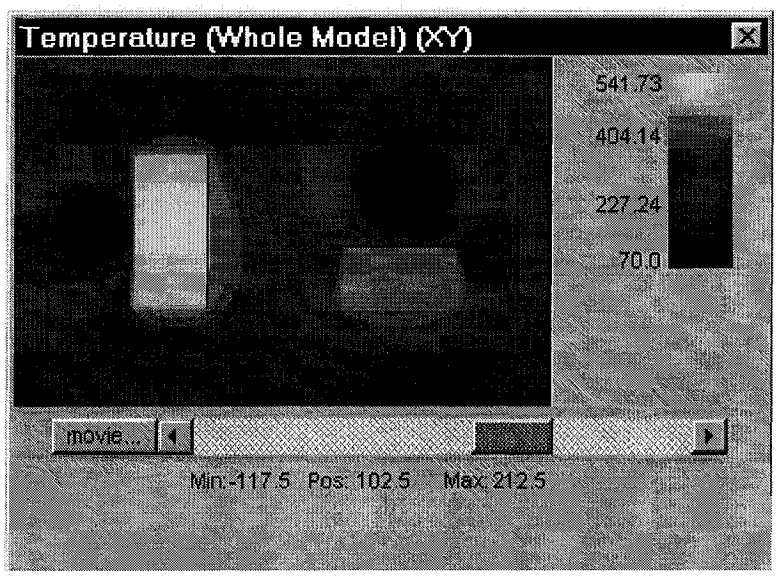

Figure 4.22. A plane cut temperature distribution results obtained from the model for the whole mold (A356 casting with heat pipe cooling)

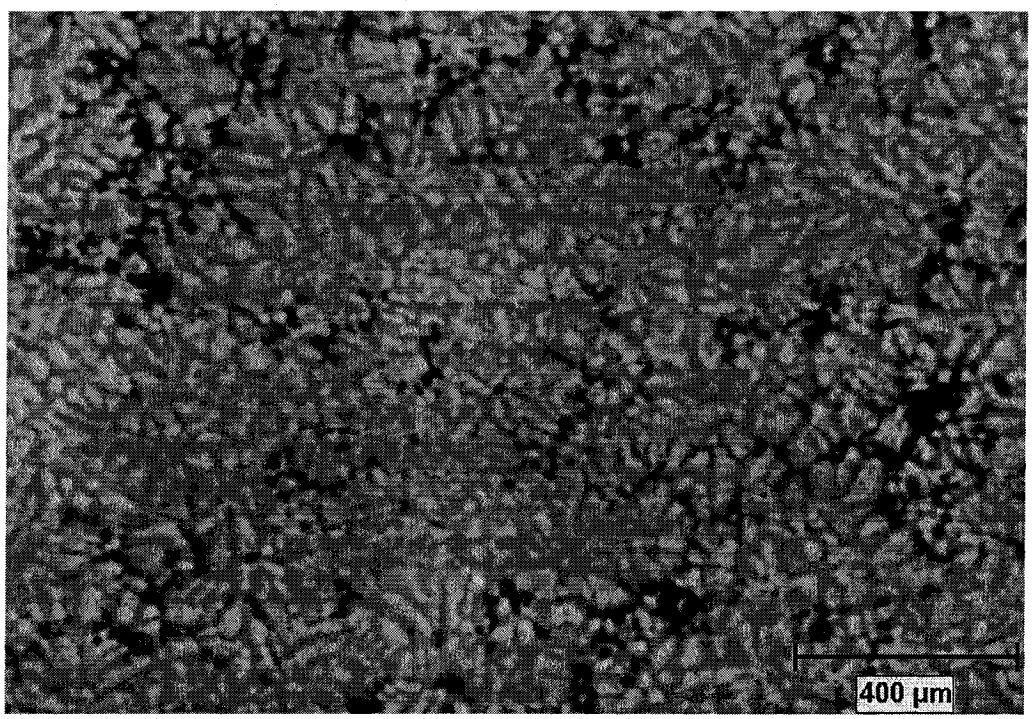

Figure 4.23. Micro-shrinkage defect in AZ91E

Figure 4.26 and figure 4.27 show the modeling results of the critical fraction solid time in minutes for the two casting sides of AZ91E and A356 respectively with heat pipe cooling.

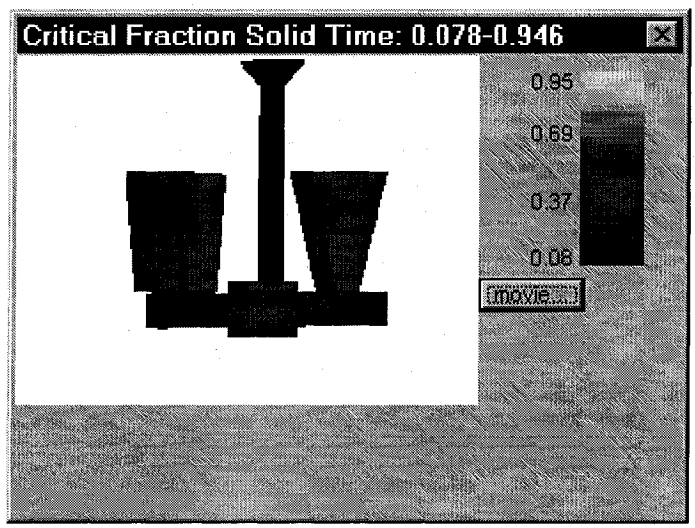

Figure 4.24. Critical fraction solid time results obtained from the model for AZ91E casting (with no heat pipe cooling)

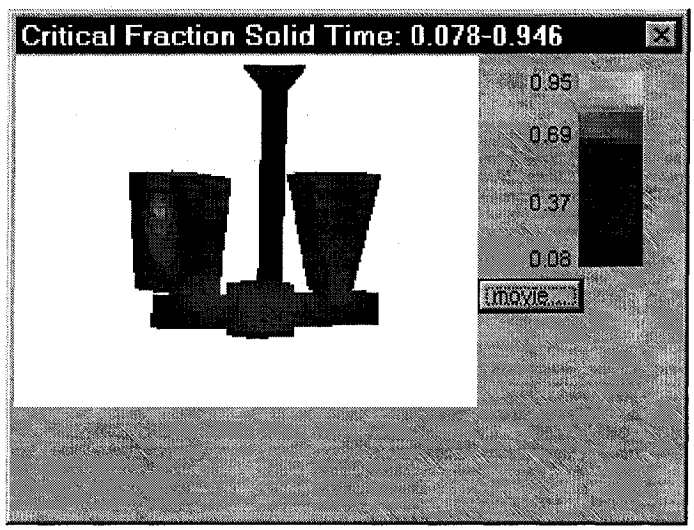

Figure 4.25. Critical fraction solid time results obtained from the model for A356 casting (with no heat pipe cooling)

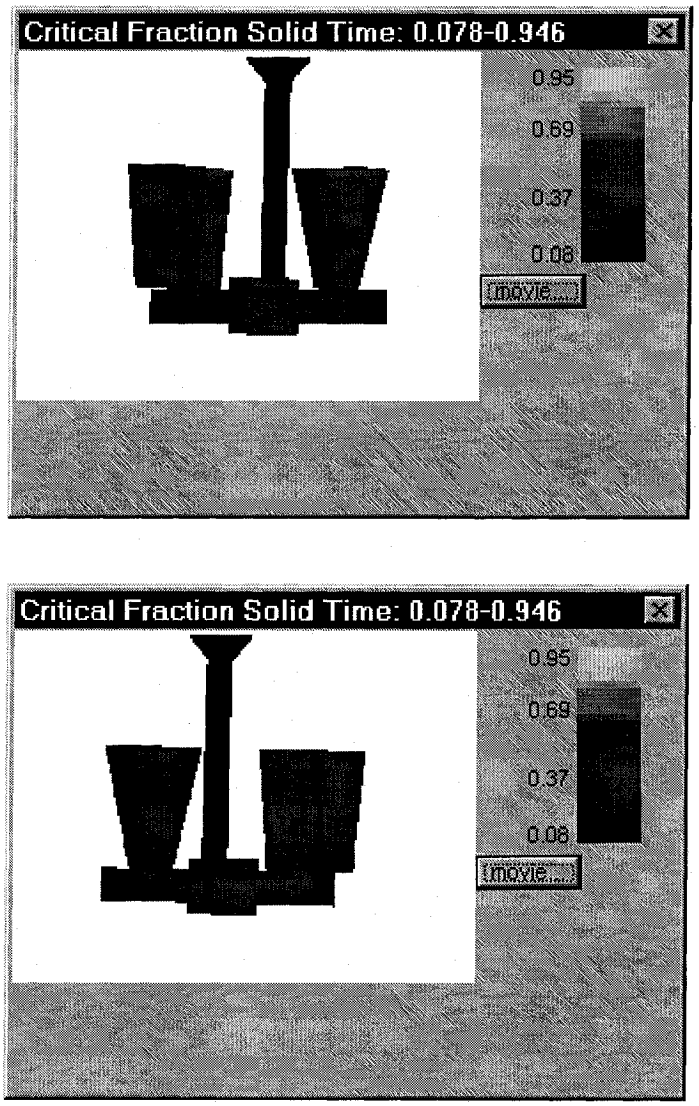

Figure 4.26. Critical fraction solid time results obtained from the model for AZ91E two casting sides (with heat pipe cooling)

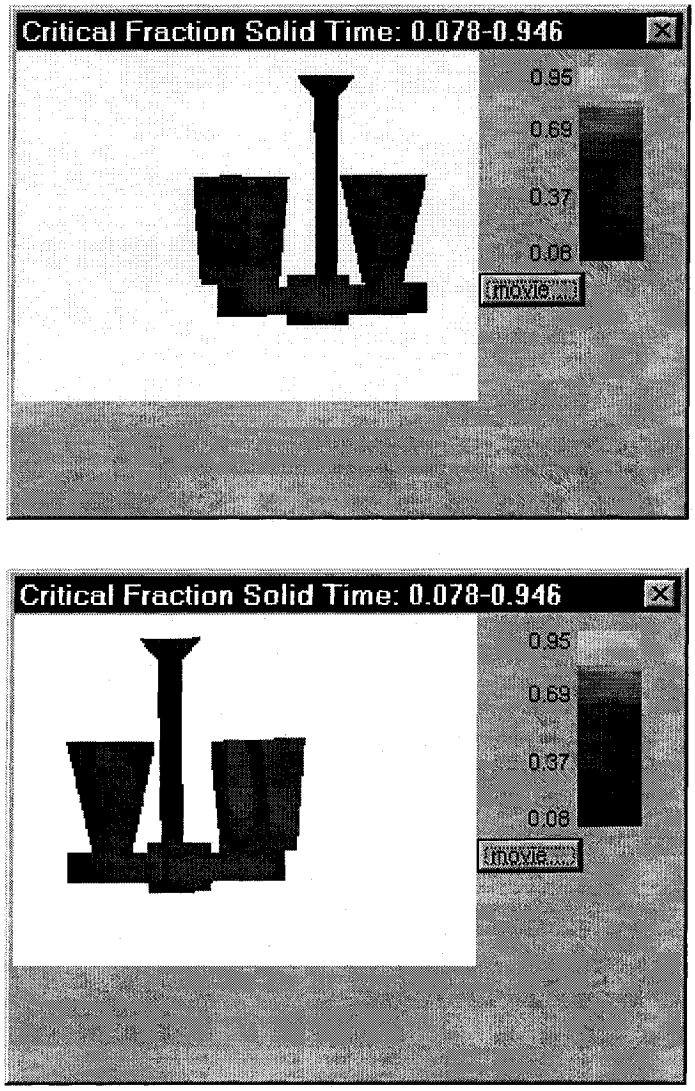

Figure 4.27. Critical fraction solid time results obtained from the model for A356 two casting sides (with heat pipe cooling)

The critical fraction solid time modeling results for both alloys showed different solidification behavior. By looking at the modeling results shown in figures 4.24 and 4.25, one can see that AZ91E solidifies faster than A356 alloy where the maximum critical fraction solid time for AZ91E is 0.76 min and for A356 is 0.95 min. This shows

that the critical fraction solid time for AZ91E is 20% less than that for A356. In both figures the time scale was set to 0.95 min for better comparison between the alloys.

Reasons for the above are related to the fact that AZ91E has a density of 1810 kg/m^3 which is substantially less than the density of A356, 2685 kg/m^3. This leads to a lower latent heat per unit volume for AZ91E (371904 J/kg) as compared to A356 (388175 J/kg) and this, in turn contributes to the poor solidification behavior of AZ91E and the presence of micro-shrinkage voids. In addition to that, it explains the critical fraction solid time difference between both alloys.

The shorter critical fraction solid time of the AZ91E alloy allowed solid islands to be formed in the early solidification stages and those islands are solid enough that liquid metal can no longer flow through. This is an important factor, which can explain the micro shrinkage defects present in the AZ91E castings as seen in figure 4.23. In the case of A356 which has a longer critical fraction solid time, the formation of those solid islands happens at later stages of the solidification process, thus there is less chance for micro shrinkage formation. The concentrated shrinkage void normally found is shown in figure 4.7.

Figures 4.28 and 4.29 show the critical fraction solid time in minutes at a plane cut (1 cm from the top of the casting) of the AZ91E and A356 castings simulated with no heat pipe cooling respectively. Figures 4.30 and 4.31 show the critical fraction solid time in minutes at a plane cut of the AZ91E and A356 castings simulated with heat pipe cooling respectively. From these figures, one can see the effect of heat pipe cooling on the critical fraction solid time where the casting side facing the heat pipe has shorter time compared to the other side.

The freezing range of the alloy is an important factor, which determines the type of shrinkage present in a casting. The two alloys studied in this work, AZ91E and A356,

have different freezing ranges. AZ91E has a long freezing range (128 °C) compared to A356 (70 °C), and that leads to different solidification patterns.

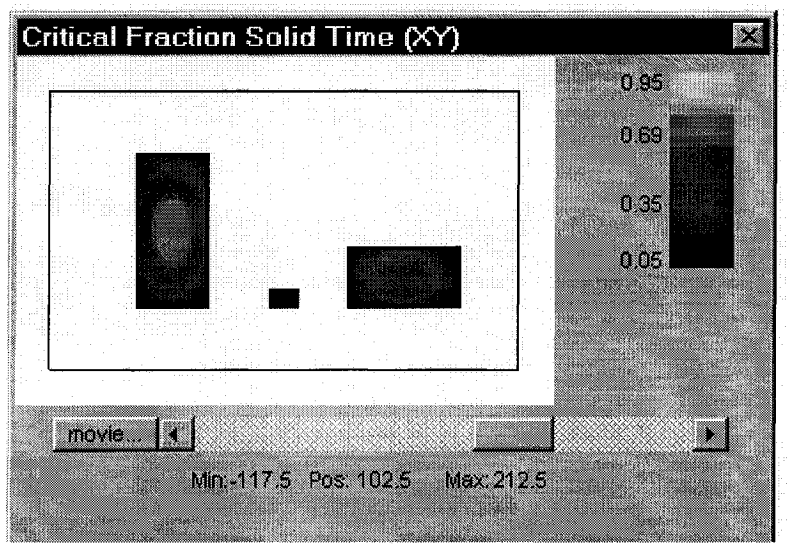

Figure 4.28. The critical fraction solid time at a plane cut of AZ91E casting simulated with no heat pipe cooling

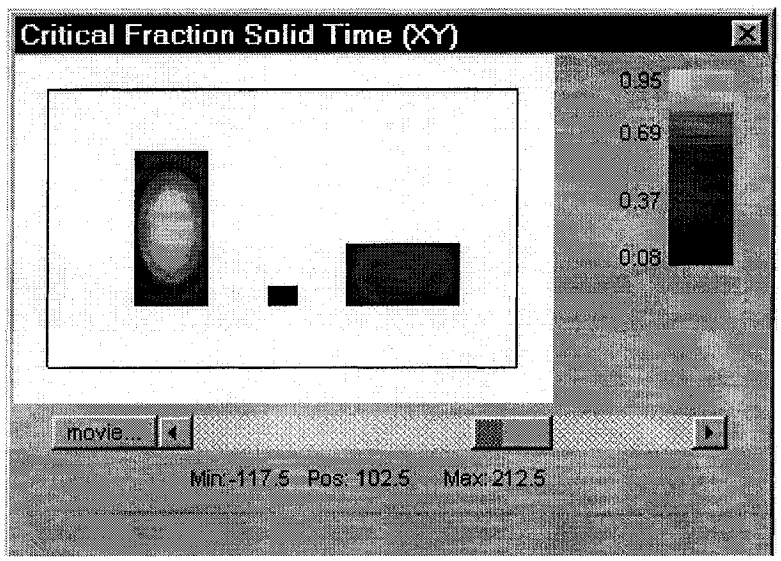

Figure 4.29. The critical fraction solid time at a plane cut of A356 casting simulated with no heat pipe cooling

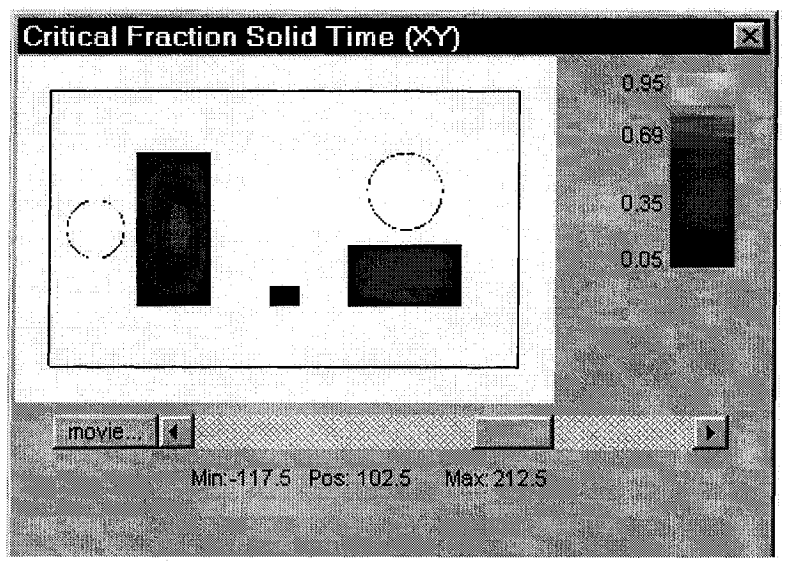

Figure 4.30. The critical fraction solid time at a plane cut of AZ91E casting simulated with heat pipe cooling

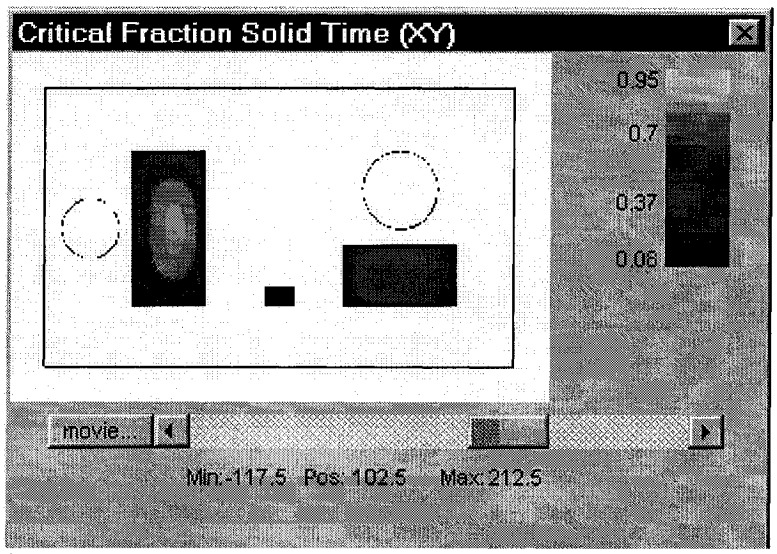

Figure 4.31. The critical fraction solid time at a plane cut of A356 casting simulated with heat pipe cooling

As mentioned earlier, in the case of alloys with long freezing range such as AZ91E a mushy or pasty solid plus liquid region develops before solidification is complete [106]. This will lead to the formation of solid and liquid islands. Because of this mushy zone, the liquid does not flow easily to compensate for the solidification shrinkage, and widespread interdendritic shrinkage is typically found. In this case, even using massive risers may not be sufficient. Figure 4.6 shows a schematic for the effect of freezing range on shrinkage.

This is not the case for A356, which has a relatively shorter freezing range with little mushy region where the liquid metal flows easily to compensate for shrinkage. In this case typical concentrated shrinkage voids can be controlled by risers. Such a shrinkage is clearly seen in figure 4.7.

The above explanation also shows the reason behind the longer critical fraction solid time for A356 compared to AZ91E.

Another look at the critical fraction solid time results was obtained by looking at the values of the critical fraction solid time at the seven points seen in figure 4.20. The results are shown in table 4.3.

Table 4.3. The critical fraction solid time for AZ91E and A356 (H2)

Casting	Critical Fraction Solid Time (min)						
	P1	P2	P3	P4	P5	P6	P7
AZ91E	0.421	0.656	0.711	0.727	0.711	0.656	0.421
A356	0.615	0.841	0.893	0.905	0.893	0.841	0.615
AZ91E (HP)	0.125	0.252	0.535	0.605	0.644	0.612	0.414
A356 (HP)	0.203	0.379	0.698	0.758	0.797	0.77	0.584

P = Point, HP = heat pipe

From the above table, one can see that AZ91E has much shorter critical fraction solid time compared to A356 and hence, AZ91E tends to have more micro-shrinkage instead of a concentrated shrinkage void.

The above table also shows the great effect of the heat pipe in reducing the critical fraction solid time for both alloys. The heat pipe with its rapid cooling reduced the overall critical fraction solid time by 13% for AZ91E and 14% for A356. However, for regions close to the heat pipe the reductions in the critical fraction solid time was substantially greater.

4.4. Microstructural Analysis of Magnesium AZ91E

The effect of heat pipe cooling on the magnesium castings was also demonstrated by measuring the secondary dendrite arm spacing, (SDAS) and the grain size. A specimen was cut from the center of each casting through the thickness of the casting. Figure 4.32 shows the specimen location. Three points were chosen for the SDAS and grain size measurements. Point number 1 is close to the heat pipe, point number 2 is inside the casting and point number 3 is on the far side of the casting. Point numbers 1 and 3 are 2 mm away from the edge to avoid mold chilling effects. The SDAS and grain size measurement results obtained for pairs of magnesium castings are given in the following sections.

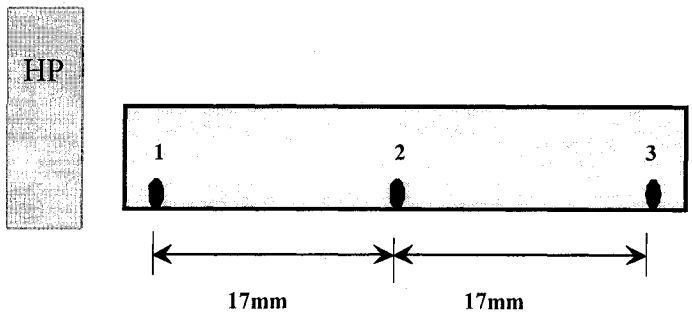

Figure 4.32. SDAS measurement specimen

After polishing and etching the specimens, the SDAS and grain size analyses were performed using an optical microscope with a digital image analysis system (CLEMEX Vision ^{TM}).

4.4.1. SDAS Analysis for Magnesium AZ91E

After polishing, the specimens were etched using acetic glycol (20ml acetic acid, 1 ml HNO_3 (conc.), 60 ml ethylene glycol, 20 ml water) for 10 seconds. The line intercept method was used to measure the SDAS. The SDAS results obtained for two pairs of castings are shown in Figures 4.33 and 4.34. The standard deviation is shown on the figures.

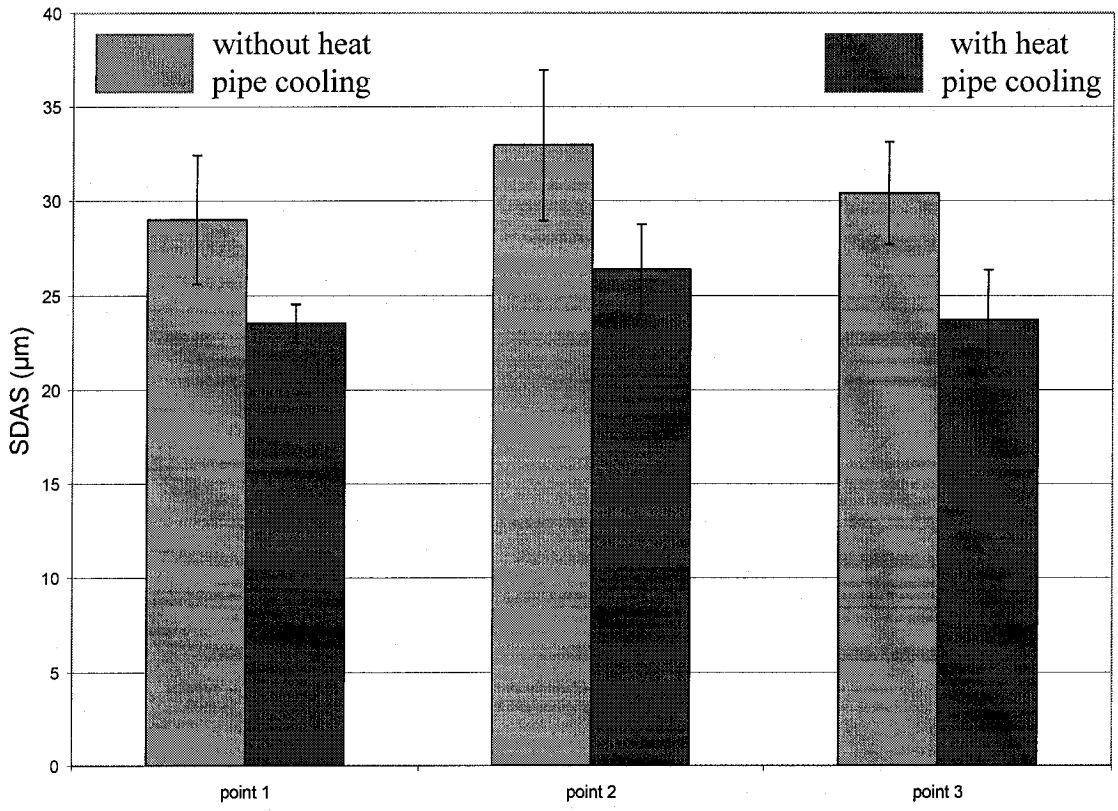

Figure 4.33. SDAS results for magnesium AZ91E (casting no. 46&47 H1)

From Figure 4.33, one can see the effect of heat pipe cooling on SDAS at all three points, especially point number 1 which is close to the heat pipe. At point number 1, a reduction of 19% in the SDAS is obtained by using heat pipe cooling. At the other two points, point 2 and point 3, reductions of 20% and 22% were obtained respectively. The

standard deviation for the SDAS analysis was reasonable (1~ 4 μm) as shown on the figure.

The SDAS results demonstrate clearly the effect of heat pipe cooling on the SDAS. The SDAS at point number 2 tends to be larger than that at point number 3. This is because there is not much mold mass near point 2 to enhance cooling. The effect of heat pipe cooling on SDAS of magnesium casting is very well pronounced in figure 4.34

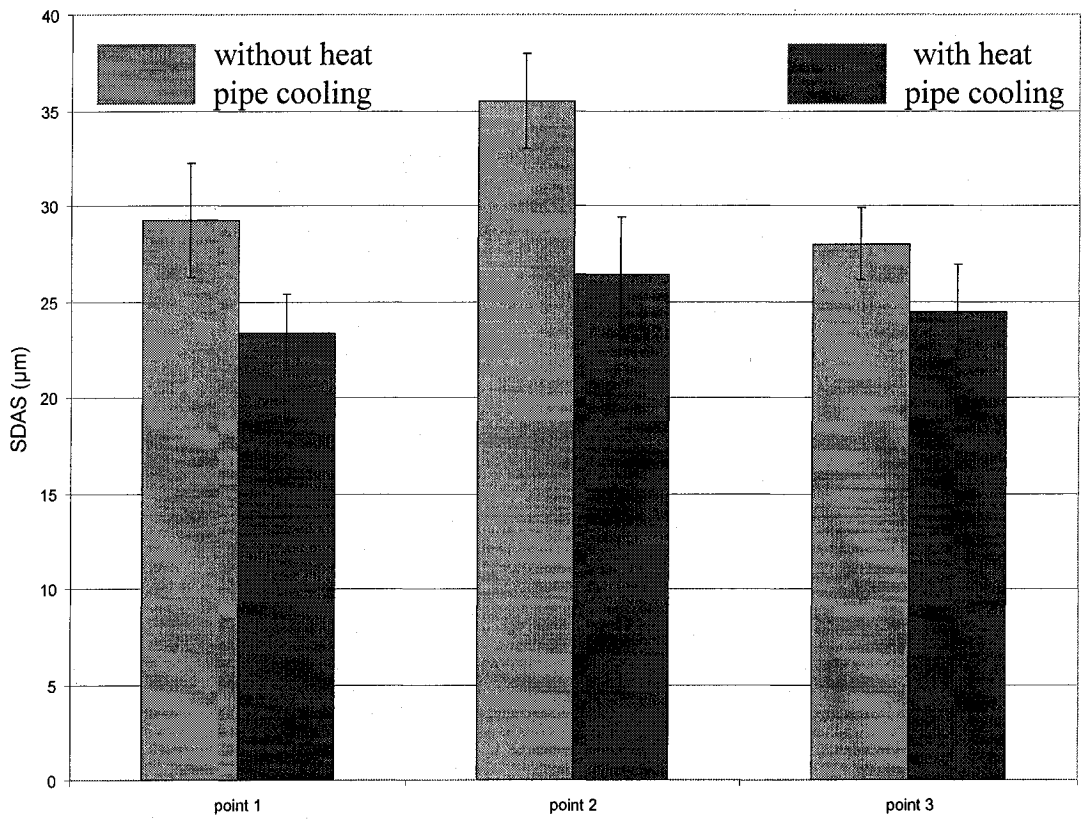

Figure 4.34. SDAS results for magnesium AZ91E (casting no. 46&47 H2)

as well. Figures 4.35 and 4.36 show the microstructure (SDAS) obtained for point number 1 for magnesium castings produced without heat pipe cooling and with heat pipe cooling respectively (casting no 52&53 H1). A reduction of 23% is observed when heat pipe cooling is applied.

Table 4.4 shows the SDAS results obtained for all selected magnesium castings for microstructural analysis. The effect of heat pipe cooling can be clearly observed from the table. The results shown in table 4.4 suggest that, in general the higher the mold temperature, the larger the SDAS. The previous observation can be seen when for example comparing castings number 46 and 52, or 46 and 49. The results also showed the effect of heat pipe cooling in reducing the SDAS. One more observation can be obtained from these results, where it shows that the heat pipes have better performance when graphite coating was used and that is shown in the larger reduction in the SDAS.

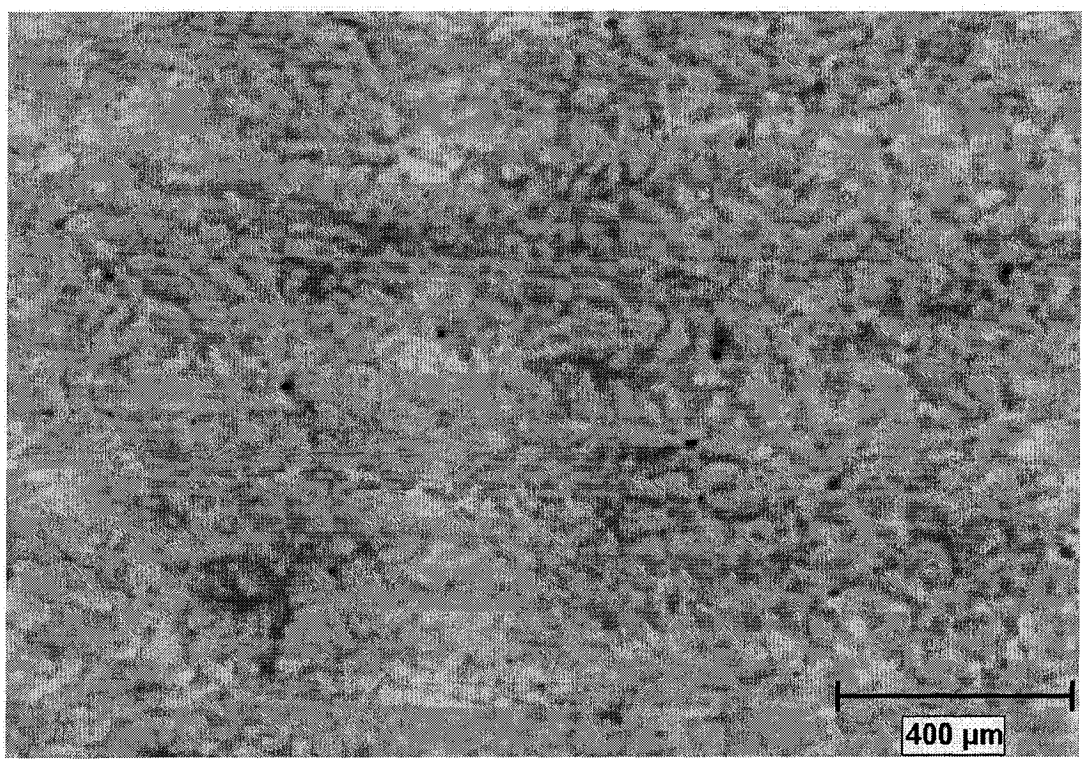

Figure 4.35. Microstructure (SDAS) obtained for point number 1
(casting no. 52 H1, without heat pipe cooling)

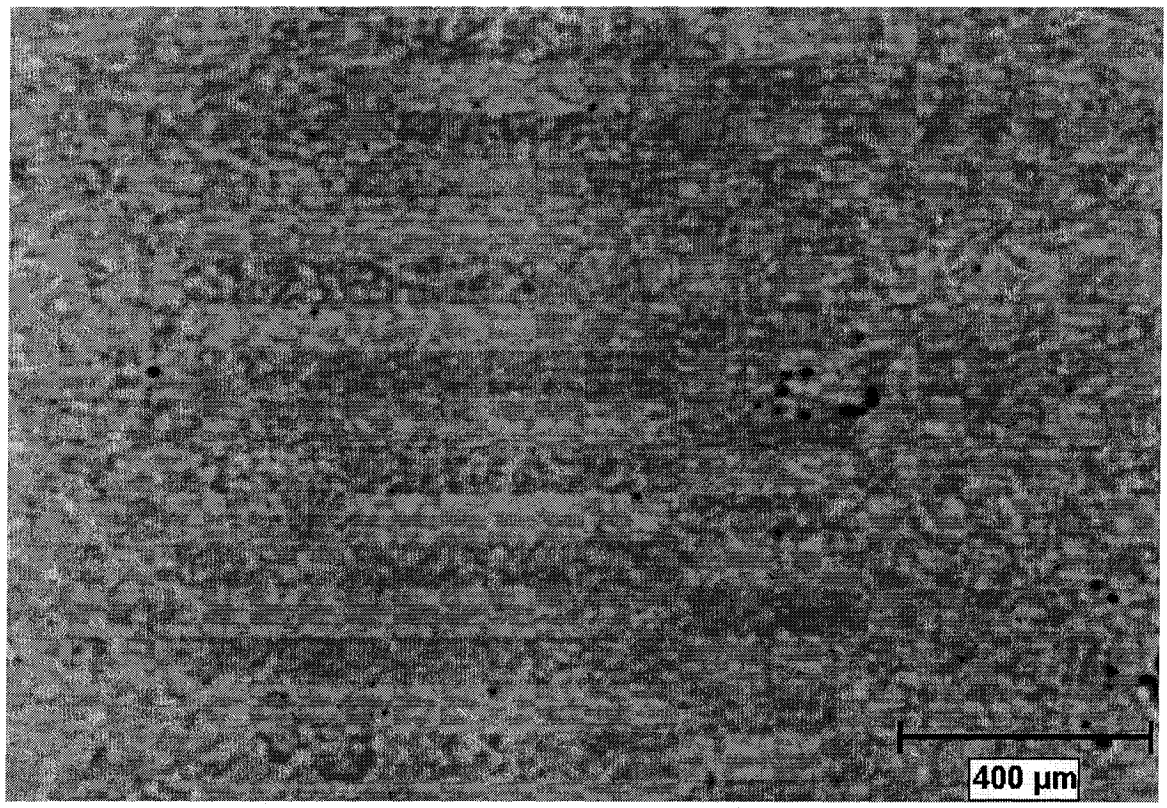

Figure 4.36. Microstructure (SDAS) obtained for point number 1
(casting no. 53 H1, with heat pipe cooling, reduction of 23%)

The previous observations obtained from AZ91E SDAS results were as expected.

Table 4.4. SDAS results obtained for magnesium castings

			Casting (H1)				Casting (H2)		
			SDAS (μm)				SDAS (μm)		
No	MT. T.	MD. T.	Coating	P1	P2	P3	P1	P2	P3
46	704	370	B. N.	29±3	33±4	30±3	29±2	35±3	28±2
47	704	365	B. N.	24±1	26±2	24±3	23±3	26±2	24±2
Percentage of reduction				19%	20%	22%	20%	26%	13%
52	704	340	B. N.	28±3	31±4	29±2	29±3	32±2	31±2
53	704	310	B. N.	22±2	25±2	24±3	21±3	26±3	25±3
Percentage of reduction				23%	18%	19%	27%	20%	18%
56	704	275	B. N.	30±3	31±3	29±2	30±3	32±3	29±2
49	704	265	B. N.	23±2	27±3	25±2	24±2	28±1	26±2
57	*704*	*290*	B. N.	*25±2*	*29±3*	*27±2*	*25±2*	*29±2*	*26±2*
Percentage of reduction				21%	13%	13%	18%	13%	11%
62	704	260	Graphite	29±4	30±3	29±4	31±3	32±3	28±3
66	704	270	Graphite	21±2	25±3	24±3	23±2	29±4	26±3
Percentage of reduction				28%	16%	19%	25%	9%	9%
68	747	370	Graphite	29±3	30±3	29±4	30±3	33±2	32±2
69	747	350	Graphite	22±3	27±2	24±4	22±2	27±3	24±3
Percentage of reduction				24%	12%	19%	27%	19%	23%

* (MT = melt, MD = mold, T = temperature, B. N. = boron nitride, P1, P2, P3 = points 1, 2 & 3 respectively, % = percentage of reduction when heat pipe cooling was used).

4.4.2. Grain Size Analysis for Magnesium AZ91E

The grain size measurements for magnesium AZ91E require a special heat treatment before polishing and etching the specimens (etched with acetic glycol). The heat treatment conducted to reveal the grain size is 413°C for 6 hours, 352°C for 2 hours, and 413°C for 10 hours. The different stages of this heat treatment were conducted with no cooling down to room temperature in between stages. The heat pipe causes an increase in grain size of AZ91E [109]. All samples were heat treated for the same length

of time. Consequently, the effect of heat treatment on the grain size should be the same for all samples.

The general intercept procedure was used in the measurements. The grain size results obtained for two pairs of castings are shown in figures 4.37 and 4.38.

From Figure 4.37, one can again see the effect of heat pipe cooling on all three points. At point number 1, a reduction of 22% in the grain size is obtained by using heat pipe cooling. At the other two points, point 2 and point 3, reductions of 21% and 18% were obtained respectively. These results demonstrate clearly the effect of heat pipe cooling on the grain size. The grain size at point number 2 tends to be larger than that at point number 3; and that is because there is not much mold mass near point 2 to enhance

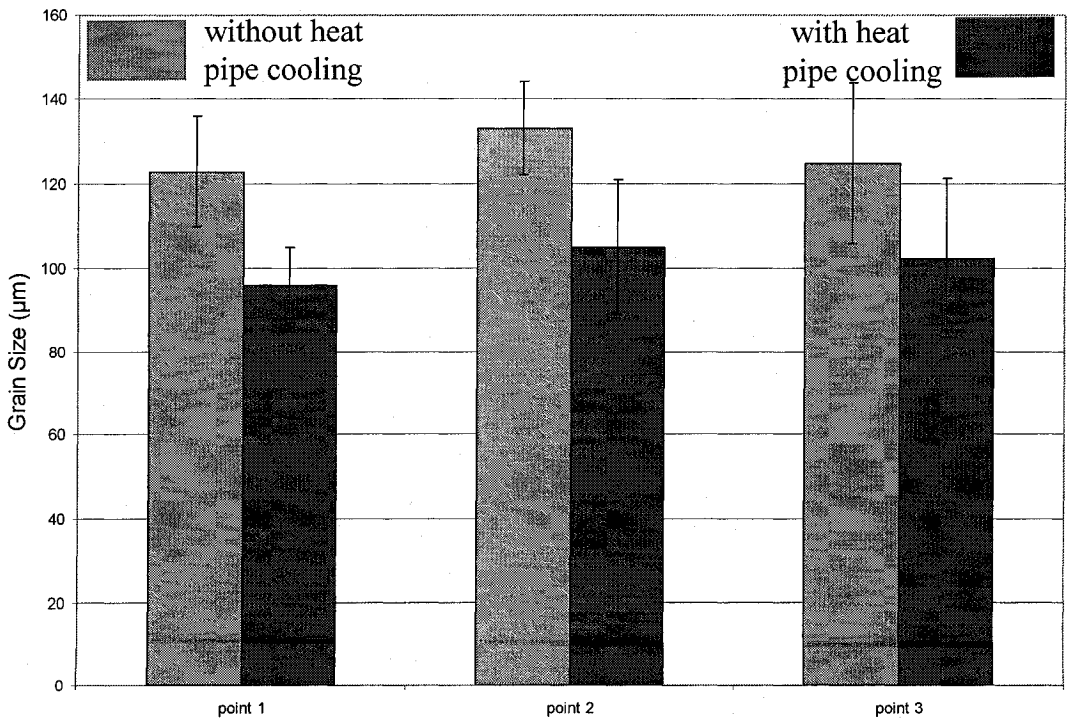

Figure 4.37. Grain size results for magnesium AZ91E (casting no. 68&69 H1)

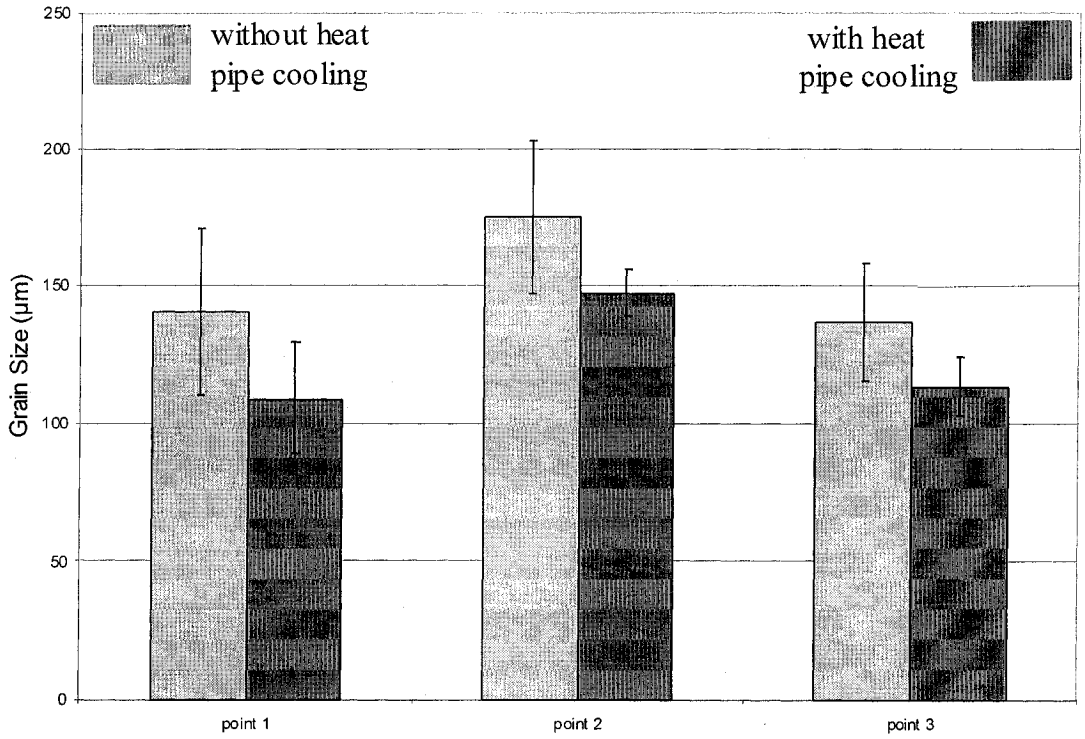

Figure 4.38. Grain size results for magnesium AZ91E (casting no. 68&69 H2)

cooling. The effect of heat pipe cooling on the grain size of the other the magnesium casting is very well seen in figure 4.38 as well.

Figures 4.39 and 4.40 show the microstructures obtained for points number 1 for castings produced without heat pipe cooling and with heat pipe cooling respectively (castings no 68&69 H1). A reduction of 22% in the grain size is accomplished.

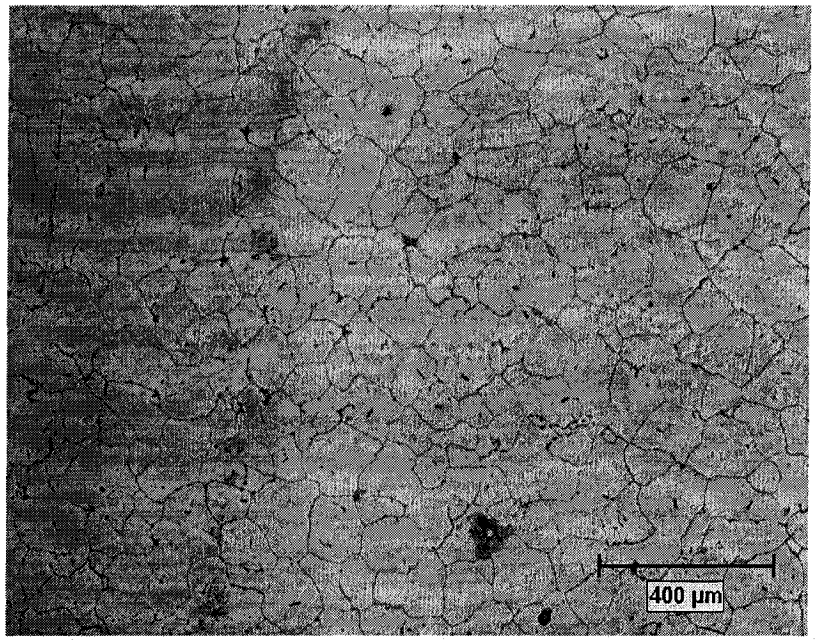

Figure 4.39. Microstructure obtained for point number 1 (casting no.68 H1) (without heat pipe)

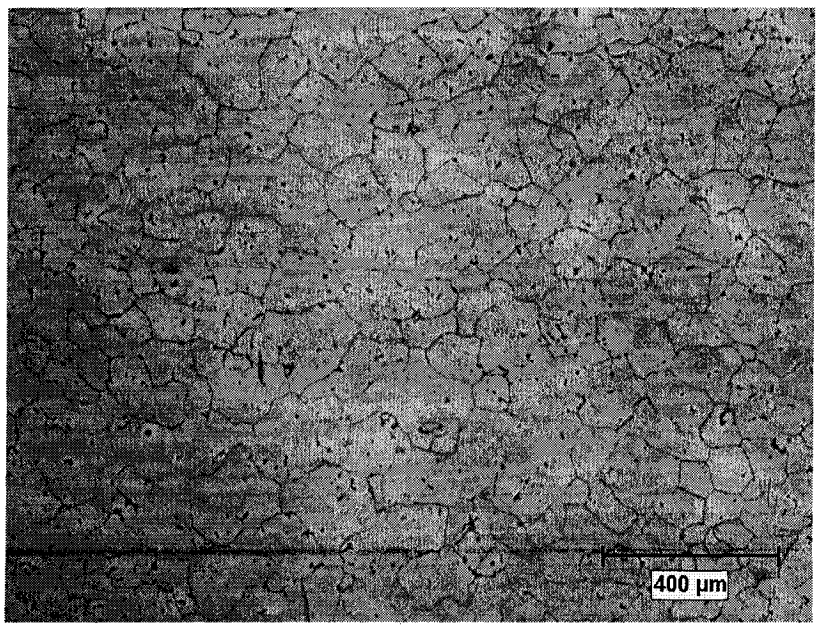

Figure 4.40. Microstructure obtained for point number 1 (casting no.69 H1) (with heat pipe)

Table 4.5 shows the grain size results obtained for all selected magnesium castings for microstructure analysis. The effect of heat pipe cooling can be clearly observed from the table. The reduction does not always follow the same trend and that is because of the non-uniformity of the mold temperature resulting from the preheating procedure.

Table 4.5. Grain size results obtained for magnesium castings

			Casting (H1)				Casting (H2)		
			Grain Size (μm)				Grain Size (μm)		
No	MT. T.	MD. T.	Coating	P1	P2	P3	P1	P2	P3
46	704	370	B. N.	196±25	210±27	208±26	245±35	236±25	262±29
47	704	365	B. N.	137±14	145±21	150±7	153±14	194±20	185±25
Percentage of reduction				30%	31%	28%	37%	18%	29%
52	704	340	B. N.	273±32	316±33	239±31	247±28	263±31	199±18
53	704	310	B. N.	173±18	231±21	218±29	182±24	229±23	189±22
Percentage of reduction				36%	27%	9%	26%	13%	5%
56	704	275	B. N.	224±28	262±31	237±20	235±31	261±31	260±35
49	704	265	B. N.	102±12	107±10	158±14	190±24	207±20	177±21
57	704	290	B. N.	108±26	112±20	164±20	187±23	210±24	180±23
Percentage of reduction				54%	59%	33%	19%	21%	32%
62	704	260	Graphite	249±33	297±31	267±33	287±33	295±35	294±33
66	704	270	Graphite	198±19	250±20	223±20	231±24	275±26	236±21
Percentage of reduction				20%	16%	17%	19%	7%	20%
68	747	370	Graphite	123±13	133±11	125±19	140±30	175±28	137±21
69	747	350	Graphite	96±9	105±16	102±19	109±20	148±8	114±11
Percentage of reduction				22%	21%	18%	22%	16%	17%

* MT = melt, MD = mold, T = temperature, B. N. = boron nitride, P1, P2, P3 = points 1, 2 & 3 respectively, % = percentage of reduction when heat pipe cooling was used.

4.5. Microstructural Analysis of Aluminum Alloy (A356)

The effect of heat pipe cooling on the aluminum castings has been conducted by measuring the secondary dendrite arm spacing, (SDAS) and the grain size. The specimens were similar to those of the magnesium alloy, and the analyses were conducted at the same points (1,2, and 3).

4.5.1. SDAS Analysis for Aluminum alloy (A356)

After polishing and etching (using nital, 100ml methanol, 3ml HNO_3) the aluminum specimens, the SDAS were measured using the line intercept method performed using CLEMEX Vision ^{TM}.

SDAS measurements for the A356 castings have been conducted to evaluate the HP cooling effect. Figure 4.41 shows the results obtained for one pair of aluminum castings. The three locations chosen for SDAS measurements are the same locations that were chosen for the analysis of the magnesium AZ91E castings. From the figure, the reduction in SDAS due to HP cooling is clearly pronounced. Reductions of 29%, 13% and 11% were obtained for points 1, 2 and 3 respectively. These results demonstrate clearly the effect of heat pipe cooling on the SDAS of A356. Similar results are obtained for a second pair of aluminum castings shown in figure 4.42.

Figures 4.43 and figure 4.44 show the microstructures of an A356 casting at point 1 for castings produced under the same casting conditions except the first was produced without heat pipe cooling and the other with heat pipe cooling.

A reduction of 29% in the SDAS by using heat pipe cooling is clearly observed in figure 4.44 compared to that shown in figure 4.43.

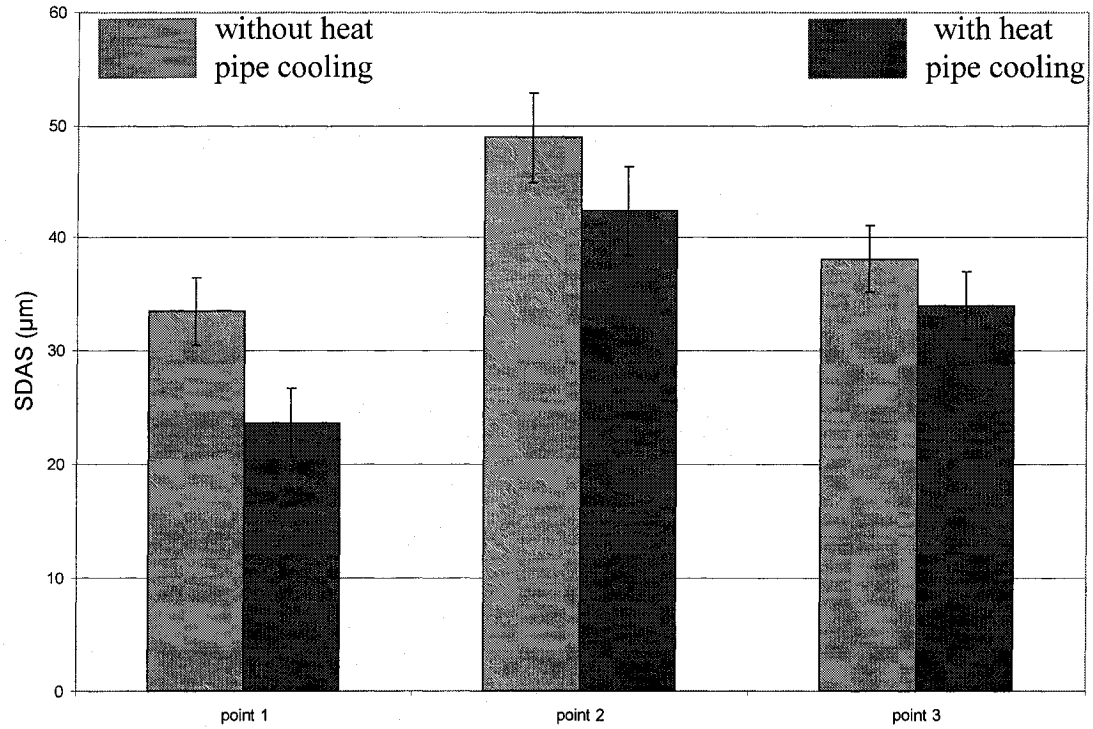

Figure 4.41. SDAS results for aluminum 356 (casting no. 81&83 H1)

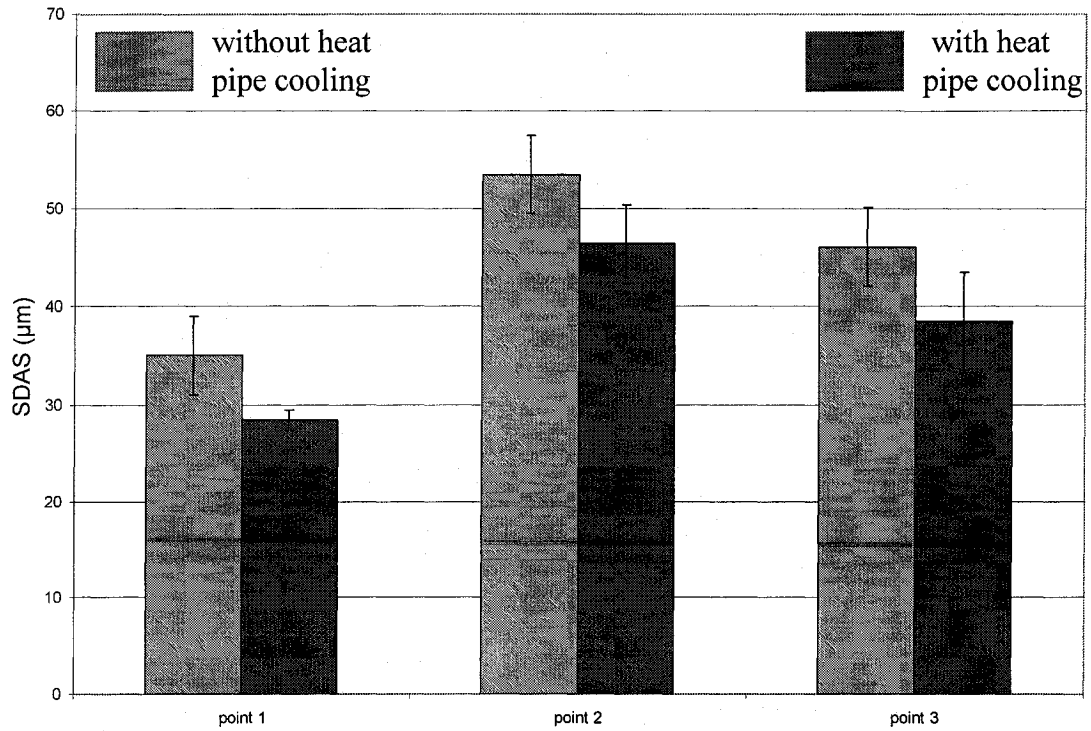

Figure 4.42. SDAS results for aluminum 356 (casting no. 81&83 H2)

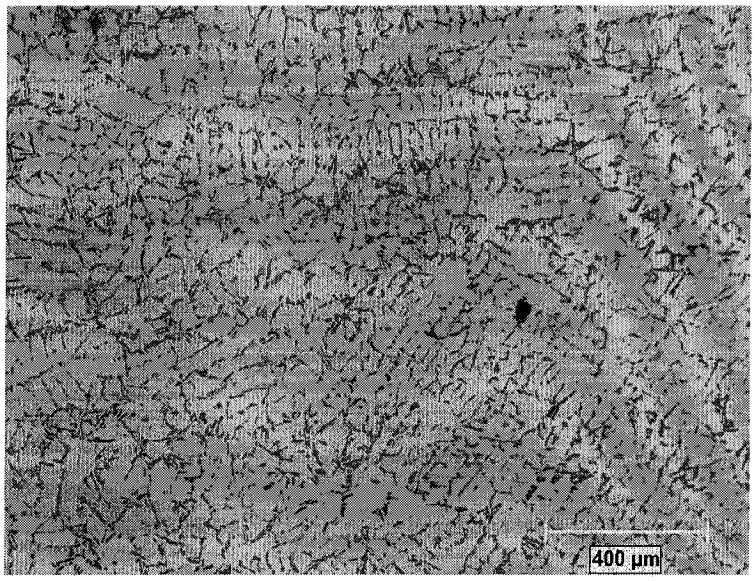

Figure 4.43. Microstructure of A356 (point 1, casting no. 81 H1)
(without heat pipe cooling)

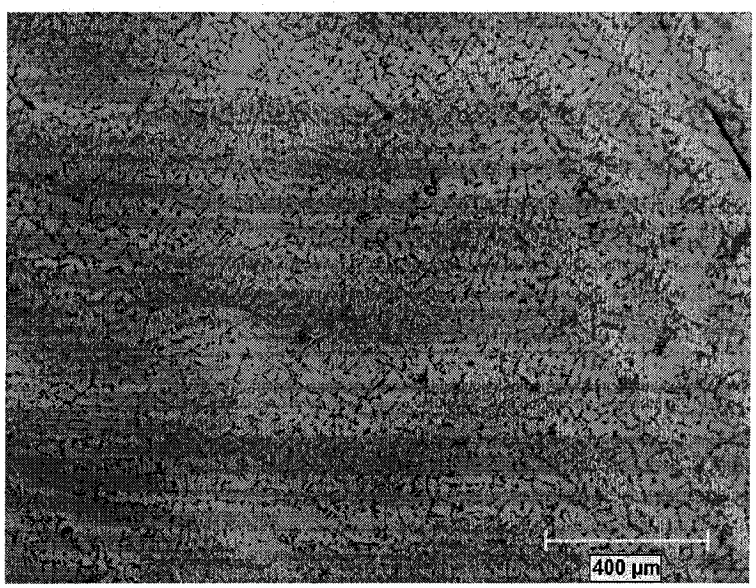

Figure 4.44. Microstructure of A356 (point 1, casting no. 83 H1)
(with heat pipe cooling)

Table 4.6 shows the SDAS results obtained for all selected aluminum castings for microstructural analysis. The effect of heat pipe cooling can be clearly observed from the table. In general, the results showed that the higher the mold temperature, the larger the SDAS. The reduction does not always follow the same trend and that is because of the non-uniformity of the mold temperature that resulted from the preheating procedure.

Table 4.6. SDAS results obtained for aluminum castings

			Casting (H1)			Casting (H2)		
			SDAS (μm)			SDAS (μm)		
No	MT. T.	MD. T.	P1	P2	P3	P1	P2	P3
74	*728*	*370*	*39*±5	*47*±6	*41*±5	*50*±4	*62*±5	*46*±3
75	728	360	39±4	53±5	44±3	45±2	56±6	49±3
76	728	360	29±2	41±3	37±3	34±2	52±5	45±5
Percentage of reduction			26%	22%	16%	24%	7%	8%
79	728	300	39±6	51±4	43±4	43±5	57±5	45±2
80	728	310	28±4	45±6	39±4	29±3	42±3	40±3
Percentage of reduction			28%	12%	10%	33%	26%	10%
81	722	260	33±3	49±4	38±3	35±4	53±4	46±4
83	722	245	24±3	42±4	34±3	28±1	46±4	39±5
Percentage of reduction			29%	13%	11%	19%	13%	16%

*MT = melt, MD = mold, T = temperature, B. N. = boron nitride, P1, P2, P3 = points 1, 2 & 3 respectively, % = percentage of reduction when heat pipe cooling was used.

4.5.2. Grain Size Analysis for Aluminum Alloy A356

A unique technique developed at McGill University was used to measure the grain size for A356 alloy [107]. After polishing and etching the sample with a proper etch (35g ferric chloride, $FeCl_3$, and 200ml water), lamps with different color filters are used to reveal the macrostructure of the A356 sample. The distance from the light source to the sample surface, as well as the incident angle were adjusted according to the contrast required. A 1 cm paper bar was placed beside the sample to be used later by the

CLEMEX Vision ™ system as a calibration reference. A digital camera with a macro feature was used to take images of the sample. The setup used is shown in figure 4.45.

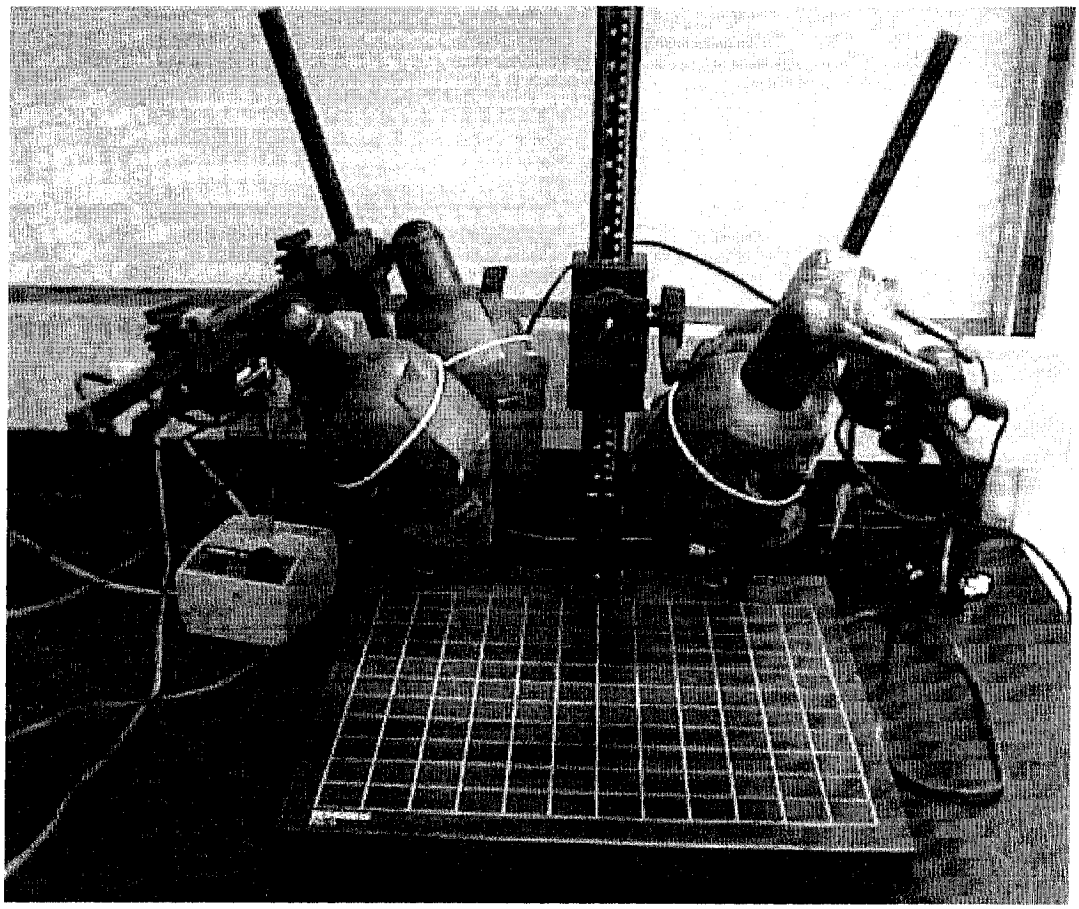

Figure 4.45. The setup used to view the macrostructure of A356

The macrostructure images obtained by the digital camera were transferred to the CLEMEX Vision ™ system. Before analysis of any image, a new calibration procedure was conducted based on the 1 cm paper bar shown in the image. Based on the calibration, the system correctly identified the magnification of the image and the measurements were taken.

The general intercept procedure was used in the measurements. The grain size results obtained for two pairs of castings are shown in figures 4.46 and 4.47.

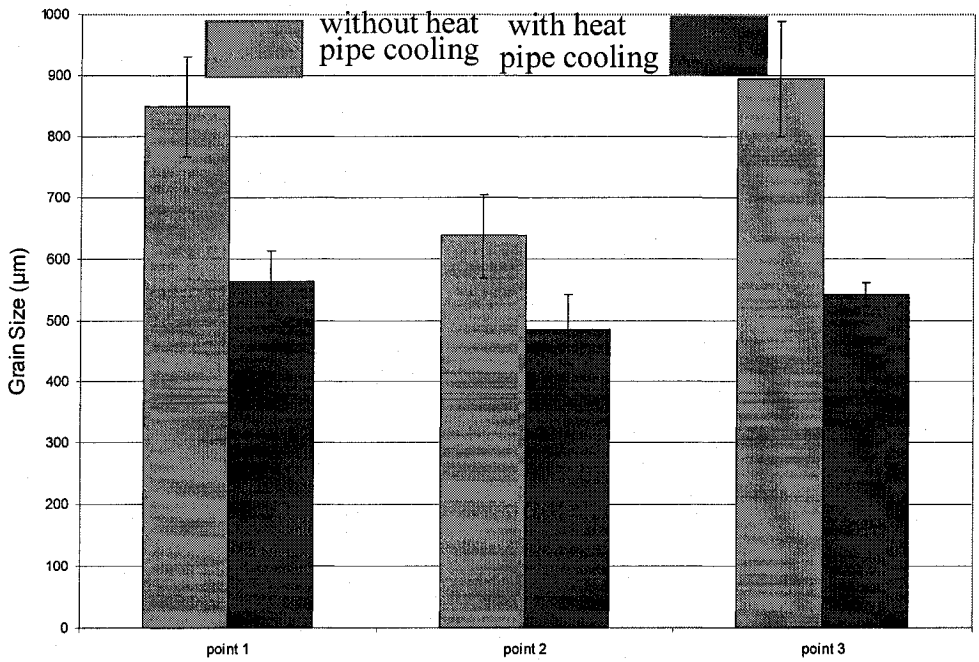

Figure 4.46. Grain size results for aluminum alloy, A356 (casting no 81&83 H1)

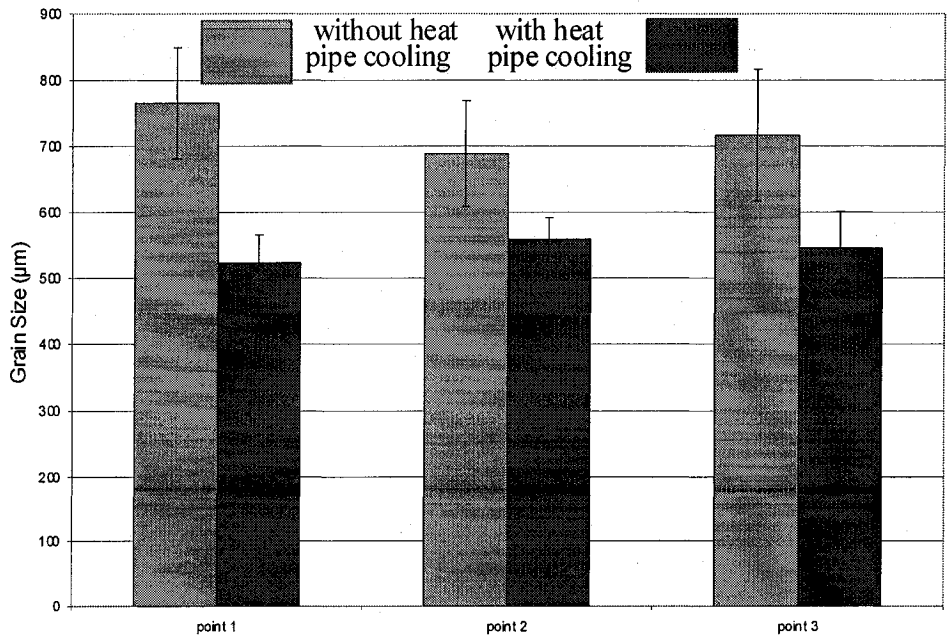

Figure 4.47. Grain size results for aluminum alloy, A356 (casting no 81&83 H2)

From figure 4.46, one can clearly see the effect of heat pipe cooling on all three points, especially point number 1 which is close to the heat pipe. At point number 1, a reduction of 33% in the grain size is obtained by using heat pipe cooling. At the other two points, point 2 and point 3, reductions of 23% and 39% were obtained respectively. These results demonstrate clearly the effect of heat pipe cooling on the grain size. The effect of heat pipe cooling on the grain size of the aluminum casting is also very well observed in figure 4.47.

Figures 4.48 and 4.49 show the macrostructure obtained for A356 castings produced without heat pipe cooling and with heat pipe cooling respectively (casting no. 74&76 H2). The effect of heat pipe cooling on the grain size can be visually observed.

Table 4.7 shows the grain size results obtained for all selected aluminum castings for macrostructure analysis. The effect of heat pipe cooling can be clearly observed from the table. Once more, the reduction does not always follow the same trend and that is because of the non-uniform mold temperature that resulted from the preheating procedure.

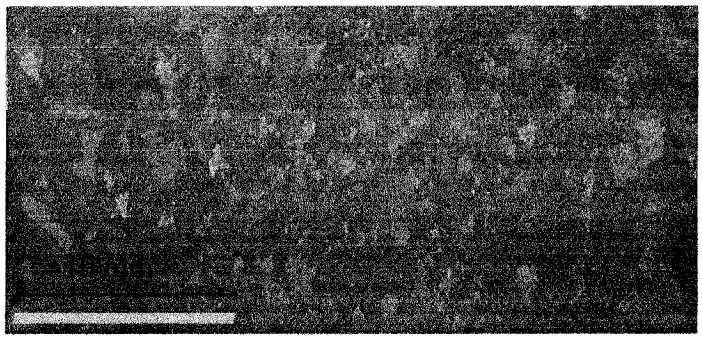

HP

Figure 4.48. Macrostructure obtained for A356 (casting no. 74 H2)
(without heat pipe cooling)

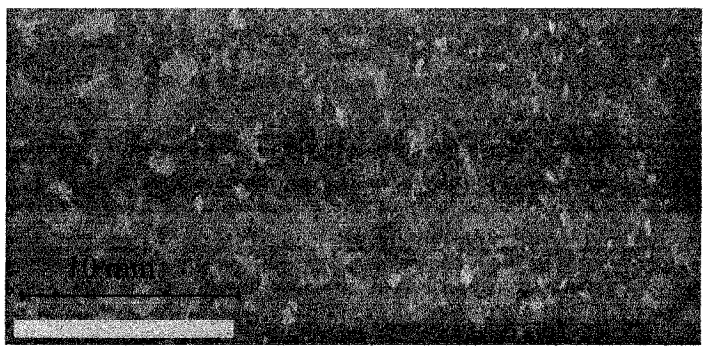

HP

Figure 4.49. Macrostructure obtained for A356 (casting no. 76 H2)
(with heat pipe cooling)

Table 4.7. Grain size results obtained for aluminum A356 castings

			Casting (H1)			Casting (H2)		
			Grain Size (μm)			Grain Size (μm)		
No	MT. T.	MD. T.	P1	P2	P3	P1	P2	P3
74	728	370	1125±122	938±98	858±49	886±55	872±61	868±118
75	728	360	1195±128	980±101	1013±110	947±59	849±88	855±110
76	728	360	783±116	765±53	818±59	641±31	681±36	654±52
Percentage of reduction			34%	22%	19%	32%	19%	23%
79	728	300	1063±115	846±77	867±66	952±89	812±71	947±110
80	728	310	680±54	660±44	647±44	629±39	752±43	776±61
Percentage of reduction			36%	22%	25%	33%	7%	17%
81	722	260	849±82	636±68	893±95	765±84	688±80	717±100
83	722	245	562±49	484±57	541±19	523±43	558±33	546±55
Percentage of reduction			33%	23%	39%	31%	18%	23%

* (MT = melt, MD = mold, T = temperature, P1, P1, P3 = points 1 to 3 respectively, % = percentage of reduction when heat pipe cooling was used).

4.6. Thermal Analysis of Heat Pipe Permanent Mold Casting Process

This section deals with the estimated heat fluxes extracted by the novel industrial heat pipes developed in the present work.

The heat pipe designed in the present work is effective and capable of absorbing the high heat fluxes generated from the mold and the molten metal poured into the casting cavity. The response of the heat pipe is rapid (less than 5 seconds) when turned on and off. The heat extraction rates were high and very well handled by the heat pipe and this is reflected in the microstructures.

As mentioned earlier, in a permanent mold casting process the mold has to be preheated for better mold filling and to eliminate some casting defects. There are reasonable heat flux values that need to be absorbed by the heat pipe in order to show a significant refinement of the microstructure. The heat fluxes extracted by the heat pipes developed in the present work were estimated based on the heat pipe and the cooling air

temperatures. As shown earlier in chapter 3 (figures 3.7, 3.10, and 3.11), each heat pipe is located facing one side of the casting cavity to extract heat.

The results of the average heat flux estimations are given in table 4.8. A sample calculation for a transient heat flux is given in section 4.6.1. The heat flux results demonstrate the ability of the designed heat pipes to extract significant heat flux values. The results showed an increase in the heat flux with the increase of mold temperature. For example, when comparing A356 castings (number 76, 80, and 83) one can clearly see that the heat flux values increase with the increase of mold temperature. Also, in the case of AZ91E, the same observation can be drawn as seen when comparing castings number 47 and 49 where casting number 47 has a higher mold temperature and higher heat flux extracted by the heat pipe. Also, when comparing the heat fluxes obtained during A356 casting processes with those obtained during AZ91E casting processes at similar mold temperatures, one can see that those obtained during A356 casting processes have higher heat fluxes and that is due to the higher latent heat of A356 compared to AZ91E.

Figure 4.50 shows a typical temperature measurement obtained during a casting process

Table 4.8. Estimated heat fluxes for both heat pips

Casting No.	Melt Temp. (°C)	Mold Temp. (°C)	Average Transient Heat Flux (kW/m^2)	
			HP 1	HP 2
AZ91E				
47	704	365	196	210
49	704	265	150	180
53	704	310	153	124
57	704	290	267	294
66	704	270	160	175
69	747	350	212	229
A356				
76	728	360	263	253
80	728	310	208	220
83	722	245	138	147

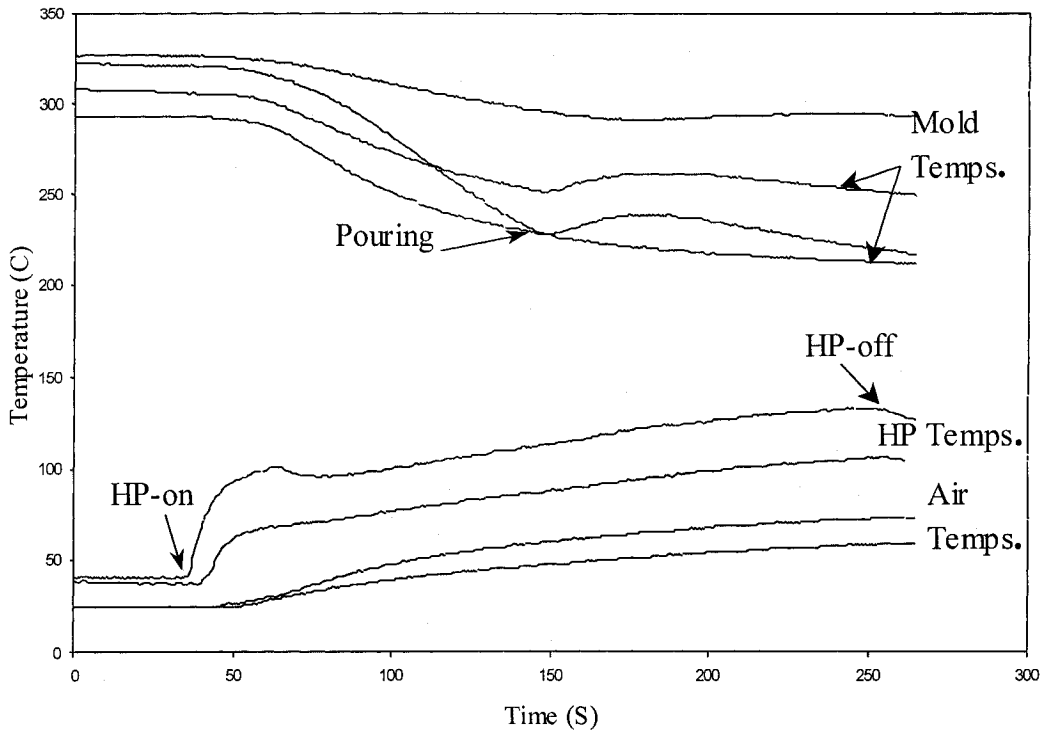

Figure 4.50. Temperature measurements obtained during aluminum casting process

From figure 4.50, one can see that the heat pipe temperature increases almost immediately after the heat pipe is switched on. One can also notice that the temperature of the air is increasing and the mold temperature is decreasing after the heat pipe is switched on. A slight jump in the mold temperature is observed due to the introduction of the molten metal into the mold cavity before it declines again due to the intensive cooling by the heat pipes. The temperature measurement is very sensitive to the thermocouple location. Measurements of the temperature of the casting and the mold at locations very close to the casting/mold interface are not possible due to space constraints around the casting machine.

4.6.1. Sample Calculation for a Transient Heat Flux

As mentioned earlier in chapter 3, the heat fluxes were estimated based on the heat pipe, air inlet and air outlet temperatures, where 70% of the heat was assumed to be

absorbed by the chill and 30% dissipated by the condenser cooling air. The following is a sample calculation for a transient heat flux at time = t second:

$$q^{\cdot} = [(T_{(\text{air outlet})t} - T_{(\text{air inlet})}) * \text{Air flow rate} * C_{p(\text{air})} * \rho_{(\text{air})} + ((T_{(HP)t} * 0.7 + T_{(\text{air outlet})t} * 0.3) - (T_{(HP)t-\Delta t} * 0.7 + T_{(\text{air outlet})t-\Delta t} * 0.3)) * \text{chill mass} * C_{p(H13)}] / \text{evaporator area}$$

where

$T_{(\text{air out let})t}$= 64.33 (°C), $T_{(\text{air inlet})}$ =20 (°C), Air flow rate =0.01413 (m^3/s), $C_{p(\text{air})}$=0.001 (J/kg-°C), $\rho_{(\text{air})}$ = 1.3 (kg/ m^3), $T_{(HP)t}$ = 114.99 (°C), $T_{(\text{air outlet})t}$ = 64.33 (°C), $T_{(HP)t-\Delta t}$ = 114.76 (°C), $T_{(\text{air outlet})t-\Delta t}$ = 64.27 (°C), chill mass = 14.5 (kg), $C_{p(H13)}$= 483 (J/kg-°C), and evaporator area = 0.01021 m^2.

Thus,

$q^{\cdot} = [(64.33 - 20) * 0.01413 * 0.001 * 1.3 + ((114.99 * 0.7 + 64.33*0.3) - (114.76 * 0.7 + 64.27 * 0.3)) * 14.5 * 483] / 0.01021 = 122.78$ (kW/m^2)

4.7. Estimation of the Local Cooling Rates from the SDAS Measurements

As mentioned in chapter 2, equations have been developed to correlate the SDAS to the local cooling rate. Equations (2.12) and (2.13) were used to estimate the local cooling rates at all casting points selected for analysis. Table 4.9 shows the results for the estimated cooling rates for AZ91E alloy. Table 4.10 shows the results for the estimated cooling rates for A356 alloy. The castings produced with heat pipe cooling were highlighted in bold numbers.

Table 4.9. Estimated cooling rates for magnesium AZ91E castings

			Casting (H1)			Casting (H2)		
			Estimated Cooling Rate (°C/s)			Estimated Cooling Rate (°C/s)		
No	MT. T.	MD. T.	P1	P2	P3	P1	P2	P3
46	704	370	2.69	1.80	2.42	2.69	1.49	3.00
47	**704**	**365**	**4.86**	**3.78**	**4.86**	**5.55**	**3.78**	**4.86**
52	704	340	3.00	2.18	2.69	2.69	1.98	2.18
53	**704**	**310**	**6.38**	**4.28**	**4.86**	**7.37**	**3.78**	**4.28**
56	704	275	2.42	2.18	2.69	2.42	1.98	2.69
49	**704**	**265**	**5.55**	**3.36**	**4.28**	**4.86**	**3.00**	**3.78**
57	**704**	**290**	**4.28**	**2.69**	**3.36**	**4.28**	**2.69**	**3.78**
62	704	260	2.69	2.42	2.69	2.18	1.98	3.00
66	**704**	**270**	**7.37**	**4.28**	**4.86**	**5.55**	**2.69**	**3.78**
68	747	370	2.69	2.42	2.69	2.42	1.80	1.98
69	**747**	**350**	**6.38**	**3.36**	**4.86**	**6.38**	**3.36**	**4.86**

* (MT = melt, MD = mold, T = temperature, P1, P1, P3 = points 1 to 3 respectively)

Table 4.10. Estimated cooling rates for aluminum A356 castings

			Casting (H1)			Casting (H2)		
			Estimated Cooling Rate (°C/s)			Estimated Cooling Rate (°C/s)		
No	MT. T.	MD. T.	P1	P2	P3	P1	P2	P3
74	728	370	3.02	1.87	2.65	1.60	0.92	1.98
75	728	360	3.02	1.38	2.22	2.09	1.19	1.68
76	**728**	**360**	**6.44**	**2.65**	**3.45**	**4.29**	**1.44**	**2.09**
79	728	300	3.02	1.52	2.35	2.35	1.14	2.09
80	**728**	**310**	**7.05**	**2.09**	**3.02**	**6.44**	**2.50**	**2.83**
81	722	260	4.63	1.68	3.22	3.98	1.38	1.98
83	**722**	**245**	**10.46**	**2.50**	**4.29**	**7.05**	**1.98**	**3.02**

* (MT = melt, MD = mold, T = temperature, P1, P1, P3 = points 1 to 3 respectively)

From the above results shown in tables 4.9 and 4.10, one can see the enhancement of the cooling rates when the heat pipe is used and that typically will reflect on the microstructure and better mechanical properties can be obtained.

The higher cooling rates were naturally achieved at point number 1, which is close to the heat pipe. Point number 2 has the lowest cooling rates compared to points 1 and 3; and that is because points 1 and 3 are closer to the casting/mold interface.

The cooling rates obtained with heat pipe cooling are considered as high cooling rates because they range from 4.2 °C/s to 10.46 °C/s at point number 1.

It is possible to further enhance the casting cooling rate using the heat pipe developed in the present work. The key here is to install the heat pipe in a location closer to the casting cavity. With such modification, further SDAS reductions could be achieved.

4.8. Comparison of a Water Cooling Channel and a Heat Pipe

As mentioned before, the value of the interfacial heat transfer coefficient, h, used at the mold/heat pipe interface during the computer modeling was 20,000 W/m^{2}K. Given that the diameter of heat pipe (H2) is 3.8 cm, a calculation for a water cooling channel with a similar 3.8 cm diameter was conducted to determine the velocity of water required to reach an interfacial heat transfer coefficient of 20,000 W/m^{2}K.

The heat transfer between a fluid flowing in a circular passage and the wall can be described for a turbulent, forced convection flow by the Dittus-Boelter equation (5) as:

$$\overline{Nu_D} = 0.023\,\mathrm{Re}_D^{0.8}\,\mathrm{Pr}^{0.4} \qquad \ldots\ldots\ldots (3.1)$$

where $\overline{Nu_D}$ = the average Nusselt number based on the pipe diameter, D

$\mathrm{Re_D}$ = the Reynolds number of the fluid

Pr = the Prandtl number of the fluid

In the experimental mold, the diameter of the passage for the heat pipe (H2) was 3.8 cm.

Equation (3.1) can be rewritten as:

$$\bar{h} = \frac{k}{D}(0.023)\left[\frac{\rho v D}{\mu}\right]^{0.8} \mathrm{Pr}^{0.4} \quad \ldots\ldots (3.2)$$

or

$$v^{0.8} = \frac{\bar{h} D^{0.2}}{(0.023)k} \frac{1}{\mathrm{Pr}^{0.4}} \left(\frac{\mu}{\rho}\right)^{0.8} \quad \ldots\ldots (3.3)$$

Thus

$$v = \left(\frac{\bar{h} D^{0.2}}{(0.023)k}\right)^{1.25} \frac{1}{\mathrm{Pr}^{0.5}} \left(\frac{\mu}{\rho}\right) \ldots\ldots (3.4)$$

where

v = average velocity of the water flow, m/s

$\bar{h}$ = average heat transfer coefficient = 20,000 W/m^{2}K

D = internal diameter of the passage = 0.038 m

k = thermal conductivity of water = 0.647 W/mK

Pr = Prandtl number of water = 3.55

μ = viscosity of water 555.1x10^{-6} Ns/m^2

ρ = density of water = 988.1 kg/m^3

The properties of water were assumed for a temperature of 50°C. Thus, substitution of the above values into Eq. (3.4) yields

$v = 6(m/s)$

The mass flow rate of water at this velocity is then computed to be:

$$\dot{m} = \pi(0.019)^2 m^2 (6 m/s)(988.1 kg/m^3) = 6.7 kg/s = 403 kg/\mathrm{min}$$

In other words, to duplicate the cooling that was achieved with the heat pipe (H2) would require a water flow of 403 kg/min. The water flow calculated is especially large when compared to the 300 g of water the heat pipe contained and this was confined in a sealed chamber. Moreover, the overall dissipation of heat from the heat pipe was with air.

Figures 4.51, 4.52, and 4.53 show the actual mold temperature measurements obtained from the AZ91E casting process with heat pipe cooling (industrial experiment), AZ91E casting process with heat pipe cooling (computer modeling), and AZ91E casting process with water channel cooling (computer modeling) respectively. The locations of the three thermocouples used in the measurements are shown in figure 4.54.

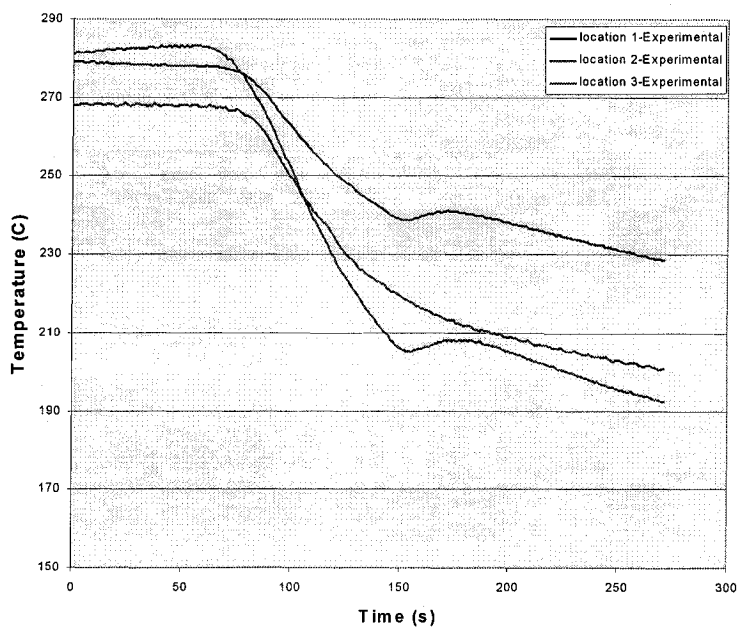

Figure 4.51. Mold temperature measurements obtained from AZ91E casting process with heat pipe cooling (industrial experiment)

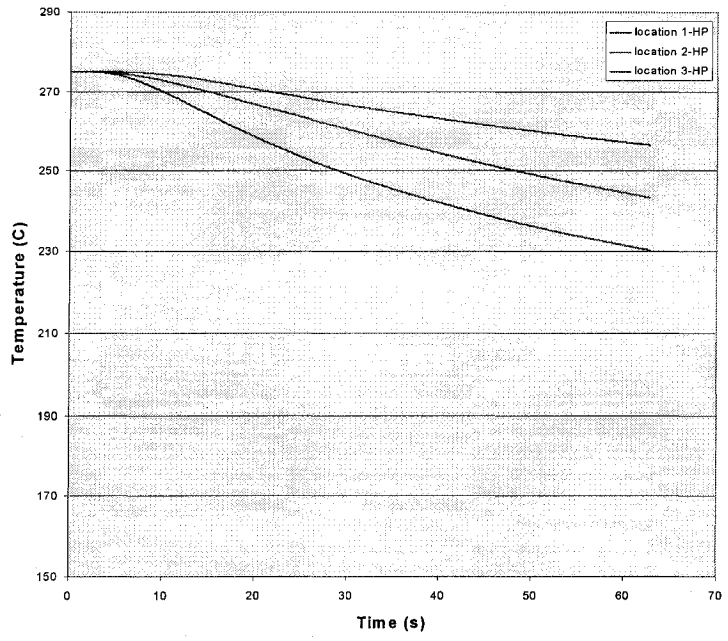

Figure 4.52. Mold temperature measurements obtained from AZ91E casting process with heat pipe cooling (computer modeling)

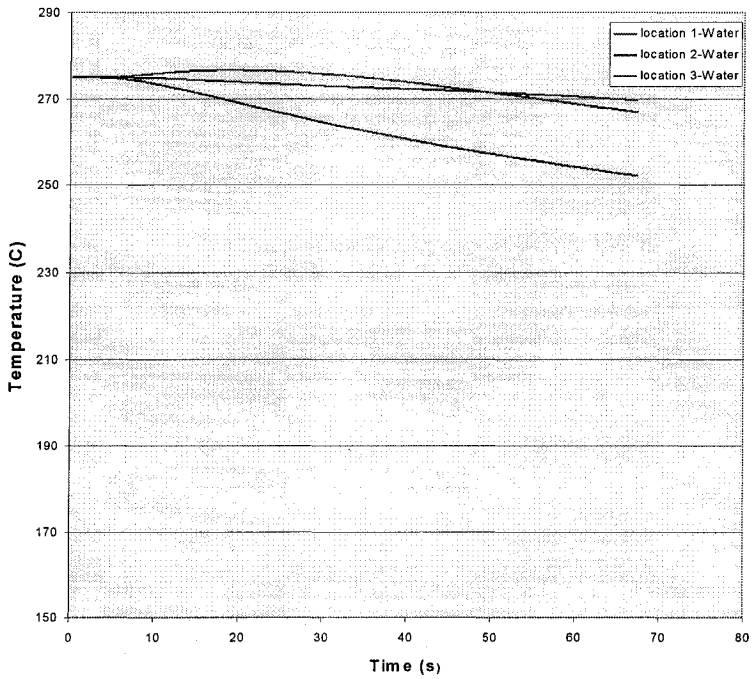

Figure 4.53. Mold temperature measurements obtained from AZ91E casting process with water channel cooling (computer modeling)

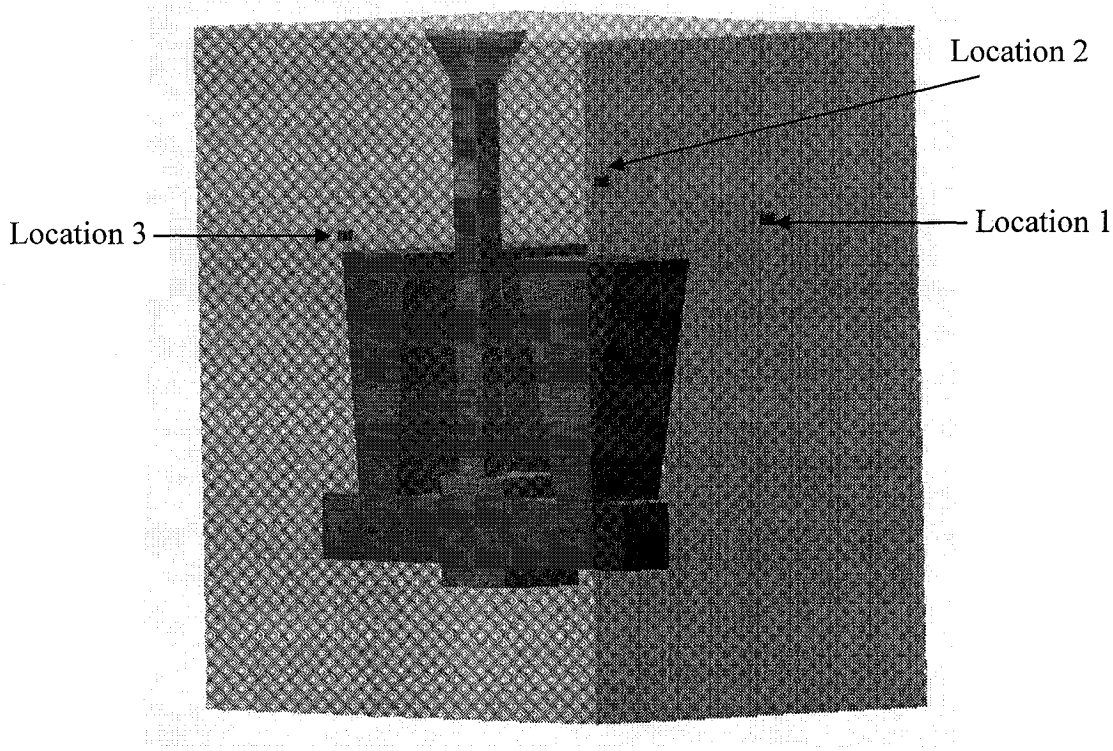

Figure 4.54. The locations of the three thermocouples used in the measurements

The initial mold temperature for all three cases was 275 °C. Also, in the case of water channel cooling, it is worth mentioning that the software package SOLIDCast recommends that if water is to be used as the coolant, the user should select a heat transfer coefficient of 1532 W/m^2K.

From figures 4.51, 4.52, and 4.53, one can clearly see that the actual mold cooling obtained by the heat pipes is substantially higher than what was expected by modeling. Also, one can see that modeling showed a higher mold cooling obtained when heat pipe cooling was used compared to water cooling. When comparing the actual heat pipe cooling with water cooling, a significantly better performance obtained by the heat pipe was observed. Thus, one can conclude that this novel heat pipe is capable of achieving

heat extraction rates that are difficult and costly to attain with conventional water cooling channels.

4.9. The Interfacial Heat Transfer Coefficient, h

As discussed in chapter 2, the interfacial heat transfer coefficient, h, is an important parameter in a casting process. The interfacial heat transfer coefficient, h, represents the behavior of the casting/mold interface during the solidification of the casting. Cooling is very much limited by the value of h during the solidification process.

When the casting is solidifying and due to the shrinkage of the casting and the expansion of the mold, a gap is present at the casting/mold interface. This gap becomes the key issue controlling the heat flow through the casting/mold interface. The value of h depends on many parameters related to the gap such as width, nature of gases present in the gap, ...etc

The external cooling is effective when a perfect contact between the casting and the mold is maintained as seen in figure 2.1. After the molten metal is poured into the mold, it takes the casting some time to start solidifying. It loses temperature and parts of the casting next to the mold wall become solid. The casting tends to shrink in size based on its thermal contraction coefficient value. The mold might increase in size depending on its thermal expansion coefficient. Here the perfect contact between the casting and the mold will transform into imperfect contact. This kind of imperfect contact will dramatically cut the heat transfer across the interface. With such an imperfect contact, the cooling provided by the heat pipe or any external source will not be efficient and the solidification pattern will be totally controlled by the thermal properties of the casting alloy.

The above contribute to the explanations of the difference in the solidification behavior between the AZ91E and the A356 where the air gap formed due to the thermal

contraction of the alloys allows the thermal properties of the alloys to play a significant role in their solidification patterns. The shorter solidification time for AZ91E reduces the effect of heat pipe cooling since the gap at the casting/mold interface forms at an early stage. This can be clearly seen in the different shrinkage types found in the AZ91E and A356 castings.

As presented in chapter 2, a considerable amount of work has been conducted by many investigators to determine the time for air gap formation. The heat pipe group of researchers at McGill University managed to determine the time for air gap formation during casting of A356 alloy in a step mold cooled by the first version of the McGill heat pipes [76], where thin thermocouples, K type, were introduced into the mold at a location very close to the casting/mold interface. They concluded that rapid temperature changes occur in the mold at the time of air gap formation, where the mold temperature suddenly declines after a sharp initial increase due to the introduction of the molten metal. The reason for the temperature decrease is the presence of the gap, which cuts the heat transfer from the casting to the mold dramatically.

In the present work, due to the limitation of space around the casting machine, it was not possible to insert thermocouples into the mold or the casting at locations close enough to the interface to monitor the change in the temperature when the air gap is formed, which indicates the air gap formation time.

As mentioned in chapter 3, the value of the interfacial heat transfer coefficient, h, between the casting and the mold for both alloys was 4000 W/m^2-K as recommended by the AFS-SolidCast manual, except for the upper edge of the cavity, where the h value chosen was 100 W/m^2-K. During modeling, the value of h is decreased by 70% when the air gap is formed.

4.9.1. Sensitivity Analysis for the Interfacial Heat Transfer Coefficient, h

As discussed in the above section, the heat transfer coefficient, h, plays a major role in the solidification process. It has been shown in this work that choosing a suitable h value will lead to better computer modeling and reasonable results can be obtained.

Sensitivity analysis was conducted to determine the effect of the h value on the casting results obtained by modeling. The shape and location of the shrinkage void in the aluminum A356 casting as shown in figure 4.7 is used to determine the sensitivity of the results to h values.

Figures 4.55 (a to f) show the temperature distributions of the A356 casting obtained by the model using different h values of 4000, 2000, 1000, 700, 300, and 100 W/m^2-K respectively at the upper casting edge interface with the mold. The value of h at the casting/mold interface at the other edges was set to 4000 W/m^2-K.

From figure 4.55, one can see that the shape and location of the hot region changes with the change of h value. When the value of h is chosen as 4000 W/m^2-K, the shrinkage was exactly in the middle of the casting. With the reduction of h value, the shrinkage started to move up and to be became U-shaped. The final position and shape of the shrinkage with an h value of 100 W/m^2-K is very close to the real shrinkage shape and position obtained in a real casting as shown in figure 4.7. The above analysis showed the importance and the effect of h value on casting solidification. It also showed the imperfect contact between the upper casting edge with the mold.

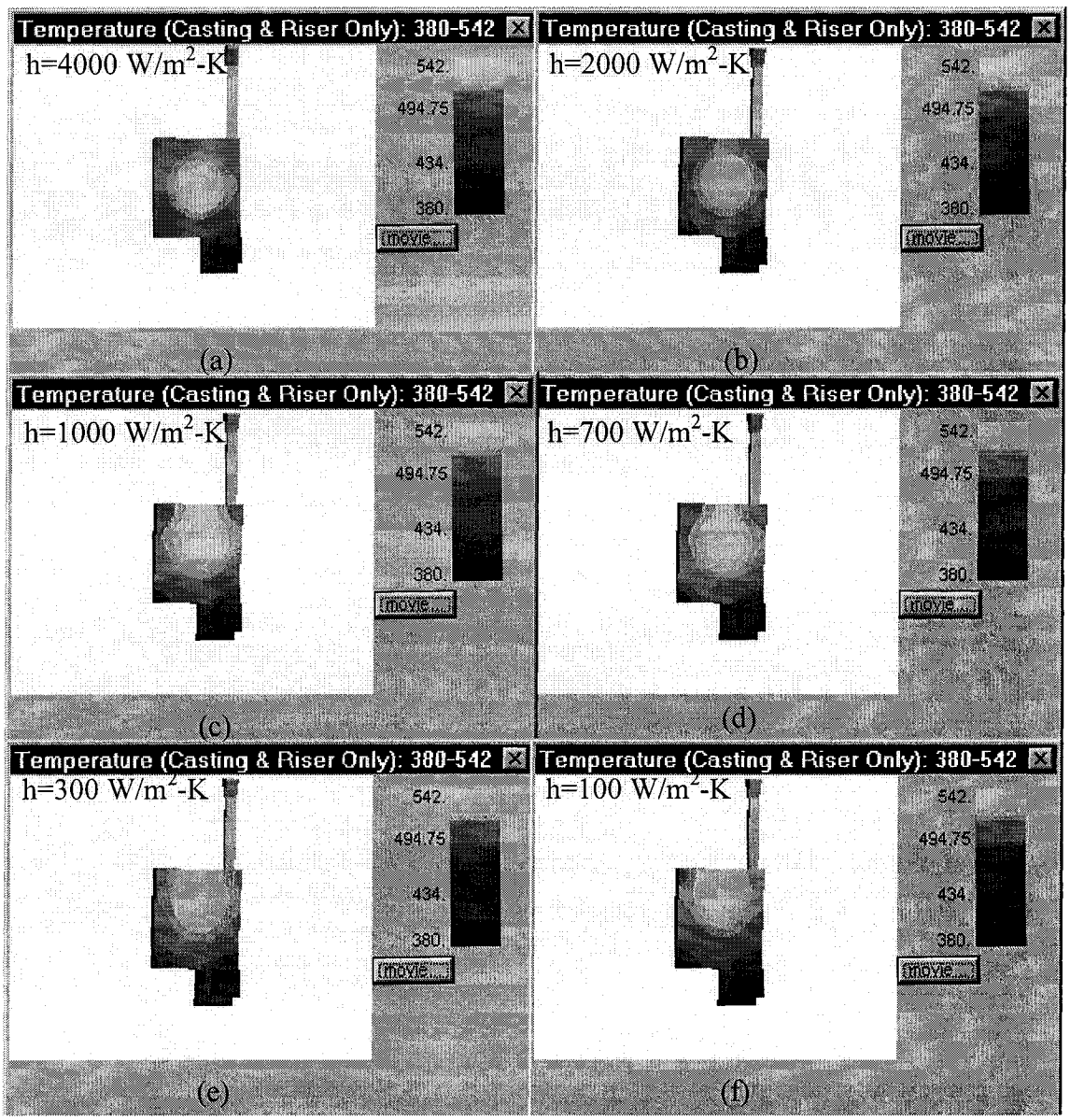

Figure 4.55. Temperature distribution results obtained from the model for A356 casting (with no heat pipe cooling)

4.10. The Importance of Thermocouple Location

It is a useful design step to determine the thermocouple locations by using computer modeling. In the present work, computer modeling was used to determine the location sensitivity of the thermocouples. Simulations of the mold temperature measurements using thermocouples during the casting processes of the magnesium and aluminum alloys (AZ91E and A356) were conducted using the AFS-SoildCast package. For each casting, one thermocouple is located 5 mm away from the face of the casting and the other one is 5 mm away from the casting side. In the simulations, when the thermocouple location is facing the casting cavity, one can see an increase in the mold temperature due to the introduction of the molten metal. If the thermocouple is not facing the cavity, not much change in the measurement can be noticed when the molten metal is introduced. Figure 4.56 shows simulated temperature measurements for thermocouples located on the mold during the AZ91E casting process. From the figure, it is clear that the thermocouple has to be close enough to the casting cavity to observe any change in the mold temperatures, and this will make it possible to determine the time for air gap formation.

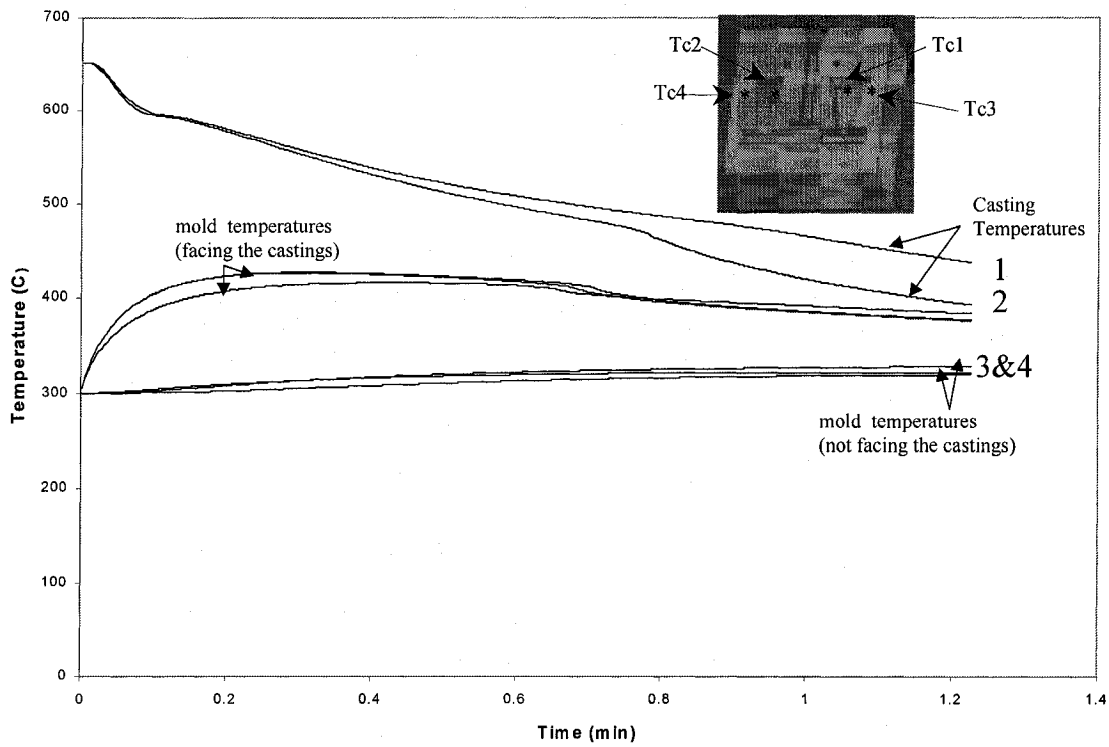

Figure 4.56. Simulation of temperature measurement for thermocouples located in permanent mold during casting of AZ91E magnesium alloy

CHAPTER 5 SUMMARY AND CONCLUSIONS

This work presents an alternative cooling method for the permanent mold casting process. The design, modeling, construction of a permanent mold and associated novel heat pipes, and industrial trials for a permanent mold casting of non-ferrous alloys are presented. The mold was designed to produce shrinkage defects and the heat pipes were designed to demonstrate that it is possible to force the shrinkage away from selected locations and hence improve the casting quality. Computer modeling was used in designing the mold and the heat pipes. Visual and microstructural analysis of selected castings are presented and discussed.

5.1. Design of Permanent Mold and Novel Heat Pipe for Nonferrous Casting Process

A novel heat pipe has been developed and comes as a continuation of the work that has been done at McGill University. The condenser and the evaporator of the heat pipe are connected by flexible hoses, which allow placing the condenser in a desired location. An external chill is incorporated in the condenser. The water inside the reservoir has been successfully returned to the bottom of the evaporator by using a separate return line. An on/off feature is incorporated in the heat pipe design.

Novel features have been incorporated in the heat pipe design such as:

1) On/Off capability: a valve is placed on the return line to fully control the heat pipe cooling operation. Another valve is placed on the hose connecting the evaporator and the condenser to prevent any water which might remain in the hose from falling back into the evaporator when the heat pipe is off.

2) Water reservoir: a water reservoir is incorporated in the design, where the condensate is collected and directly returned to the bottom of the evaporator. The water inside the reservoir has been successfully returned to the bottom of the evaporator by using a separate return line.

3) Flow modifier: a flow modifier has been used to reduce the chance of forming film boiling inside the evaporator.

4) Flexible hoses: the condenser and the evaporator of the heat pipe are connected by flexible hoses, which allow placing the condenser in the desired location. This feature proved to be a desirable feature in the industrial environment where the space is limited. Flexible hoses are also used as a return line and as a vent line.

5) Sleeve: a novel technique to cool only the desired locations and not the entire evaporator has been developed where inserts (sleeves) have been used to control the heat extraction areas. This novel technique could be used in many different applications and equipment where selected areas need to be cooled or perhaps heated.

From the above five features one can conclude that a new novel heat pipe was developed and tested successfully in a laboratory and in an industrial environment.

In order to evaluate the effect of mold cooling using heat pipes, a permanent mold for magnesium and aluminum casting has been designed and constructed with the intention of introducing shrinkage defects.

Computer modeling has been used to design the mold and the heat pipes. The AFS SolidCast modeling package was used. The modeling results showed promising applications for heat pipes in permanent mold casting of nonferrous alloys.

The preliminary testing of the heat pipe conducted in the laboratory and in the plant showed good results.

From this work, one can clearly see that the developed heat pipe can handle high heat fluxes. The preliminary testing of the heat pipe showed that it could handle heat fluxes as high as 800 kW/m^2, and this provided more confidence in handling heat fluxes obtained in a typical permanent mold casting process.

Mathematical calculations and computer modeling showed that the novel heat pipe developed in this work is capable of attaining heat extraction rates that exceed those of comparable water cooling passages.

Thus, this work showed that the developed heat pipe with a small amount of water could achieve high cooling rates without any external pumping requirements. The heat transfer coefficient at the heat pipe/mold interface can reach 20,000 W/m^2K. The high heat transfer coefficient can be reached because of the turbulence generated inside the evaporator of the heat pipe. Such a high heat transfer coefficient is not achievable with conventional water cooling.

5.2. Analysis of Permanent Mold Castings of Magnesium and Aluminum Alloys

Visual and microstructural assessments have been conducted for AZ91E and A356. The effect of freezing range on the shrinkage type has been discussed.

From the discussion given in this work, one can conclude that heat pipe cooling is very effective in reducing the SDAS and the grain size for AZ91E and A356. Aluminum A356 showed a slightly better response to heat pipe cooling compared to magnesium AZ91E in term of SDAS and grain size measurements. Also, heat pipe cooling is very effective in reducing the shrinkage defect for A356 where the shrinkage is a typical concentrated shrinkage void, but not effective to deal with the micro-shrinkage voids found in AZ91E.

A typical shrinkage void was found in A356 castings and the heat pipe managed to push it to the other side of the casting as expected. This was not the case when AZ91E alloy was cast. The metallurgical differences between AZ91E and A356 were discussed. Extensive computer modeling was conducted to enhance the design and to understand the metallurgical differences between the two alloys.

This work showed clearly that cooling is better used to improve the casting quality of alloys with short freezing range. The results presented showed an obvious reduction in casting shrinkage defects when the casting was of an alloy with a short freezing range.

The SDAS was directly related to the cooling rate. The local estimated cooling rates were calculated. Higher cooling rates lead to smaller SDAS. In the setup developed in the present work, the distance between the heat pipe and the casting was 10mm. It is possible to obtain higher casting cooling rates with the existing setup, however, would one need to move the heat pipe closer to the casting cavity. This will

increase the casting cooling rate provided by the heat pipe and will consequently provide further reduction in the SDAS and grain size.

The interfacial heat transfer coefficient, h, and the time for air gap formation were discussed. Interfacial heat transfer coefficient sensitivity analysis was conducted using computer modeling and the results were presented.

This work showed the importance of the effect of the gravity force on the casting during solidification. Gravity will pull the casting downward away from the upper mold surface. Thus, this effect has to be considered in permanent mold casting design.

Because of the thermal properties of AZ91E, it is relatively difficult to cast this alloy. A proper design and choice of an effective casting process are necessary.

Based on the present work, one might conclude that the pressure casting process is the solution to improve the casting quality of AZ91E castings by reducing the micro-shrinkage defects typically present.

The results showed that AZ91E is not a good alloy to be used to study casting parameters such as mold temperature and coating type. Its low thermal conductivity (almost half of A356), low latent heat per unit volume, and long freezing range make it behave in a different way during solidification compared to A356 alloy.

The industrial trial results of magnesium AZ91E and aluminum A356 showed an encouraging future for heat pipes in permanent mold casting.

STATEMENT OF ORIGINALITY

The present work marked the application of heat pipes in the permanent mold casting of magnesium alloys for the first time in both laboratory and industrial environment. InterMag Technologies was the first company to test this novel heat pipe in a commercial casting process. The door is now open for more companies to incorporate heat pipes in their cooling systems for permanent mold casting. This work focused on developing a novel heat pipe, permanent mold design and studying the cooling effect on two popular nonferrous alloys, AZ91E and A356. This research comes as a continuation of novel work that has been conducted at McGill University. The major original contributions to knowledge made in this particular research are summarized as follows:

1. Development of a Novel Heat Pipe

This is the first time that a McGill heat pipe with the following features has been designed, constructed, and tested in the permanent mold casting of AZ91E magnesium alloy. The features of the McGill heat pipe are:

- The heat pipe is fully controlled by inserting valves on the return line and on the main line.

- Flexible hoses are used and the condenser is located away from the heat pipe to suit the industrial environment.

- Sleeves (inserts) have been used. This technique made it possible to cut down the area of the evaporator.

- High heat flux can be easily handled by the heat pipe.

- The water inside the reservoir has been successfully returned to the bottom of the evaporator by using a separate return line.

- The heat pipe performance has been improved by incorporating a flow modifier in the design. The flow modifier reduces the chance of operating in the film boiling regime.

2. Heat Pipe Cooling of Permanent Mold Casting

- This work was the first application of heat pipes in an industrial permanent mold casting environment where the heat pipe installation and handling have to follow the regulations of the plant.

- The chill, which is normally inserted into the mold, has been moved away from the mold and can be located at any desired location. Such a technique made it possible to absorb the heat when required and to continuously dissipate the heat into the air during the entire casting cycle.

- This is the first time that heat pipe cooling technology has been successfully applied to a magnesium alloy casting process.

- It is the first time that a comparison is made of the heat pipe cooling of castings of both aluminum and magnesium alloys in permanent molds.

- The studies conducted in this work showed the improved cooling capabilities of the novel heat pipe developed in this work compared to conventional water cooling systems.

REFERENCES

1. N. Church, P. Wieser, and J.F. Wallace, Modern Casting, Vol. 49, 129-144, (1966).
2. J.J. Burke and V. Weiss, Ultrafine-Grain Metals, Syracuse University Press, New York, NY, (1970).
3. M. C. Flemings, Solidification Processing, McGraw -Hill, New York, NY, 341-344, (1974).
4. G.S. Cole and G.F. Bolling, J.J. Burke and V. Weiss, Ultrafine-Grain Metals, eds., Syracuse University Press, New York, NY, 31–69, (1974).
5. J.R. Picken: J. Mater, Science, Vol. 16, 1437-1457, (1981).
6. R.M. German, Powder Metallurgy Science, Metal Powder Industries Federation, Princeton, NJ, (1984).
7. R.E. Maringer and C.E. Mobley, Rapid Solidification Process Principle and Technologies, Proc. Int. Conf. On Rapid Solidification Processing, Claitor's Publishing Division, Vaton Rouge, LA, 208-221, (1977).
8. P. K. Domalavage, N.J. Grant, and Y. Gefen, Metall. Trans. A, Vol. 14A, 1599-1606, (1983).
9. James V. Beck, " Non-linear Estimation Applied to the Non-linear Inverse Heat Conduction Problem, " International Journal of Heat and Mass Transfer, Vol. 13 703-716, (1970).
10. Irani D. R. and Kondic V., "casting and mold Design Effects on shrinkage Porosity in Light Alloys", AFS Transactions, Vol. 77, 208-211, (1969).
11. Jones H., "A comparison of Approximate Analytical Solution of Freezing from a Plane Chill", Jl. of the Institute of Metals, Vol. 97, 38-43, (1969).
12. Henzel J.G. and Keverian J., "Gap Formation in Permanent Mold Castings", AFS Transactions, Vol. 68, pp. 373-379, (1960).

13. Srinivasan M.N., Seshadri M.R. and Ramachandran A., "Studies on Solidification of Thermal Behaviour of the Molds ", AFS Cast Metals Research Journal, 23 - 26, March, (1971).
14. Srinivasan M.N., Seshadri M. R. and RamachandranA.," Thermal Aspects of Metallic Molds", AFS Transactions, Vol. 78, 395-400, (1970).
15. Nehru K.V.K., Seshadri M.R. and Ramachandran E.G., "Influence of Insulating Mold Coating on the Solidification of Copper Castings in Metallic Molds and Thermal Behaviour of Molds", AFS Cast Metals Research Journal, 111- 116, September, (1974).
16. Chunhui Zhang, Frank Mucciardi and John E. Gruzleski: "Controlled Cooling of Permanent Molds in the Casting of Aluminum", Light Metals, 431-441, (2001).
17. Desars, Rev. de Metall., pp.137, June, (1946).
18. Mohan V. and Shenoy R. N., " Prediction of Solidification Time of Iron Castings in Coated Cast Iron Molds", AFS Transaction, Vol. 90, 435-449, (1982).
19. Winter B. P. , Pehlke R. D. and Trojan P. K., " Volumetric Shrinkage and gap Formation During Solidification of Cu-Base Alloys ", AFS Transactions, Vol. 91, 81-88, (1983).
20. Matuschka B., Archir F. Eisenhuttenwesen, Vol. 2, pp. 405, January, (1929).
21. Paschkis V., " Theoretical Thermal Studies of Steel Ingot Solidification ", ASM Transactions, Vol. 38, 117-147, (1947).
22. Bishop H. F., Brandt F. A. and Pellini W. S., "Solidification of Steel Against Sand and Chill Walls ", AFS Transactions, Vol. 59, 435-450, (1951).
23. Panchanathan V., Seshadri M. R. and Ramachandran A., " Some Thermal Aspects of Metallic Molds ", AFS Transactions, Vol. 71, 158-166, (1963).
24. Mackenzie I. M. and Andrie Donald, " The Distribution of Temperature in Ingot Molds and its relation to Ingot Structure", Journal of the Iron and Steel Institute, 19- 28, September, (1950).
25. Bishop H. F. and Pellini W. S., " Solidification of Metals ", Foundry, Vol. 80, 86-261, (1952).
26. Sharma D.G.R. and Mythily K., " Simulation of Heat Transfer at Casting Metal-

Mold interface ", AFS Treansactions, Vol. 99, 429-438, (1991).

27. Nehru K. V. K., Seshadri M. R. and Ramachandran E. G., " Influence of Insulating Mold Coatings on the Solidification of Copper Castings in Metallic Molds and Thermal Behaviour of Molds ", AFS Cast Metals Research Journal, 111 - 116, September, (1974).
28. Isaac J., Reddy G.P. and Sharma G.K., "Numerical Simulation of Solidification in Metallic Molds", AFS transactions, Vol. 93, 123-132, (1985).
29. Thamban M. I. and Panchanathan V., " Numerical Simulation of solidification of Al Alloys in Cast Iron Molds", AFS Transactions, Vol. 88, 167-174 (1980).
30. Kutumba Rao G.V. and Panchanathan V., " End Chills Influence on Solidification Soundness of Al-Cu-Si (LM4) Alloy Castings", AFS Cast Metals Research Journal, 135-138, September, (1973).
31. Thamban M. I., Gopalakrishnan S. and Panchanathan V., " Thermal Behavior of Cast Iron Molds with long Freezing Range Aluminum Alloys", AFS Transactions, Vol. 87, 171-176, (1979).
32. Prabhakar K. V. and Seshadri M. R., "Influence of Chills on the Soundness of Al-12% Si Alloy Castings ", AFS Transactions Vol. 87, 377-386, (1979).
33. Srinivasan M.N., "Heat Transfer Coefficients at the Casting-Mold Interface During Solidification of Flake Graphite Cast Iron in Metallic Molds ", Indian Journal of Technology, Vol. 20, 123-129, April, (1982).
34. Mohan V. and Shenoy R. N., "Prediction of Solidification Time of Iron Castings in Coated Cast Iron Molds", AFS Transactions, Vol. 90, 435-449 (1982).
35. Pathak S. D. and Prabhakar O., "Feeding Range of Aluminium 11.8 % Si Alloy in Metallic Molds", Aluminium, 599-601, (1980).
36. Ayyamperumal M. , " Feeding Bar and Cylinderical Castings of Aluminium Base Alloys in Metallic Molds", Ph.D Thesis, ITT Madras-36, (1984).
37. Chinnathambi K. , " Feeding Aluminium Base Alloys in Metallic Molds ", Ph.D. Thesis, ITT Madras-36, (1979).
38. Morales A., Glicksman M. E. and Biloni H., "Influence of Mold Wall Microgeometry on Casting Structure ", Solidification and Casting of Metals, The Metals Society,

London, 184-192, (1979).

39. Durham D.R., Verma D. and Berry J.T., " Some Further Observations on Freezing From Chills", AFS Transactions, Vol. 84, 787-792, (1976).
40. Hou T. X. and Pehlke R. D., " Computation of Solidification of a Steel Casting Against a Chill Mold Wall", AFS Transactions, Vol. 96, 151-160, (1988).
41. Chatterjee S. and Das A.A., "Effect of Pressure on the Solidification of Some Commercial Aluminium-Base Casting Alloys ", British Foundryman, Vol. 65(11), 420-428, November,(1972).
42. Chatterjee S. and Das A.A., " Some Observations on the Effect of Pressure on the solidification of Al-Si Eutectic Alloys ", British Foundryman, Vol. 66(4),118- 124, April, (1973).
43. Veinik A.I., " Thermodynamics for the Foundry ", Maclaren and Sons Ltd., (1968).
44. Ho K. and Pehlke R. D., "Mechanisms of Heat Transfer at a metal-mold Interface", AFS Transactions, Vol. 92, 587-598, (1984).
45. Ho K. and Pehlke R. D., " Thransient Methods for Determination of Metal- Mold Interfacial Heat Transfer", AFS Transactions, Vol. 91, 689-698, (1983).
46. T. S. Prasanna Kumar and Narayan Prabhu, " Heat Flux Transients at the Casting/Chill Interface during Solidification of Aluminum Base Alloys", Trans. AFS, Vol. 99, 661-665. (1991).
47. Sully L. J. D., "The Thermal Interface Between Castings and Chill Molds ", AFS Transactions, Vol. 84, 735-744, (1976).
48. Sun R. C., " Simulation and study of surface conductance for Heat Flow in the Early stage of Casting ", AFS Cast Metals Research Journal, 105-110, September, (1970).
49. Nishida Y. and Matsubara H., " Effect of Pressure on Heat Transfer at The Metal-Mold Casting Interface ", British Foundryman, Vol. 69, 274-278, (1976).
50. N. R. Eyers, D. R. Hartree, J. Ingham, R. Jackson, R. J. Sarjant and J. R. Wagstaff, "The calculation of variable heat flow in solids", Philosophical transactions of the Royal Society of London, Series A, Vol.240, 1-57, (1948).
51. W. C. Erickson, " Computer simulation of solidifica- tion ", AFS International Cast-Metals Journal, March, 30-41, (1980).

52. R. J. Sarjant and M. R. Slack, "Internal temperature distribution in the cooling and re-heating of steel ingots", Journal of the Iron and Steel Institute,Vol.177, 428 - 444 (August 1954).

53. R. D. Pehlke, R.E. Marrone and J.O.Wilkes,"Computer simulation of solidification", American Foundrymen's Society, Des Plaines, Illinois, (1976).

54. J. B. J. Fourier, Theorie Analytique de la Chaleur, Gauthier-Villars, 1822; English translation by Freeman, Cambridge, (1878).

55. Stahland W.K., Whaler R.K., "Reviewing Permanent Mold Process – Part 1," Modern Casting, Oct., 45-49, (1981).

56. Lerner S. Y., "Water or Air? – Examining Permanent Mold Cooling Methods,", Modren Casting, 23-26, February (2002).

57. Mechanical engineers handbook, New York; Chichester [England] : Wiley, pp. 283, (1998).

58. Chiesa F., " Controlling Permanent Mold Coating Application Parameters", Modern Casting, Vol. 86, No. 10, 28-30, (1996).

59. Chiesa F., :Quantifying Permanent Mold Coating's Functional Properties", AFS Transactions, Vol. 106, 589-594, (1998).

60. Kuo J. H., Hsu F. L., Hwang W. S., Yeh J L., Chen S. J., "Effects of Mold Coating and Mold Material on the Heat Transfer Coefficient at the Casting/Mold Interface for Permanent Mold Casting of A356 Aluminum Alloy", AFS Transactions, Vol. 109, 469-484, (2001).

61. Wells, K. J., Colwell, G. T., Berry, J. T., :Two-Dimensional Numerical Simulation of Casting Solidification with Heat Pipe Controlled Boundary Conditions", Transactions of AFS, Vol. 92, 429-434, (1984).

62. A. Faghri, Heat Pipe Science and Technology, Taylor & Francis, Washington D. C., (1955).

63. R. S. Gaugler, "Heat Transfer Device," U.S. Patent 2,350,348, (1944).

64. G. M. Grover, " Evaporation - Condensation Heat Transfer Device," U.S. Patent 3,229,759, (1964).

65. Grover, G. M., Cotter, T. P. and Erikson, G. F., "Structures of Very High Thermal

Conductivity", J. Appl. Phys., 35, 1990 (1964)

66. Deverall, J. E. and E. W. Salmi (1967) " Heat Pipe Performance in a Space Environment," (1967) 1967 IEEE Thermionic Conversion Specialist Conference, Palo Alto, California, October 30-November 1, (1967).
67. Girrens, S. P., Meier, K. L. and J. M. Dickinson (1980) " Titanium Heat Pipes for Space Power Systems," LA- UR- 80 - 1033, 15th Intersociety Energy Conversion Engineering Conference, Seattle, WA, August 18-22, (1980).
68. Kemme, J. E., E. S. Keddy, and J. R. Phillips (1978) "Performance Investigations of Liquid-Metal Heat Pipes for Space and Terrestrial Applications," III International Heat Pipe Conference, Palo Alto, CA, May 22-24, (1978).
69. Kay J., Mucciardi F.,"A Computational Investigation of a Heat Pipe Injection "Lance, " Steel Research, Vol. 66, No. 1, 8-13, (1995).
70. Mucciardi F., Jin N., " Top Blowing Oxygen Lance for Copper Smelting and Converting," Canadian Metallurgical Quarterly, Vol. 35, No. 5, 395-408.
71. Jin N., " Heat Pipe Cooled Injection Lances - Experimental Investigation and Mathematical Modeling," Ph.D. Thesis, McGill University, Montreal, Canada
72. Mucciardi F., " Improved Injection Lances with Heat Pipe Technology, " The Brimacombe Memorial Symposium, CIM, (2000).
73. Mast E, Mucciardi F, Brown M., " Self - Cooling Lance or Tuyere," US Patent 5,310,166, (1994).
74. Mafoud M., Mucciardi F., J.E. Gruzleski, "On-line control of Heat Extraction During Thermal Analysis of Aluminum Alloys,"International Journal of Cast Metals Research Vol. 10, 191-200, (1998).
75. Mafoud M., " Controlled Thermal Analysis Using Heat Pipe Technology," Ph. D. Thesis, McGill University, Montreal, Canada.
76. Zhang C., Mucciardi F., Gruzleski l. E., " Heat Pipe Cooling of Permanent Mold Castings of Aluminum Alloys," AFS Transactions, Vol. 110, 435-448, (2002).
77. Zhang C., Mucciardi F., Gruzleski l. E., "Effects of Heat Pipe Cooling on Permanent Mold Castings of Aluminum Alloys," Light Metals, 321-334, (2002).

78. Zhang C., Mucciardi F., Gruzleski J., E., Burke P., Hart M., " Application of Controllable Heat Pipe Cooling During the Low Pressure Die Casting of Aluminum Alloys," AFS Transactions Vol. 111, 03-010, (2003).

79. Leefer, B. I., " Nuclear thermionic energy converter", Proceedings of 20th Annual Power Sources Conf., 172 – 175, (May 1966).

80. Atsugi H. K., etal, "Method for Manufacturing Molded Resin Product and Plastic Mirror," U. S. Patent 5,603,871, (1997).

81. Peterson G.P., Ma H.B., "Temperature Response of Heat Pipe Transport in a Micro Heat Pipe," Journal of Heat Transfer, VoL 121, No. 2, 438-445, (1999).

82. Scott D., Garner P.E., "Heat pipes for electronics cooling applications," Electronics Cooling Online, Vol. 2, No.3, http://www.coolingel ectronics.com/html/articles html, (1996).

83. Ali A, DeHoff R, Grubb K, " Advanced Heat Pipe Thermal Solutions for Higher Power Notebook Computers," Thermacore International, Inc. LANCASTER, P.A., USA, http://www.th_rmacore.com/papers.htm.

84. Xie H, Aghazadeh M, Toth J, "The Use of Heat Pipes in the Cooling of Portables with High Power Packages -.A Case Study with the Pentium Processor - Based Notebooks and Sub - notebooks," Thermacore International, Inc. LANCASTER, P A USA, http://www.thermacore.com/papers.htm.

85. Toth J., DeHoff R., Grubb K., " Heat Pipes: The Silent Way to Manage Desktop Thermal Problems," Presented at I-THERM Conference, Seattle, W A, (May 1998).

86. Waters, E. D., "Arctic tundra kept frozen by heat pipes", The Oil and Gas Journal (US), 122-125, August 26, (1974).

87. Busse, C. A., "Theory of the Ultimate Heat Transfer Limit of Cylindrical Heat Pipes", The International Journal of Heat and Mass Transfer, Vol. 16, 169-186, (1973).

88. Holman, J. P., "Heat Transfer", Sixth Edition, McGraw-Hill, 1986.

89. Chi S. W., "Heat Pipe Theory and Practice," Hemisphere Publishing Corporation, (1976).

90. Dunn P. D., and Reay D. A., "Heat Pipe," 3rd Edition, Permagon Press, (1982).

91. Peterson G. P., " An Introduction to Heat Pipes: Modeling, Testing, and

Applications", John Wiley & Sons, Inc., (1994).

92. Mucciardi F., "Introduction to Process Engineering", class notes for Advance Process Engineering course, McGill University, (2003).
93. Andresen, W. T., " Computer Simulation and Analysis of Liquid Metal Flow and Thermal Conditions in Die Casting Dies," SDCE 14th International Die Casting Congress and Exposition, Toronto, Ontario, Canada, Society of Die Casting Engineers, Inc., 1-5,11-14 (May 1987).
94. Bounds, S; Davey, K; Hinduja, S, "Modeling the pressure die casting process using a hybrid finite-boundary element model," International Journal for Numerical Methods in Engineering (UK), Vol. 45, no. 9, 1165-1185, (1999).
95. Nyamekye, K; Wei, S; Martinez, KM, "A CAD/CAE Model for Predicting Thermal Fatigue Life of a Permanent Mold," Transactions of the American Foundry Society, Vol. 105, 557-572, (1997).
96. Fjar G. H., Mortensen D., Hakonsen A., S_rheim A. E., "Couple Stress, Thermal and Fluid Flow Modelling of the start-up Phase of Aluminum sheet Ingot Casting," Light Metal, 743-748, (1999).
97. Lorstad L. J Rasmussen M. W., " Aluminum Casting Technology," 2nd Edition, American Foundry Society, Des Plaines, IL USA, (1993).
98. Fang Q. T. Granger D. A., " Porosity Formation in Modified and Unmodified A356 Alloy Castings," AFS Trans. Vol. 97, 989-1000, (1989).
99. ASM International. Handbook Committee, " ASM Metals Handbook, Casting," 9th Edition, Metals Park, Ohio, USA, Vol. 15, pp. 749, (1998).
100. I. S. Kim, M. Isac and R. I. L. Guthrie, " Casting Strips of Magnesium Alloy AZ91 on a Moving Mold System", Light Metals, 455-469, (2002).
101. Backerud L., Krol E., and Tamminen J., " Solidification Characteristics of Aluminum Alloys, Volume 1, Wrought Alloys", American Foundry Society, pp.82, (1986).
102. France D.M., Minkowycz W.,J., Chang C., "Analysis of Post-CHF Swirl Flow Heat Transfer," International Journal of Heat Mass Transfer, Vol. 37, Suppl. 1, 31-40, (1994).

103. Agarwal S.K., Rao M., " Heat Transfer Augmentation for the Flow of a Viscous Liquid in Circular Tubes Using Twisted Tape Inserts," International Journal of Heat Mass Transfer, Vol. 39, No. 17, 3547-3557, (1996).

104. Manglik R.M., Bergles A. E., " Heat Transfer and Pressure Drop Correlations for Twisted-Tape Insert in Isothermal Tubes: Part 1- Laminar Flows," Journal of heat Transfer, Vol. 115, 881-889, (Nov. 1993).

105. AF-SOLD 2000, "Training Course Workbook", Finite Solution Inc., (2000).

106. Donald R. Askeland, The Science and Engineering of Materials, Brooks/Cole Engineering Division, Monterey, CA, (1984).

107. A. Tronche, D. Gloria and J. E. Gruzleski, " A Grain Size Determination Technique for Al - Si Casting Alloys ", International Journal of Cast Metals Res, Vol. 11, 211-218, (1999).

108. J. F. Wallace, D. Schwam and Y. Zhu, "The Influence of Potential Grain Refiners on Magnesium Foundry Alloys", AFS Transactions, Vol. 111, Paper #03-141, 2003.

109. J. P. Thomson, P. Liu, M. Sadayappan, and M. Sahoo, "Effect of C_2Cl_6 on Mechanical Properties and Microstructure of Gravity Permanent Mold Cast AZ91E", AFS Transactions, Vol. 112, #04-121, 2004.